Phosphoglucomutase 1 (PGM1) expression and regulation in cancer cells

Hapiloe 'Mabaruti Maranyane

Thesis presented for the Degree of

DOCTOR OF PHILOSOPHY

in the Department of

Clinical Laboratory Sciences

Division of

Medical Biochemistry

FACULTY OF HEALTH SCIENCES

UNIVERSITY OF CAPE TOWN

February 2015

ACKNOWLEDGEMENTS

I would like to extend my heartfelt thanks to the following people:

My supervisor, A/Prof Virna Leaner for her faith in me, supervision, mentorship and counsel, patience and encouragement, guidance and tutelage

A/Prof Denver Hendricks for his advice and support and occasional pat on the back
Prof Peter Meissner and Jene Ward for administration and coordination of the department

Dr Pauline van der Watt for her immeasurable support, encouragement, patience experimental and conceptual assistance, guidance and mentorship
Dr Kate Hadley for her encouragement, advice and critical input
Dr Nina A.V. Holderness-Parker for her insight, support, friendship and genuine faith in me

All the past and current 'Cancer Lab' members:

The friendship and genuine support and comradery of the following people has made it a worthwhile journey:
Dr Nelusha Shunmoogam-Gounden, Dr Luke Esau, Dr Lise-Lotte Angus, Dr Jacqueline Bracher, Londiwe Khuzwayo, Gannie Tzoneva, Boris Krivochiev, Cherise Dunn, Alicia Chi, Erin Strydom, Tamara Stelma, Tamlyn Shaw, Cleo Julie-Jean Willams.

A special thanks to Hajira Guzgay (lab manager) for your support and aid and Robert Samuels (lab technician) for your help and assistance.
Dr Fierdoz Omar for her assistance and expertise with lactate assays
Susan Cooper for her guidance and direction with microscopy
Dr Dee Blackhurst for her help with all things lipid

Thank you to the following institutions and individuals for financial support throughout my postgraduate studies:

The Mandela Rhodes Foundation and Leshego Ledwaba
Council of Scientific and Industrial Research (CSIR) with special mention of Nokuthula Zama and Joseph Tshikomba (as direct liaisons) for their assistance and support.
The University of Cape Town (Linda Vranas and the PGFO team for administrative and invaluable support and assistance)

My family and friends:

My parents, Mr and Mrs Maranyane for their encouragement, prayers and value for education that has rubbed off on me.
My siblings, Matala Maranyane, Napo Maranyane and Lebogang Diale, (I had no better fan club) for every prayer and word of hope and encouragement they shared.

A special thank you to the following people who have been my family away from home:

Geraldine Majoro, Kutlwano Rasodi, Rian Eikelboom, Takalani Mulaudzi, Melina Ojiambo, Phuti Senyantsi and Domingo Joao, Jason and Jessica Stanier, Carmelita Lee-Shong for their prayers, support, friendship and counsel in their different capacities.

You desire truth in the innermost being, and in the hidden part you make me know wisdom.

Psalm 51:6 (NASB)

CONTENTS

ABBREVIATIONS

ADP	Adenosine Diphosphate
Amp	Ampicillin
APS	Ammonium Persulphate
ATP	Adenosine Triphosphate
BCA	Bicinchoninic acid
BSA	Bovine Serum Albumin
bp	Base pairs
CDK	Cyclin-Dependent Kinase
CAMP	Cyclic adenosine monophosphate
ChIP	Chromatin Immunoprecipitation
^{o}C	Degrees Celsius
$CoCl_2$	Cobalt (II) Cholride
Ctl	Control
DAPI	4', 6' –diamidino-2'-phenylindole hydrochloride
DCF-DA	2',7' –dichlorofluorescein diacetate
DMEM	Dulbecco's Modified Eagle's Medium
DMSO	Dimethyl Sulphoxide
DNA	Deoxyribonucleic acid
dNTP	Deoxynucleoside Triphosphate
Dox	Doxorubicin
DP1	Dimerization partner 1
ECL	Enhanced Chemiluminescence
ENO1	Enolase 1
FBS	Fetal Bovine Serum
G1P	Glucose-1-phosphate
G6P	Glucose-6-phosphate
G6PDH	Glucose-6-phosphate Dehydrogenase
GYS	Glycogen Synthase
Gus B	β-glucuronidase
HIF	Hypoxia inducible Factor

HRE	Hypoxia Response Element
HK	Hexokinase
HPV	Human Papilloma Virus
Hr	hour
HRP	Horse Radish Peroxidase
IPTG	Isopropyl β-D-1'-thiogalactopyranoside
LB	Luria Broth
LDH	Lactate Dehydrogenase
Luc	Luciferase
M	Molar
mM	Millimolar
µM	Micromolar
mg	Milligrams
µg	Microgram
ml	Millilitre
µl	Microliter
MTT	3-[4,5-dimethylthiazol-2-yl]-2,5 diphenyl tetrazolium bromide
NADP+	nicotinamide adenine dinucleotide phosphate
NADPH	reduced nicotinamide adenine dinucleotide phosphate
ng	Nanograms
$NiSO_4$	Nickel (II) Sulphate
nM	Nanomolar
nm	Nanometres
N_2	Nitrogen gas
OD	Optical Density
PAGE	Polyacrylamide Gel Electrophoresis
PBS	Phosphate Buffered Saline
PCR	Polymerase Chain reaction
PEG	Polyethylene Glycol
PGAM	Phosphoglycerate mutase
PGK1	Phosphoglycerate Kinase 1

PGM1	Phosphoglucomutase 1
PKM2	Pyruvate Kinase Mutase 2
PDHs	Proly hydroxylases
PFA	Paraformaldehyde
PMSF	Phenylmethanesulfonyl fluoride
PPP	Pentose Phosphate Pathway
p/s	Penicillin and Streptomycin
PYGL	Glycogen Phosphorylase
Rb	Retinoblastoma protein
RIPA buffer	Radio-immunoprecipitation assay buffer
RNA	Ribonucleic acid
RNAsin	Ribonuclease inhibitor
ROS	Reactive oxygen Species
RFU	Relative fluorescence units
rpm	Revolutions per minute
siRNA	Small interfering RNA
SV40	Simian Virus 40
Ta	Annealing Temperature
TBST	Tris-Buffered Saline Tween-20
TCA cycle	Tricarboxylic acid cycle
TK	Thymidine Kinase
TF	Transcription factor
UTR	Untranslated region
X-gal	5-bromo-4-chloro-3-indolyl-β-D-galactopyranoside

ABSTRACT

Cancer cells undergo metabolism that is significantly different to normal cells, with an increased dependence on glucose metabolism as a hallmark of most cancers. Changes in global gene expression patterns are the major driving forces behind cancer progression. These changes trigger events that result in the dysregulation of key enzymes associated with metabolic processes. Gene expression profiling studies done previously in our laboratory identified a group of genes involved in glucose metabolism to be differentially expressed in cervical cancer patient material. Of these, Phosphoglucomutase 1 (PGM1) was identified to have elevated expression in the cancer group. PGM1 is a phosphotransferase that catalyses the reversible conversion of the glycogen breakdown product, glucose-1-phosphate into glucose-6-phosphate, a substrate for glycolysis and the pentose phosphate pathway. This places PGM1 at a critical traffic point of glucose metabolism. In this study we investigated the expression, regulation and biological significance of PGM1 in cancer cells. Our results showed that PGM1 expression was elevated in cervical cancer tissue compared to normal. Its expression was also high in cervical, oesophageal and breast cancer cell lines. Elevated PGM1 expression associated with high promoter activity as well as with E2F and HIF1α activities in cancer cells. PGM1 expression at the level of mRNA, protein and promoter activation was significantly stimulated in hypoxia mimicking conditions. Our data showed that PGM1 expression in cancer cells was required mainly for glycogen accumulation with marginal changes on glycolysis and the pentose phosphate pathway. While PGM1 expression did not appear necessary for cancer cell proliferation in normoxia and nutrient sufficiency, our data shows that it is required for proliferation under conditions of glucose deprivation combined with hypoxia. Together these findings suggest that PGM1 expression is altered in cancer cells,

that it is required for aberrant glycogen expression in cancer cells and that it has a role in cancer biology during severe stress conditions.

CHAPTER 1

LITERATURE REVIEW

1.1 Global cancer burden

"The diseases that are grouped together as cancers are among the major liabilities to human life." This was an opening line in a recent commentary addressing leaders in cancer research and policy from 15 economically diverse countries meeting to discuss opportunities to reduce cancer incidence and mortality. The main aims were to improve cancer care, and increase current understanding of disease pathophysiology, thereby enabling faster progress in confronting the growing challenge of cancer worldwide (Varmus & Kumar 2013).

The World Health Organization published in 2008, that cancer is the leading cause of death in economically developed countries and the second leading cause of death in developing countries (World Health Organization 2008). According to Jemal and co-workers (2011) the burden of cancer is emergent in economically developing countries as a result of population aging and growth (Edwards et al. 2002) as well as, increasingly, an adoption of cancer-associated lifestyle choices including smoking, physical inactivity, and ''westernized'' diets (Jemal et al. 2011; Hanahan 2014). Globally, there are about 12.7 million newly diagnosed cancer cases per year and a reported 7.6 million cancer deaths are estimated to have occurred in 2008; of these, 64% occurred in the economically developing world (Jemal et al. 2011; Varmus & Kumar 2013). Cancer in the developing world thus poses a major health risk which is exacerbated by poorer cancer survival in developing countries, most likely due to a combination of a late stage diagnosis and limited access to timely and standard treatment approaches (Lingwood et al. 2008; Jemal et al. 2011). New drugs and treatment regimens and modern technologies are generally unaffordable or logistically impractical to deliver to

patients (Hanahan 2014). As such, the search for new diagnostic tools and therapeutic strategies against cancer continues. Our research in the field is directed towards obtaining a better understanding of the molecular mechanisms that underpin cancer development with the hope to discover of novel cancer biomarkers and therapeutic targets.

1.2 Therapeutic targeting of cancer hallmarks

Cancer is a complex disease involving numerous tempo-spatial changes in cell physiology, which ultimately lead to malignant tumours. The consequent abnormal cell growth (or neoplasia) is the biological endpoint of the disease (Seyfried & Shelton 2010). Transformation of normal human cells into malignant cancers is preceded by the progressive acquisition of specific characteristics which become definitive of the cancer phenotype, and these characteristics are collectively termed 'cancer hallmarks' (Hanahan et al. 2000). 'Hallmarks' constitute an organizing principle for rationalizing the complexities of neoplastic disease (Hanahan & Weinberg 2011). From an initial six capabilities, described by Hanahan and Weinberg (2011), research in the last decade has advanced to the adoption of the following ten cancer hallmarks: 1) sustained proliferative signals 2) evasion of growth suppressors 3) avoidance of immune destruction 4) replicative immortality 5) enabling of tumour promoting inflammation 6) activation of invasion and metastasis 7) induction of angiogenesis 8) allowance of genomic instability and mutation 9) resistance of cell death and 10) deregulated cellular energetics Figure 1.1 (Hanahan & Weinberg 2011). These cancer hallmarks form a molecular signature of cancer cells that differentiates them from normal cells and therefore offers the selectivity necessary for target discovery. Research efforts have investigated the

targeting of these different cancer capabilities as distinct therapeutic approaches. and Figure 1.1 shows illustrative examples of candidate drugs against the specified molecular targets.

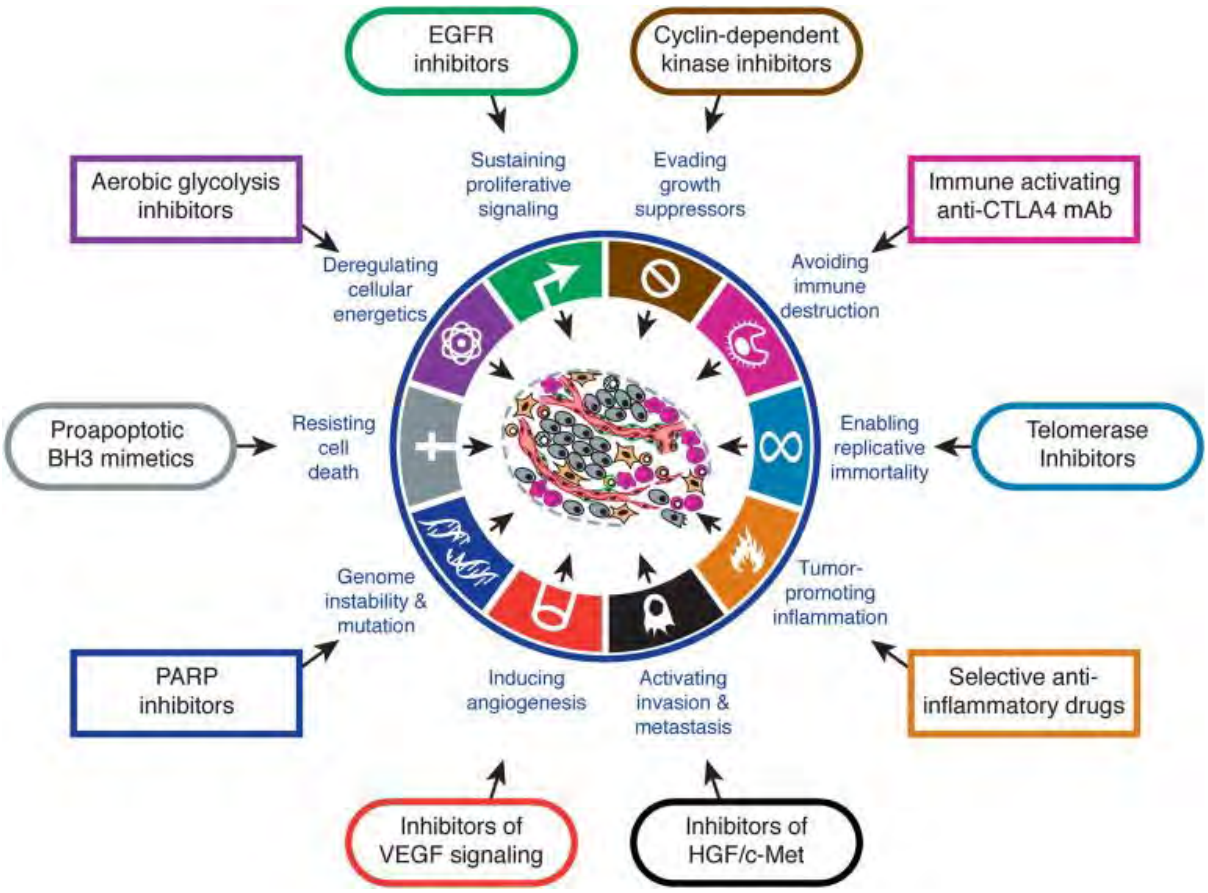

Figure 1.1. Therapeutic targeting of the hallmarks of cancer

Drugs that interfere with each of the acquired capabilities necessary for tumour growth and progression have been developed and are in clinical trials or in some cases approved for clinical use in treating certain forms of human cancer. Additionally, the investigational drugs are being developed to target each of the enabling characteristics and emerging hallmarks which also hold promise as cancer therapeutics. From (Hanahan & Weinberg 2011)

The investigation of gene expression patterns across cancer cohorts typically directs the search for novel potential targets and often reveals a contextual profile of genomic and epigenetic changes that underlay the tumourigenic landscape of any particular cancer. Studies have shown that certain cancers demonstrate specific hallmark changes that provide

an opportunity for targeted therapy. For example, some breast cancers show an overexpression of the human epidermal growth factor receptor (HER2) and as such, tyrosine kinase inhibitors have been used to selectively target these malignant cancer cells, the drug Herceptin (trastuzumab) being one such example (Vogel et al. 2003).

The discovery of drugs such as Gleevac (Imatinib) certainly speaks to the promise of the 'silver/magic bullet' approach to finding new and effective cancer therapies with reduced toxicity towards normal cells and reduced side effects that often follow off-target drug binding. In this specific example, much success was seen, in which genomic instability was targeted through the design of an inhibitor specific to the BCR-ABL tyrosine kinase, a fusion protein that results from a reciprocal translocation between chromosome 9 and 22q, and is responsible for the onset of chronic myelogenous leukaemia (CML). CML patients treated with Gleevac, had an estimated overall survival rate in a 5-year follow-up trial of 89%, with a relapse rate of only about 17%, compared to an initial 30% patient survival rate following prior traditional treatment protocols which were also expensive (Druker et al. 2006; Pray 2008). This is a success story, however, an exceptional case as unlike most other cancers, which are caused by a multitude of complex interacting genetic and environmental factors (and therefore involving multiple targets), CML is caused by a single aberrant protein related to a consistent chromosomal translocation (Pray 2008).

Although a growing number of inhibitors that target specific components of the altered cancer capabilities are in clinical use, the success and efficacy of these agents has been limited by resistance to inhibitor therapy (Logue & Morrison 2012; Locasale 2012). Detailed bioinformatic analyses have suggested that cancer-related driver mutations affect a dozen or more core signalling pathways and processes responsible for tumourigenesis, leading to

questions about the usefulness of targeting individual signalling molecules as a practical therapeutic strategy. This singular approach towards treatment does not cater for cancer's ability to adapt signalling circuitry, which enables cancer cells to take advantage of pathway redundancy and routes of feedback and cross-talk in order to sustain their progression (Cairns et al. 2011; Logue & Morrison 2012). The challenge of better understanding of carcinogenesis therefore still remains.

1.3 The Tumour Microenvironment

"Tumours are complex tissues in which mutant cancer cells have conscripted and subverted normal cell types to serve as active collaborators in their neoplastic agenda" (Hanahan et al. 2000). The tumour microenvironment describes the local conditions experienced by cells in a tumour, including the levels of nutrients, oxygen and signalling molecules such as growth factors and cytokines (Vander Heiden 2011). The interactions between these 1) local conditions, 2) genetically altered neoplastic cells and 3) 'normal' supporting cells around solid tumours are proving to be all critical to understanding cancer pathogenesis and have implications on the development of novel, effective therapies. A good example to illustrate this, is in a study conducted by Smith and co-workers (Smith et al. 2013). Their data showed that tumours assume a differential architecture that either makes them resistant or susceptible to anti-angiogenic treatment in this case, VEGF inhibition. In this study, xenograft tumour cells that displayed a 'stromal-vessel' (SV) phenotype appeared somewhat resistant to the VEGFR2 inhibitor, DC101 (a monoclonal neutralizing antibody); SV-type tumours being characterized by a dominant pattern of tumour cell nests surrounded by well-developed stromal structures containing the majority of the vessels. Their study showed that in contrast

to tumours of the SV-type architecture, the 'tumour-vessel' (TV) phenotype, in which the tumour structure showed vessels embedded throughout the tumour cell mass, showed greater sensitivity to this anti-angiogenic treatment *in vivo* (Smith et al. 2013). Their observations highlight the importance of considering the contribution of the supporting cellular compartment in and around cancer cells in evaluating and developing a holistic understanding of carcinogenesis, the tumour microenvironment and consequent implications upon treatment approaches. The stromal architecture may influence the intrinsic metabolic status of the tumour cells either directly, or by creating a dependency on metabolic coupling between the stromal fibroblast and tumour to promote anabolic growth (Whitaker-Menezes et al. 2011).

The cellular compartment of the tumour microenvironment is comprised of neoplastic cancer cells that initiate the creation of the tumour niche, and cells that maintain the structural framework of tumour tissue. These tumour cells are a collective grouping of mesenchyme-derived cells called cancer-associated fibroblasts (CAFs) recruited from local tissues to the tumour site (Polanska & Orimo 2013). CAFs differ from normal fibroblasts in that they display increased proliferation, enhanced extracellular matrix production and a unique cytokine secretion profile (e.g. VEGF, Stromal cell-derived factor 1; SDF1, platelet derived growth factor (PDGF) and others) (Polanska & Orimo 2013; Junttila & de Sauvage 2013). Maintenance of cells requires tumour vasculature composed of endothelial cells and pericytes which assume a diverse morphology compared to the normal vasculature. The host vessels provide the structure from which new blood vessels are formed. The ability to recruit *de novo* formed vessels not only supplies oxygen and nutrients for the growing tumour mass (Fiaschi & Chiarugi 2012) but allows for the infiltration of immune cells. Both the innate and adaptive immune systems have been implicated in promoting and preventing tumour growth.

Although the immune system has the ability to mount anti-tumour responses, mechanisms of immune suppression can prevent this process (Junttila & de Sauvage 2013). Figure 1.2 shows a comprehensive overview of the cellular compartment of the tumour microenvironment and the functions of the individual players in propagating and maintaining cancer proliferation and survival.

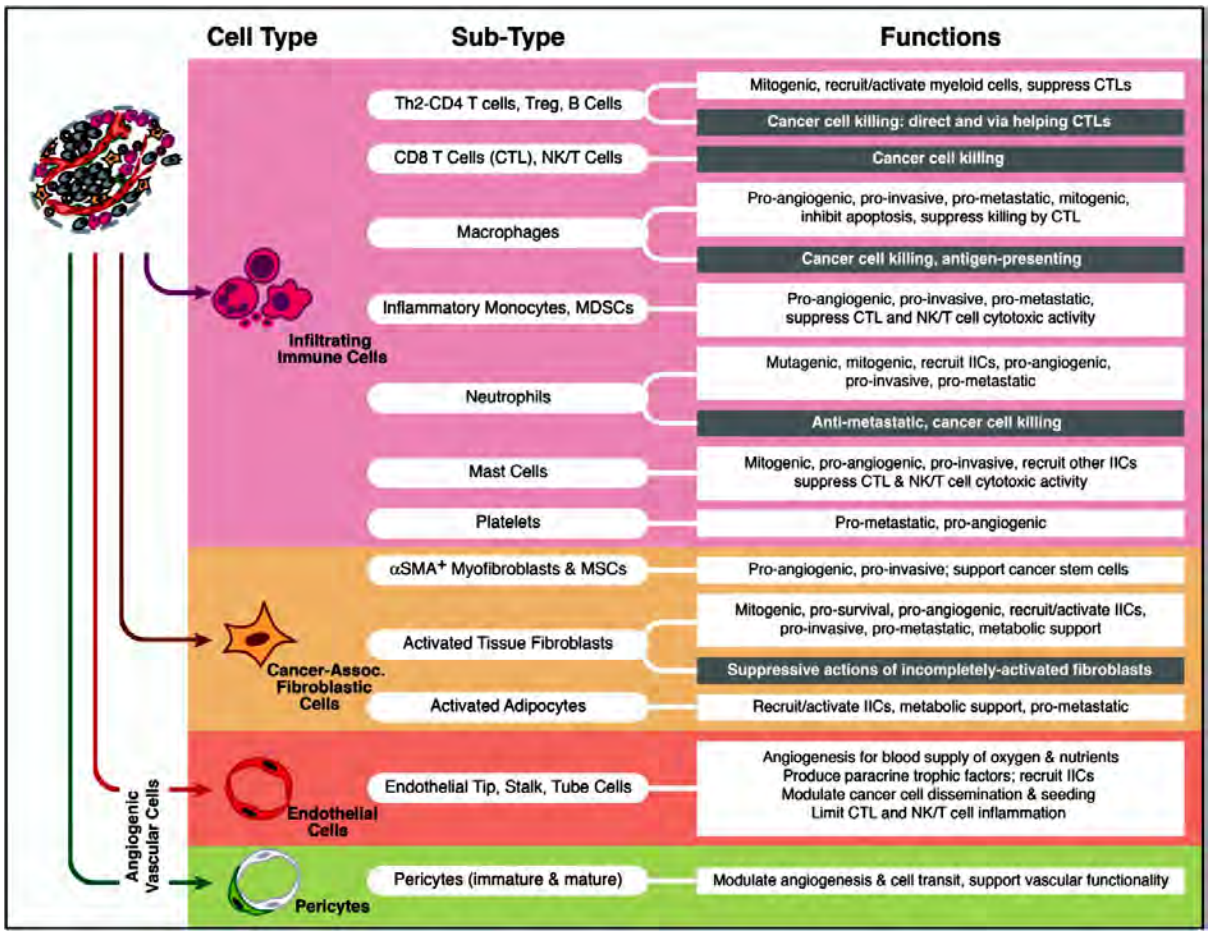

Figure 1.2. Multiple stromal cell types and sub-cell types of the tumour microenvironment can variably contribute to, or in some cases oppose, acquisition of hallmark functional capabilities in different organ sites, tumour types and subtypes, and stages of progression. Major stromal cell subtypes are indicated, along with a synopsis of key functional contributions that such cell subtypes can make. The antagonistic functions of certain subcell types are highlighted in gray. The lists of subtypes and of their key functions are not comprehensive, but rather prominent examples. Th2, helper type 2; CD4 T cell, CD4-positive lymphocyte; Treg, regulatory T cell; CTL, cytotoxic T lymphocyte; NK/T, natural killer and natural killer T cell; MDSCs, myeloid-derived suppressor cells; αSMA, alpha smooth muscle actin; MSCs, mesenchymal stem cells. From (Hanahan & Coussens 2012).

In order to adequately delineate the local conditions within the tumour microenvironment, it is important to consider that cancer cells are typified by deregulated cellular energetics (Hanahan & Weinberg 2011) or metabolic reprogramming (Ward & Thompson 2012). The altered metabolic profile of tumours occurs in the context of the previously mentioned physical and morphological features of the tumour microenvironment which often include hypoxia, hypoglycemia and acidity, all of which contribute to tumour pathogenesis (Estrella et al. 2013). Reprogrammed metabolic pathways have been the basis behind the design of imaging techniques such as positron emission tomography (PET) with F-18 fluorodeoxyglucose (FDG) (Som et al. 1980; Rohren et al. 2004; Xue et al. 2006; Upadhyay et al. 2013). FDG-PET is a technique that exploits the tumour's affinity for glucose as a means to locate and aid in the diagnosis and staging of cancer. A detailed overview of the molecular mechanisms and metabolic pathways that underpin the local conditions of the tumour microenvironment will be the focus in the upcoming section.

1.4 Reprogramming of metabolism in cancer

Metabolism can be described simplistically as a combination of biochemical processes that occur in living things for the maintenance of life. These processes have been categorized into two main branches; anabolic metabolism, which refers to the building up of biosynthetic molecules and catabolic metabolism, which refers to the breaking down or utilization of the molecules imported from the extracellular environment or internally synthesized macromolecules. Both anabolic and catabolic processes in cancer cells differ from those of normal cells (Zhao et al. 2013). Cell proliferation requires nutrients, energy, and biosynthetic activity to duplicate all macromolecular components during each passage through the cell cycle, therefore it is not surprising that metabolic activities of highly proliferating cancer cells would be appear different from those in normal cells (DeBerardinis et al. 2008).

Multiple molecular mechanisms, both intrinsic and extrinsic, converge in cancer to alter core cellular metabolism and provide support for the three basic needs of dividing cells: rapid ATP generation to maintain energy status; increased biosynthesis of macromolecules to support cellular replication; and maintenance of appropriate cellular redox status for survival (Cairns et al. 2011).

Cancer's adaptations to meet these needs was first investigated by Otto Warburg. He observed a shift in ATP generation from oxidative phosphorylation to glycolysis, even under normal oxygen concentrations (Warburg 1956). While Warburg interpreted dependency on glycolysis as a function of mitochondrial impairment (Warburg 1956; Carew & Huang 2002), this deduction was found to be controversial as more recent evidence has shown that mitochondria in cancer cells are both functional and re-programmed to support carcinogenesis (Grupp et al. 2013; Moreno-Sánchez et al. 2007). Most cancers readily take up

and use glucose as an immediate energy source through accelerated glycolysis (Sonveaux et al. 2012; Marín-Hernández et al. 2011; Bao et al. 2013).

To fuel metabolic requirements of the cell and to supply biosynthetic precursors (DeBerardinis et al. 2008), glutamine, one of the most abundant amino-acids is also thought to be processed through the mitochondria. Glutamine participates in metabolism as a nitrogen and carbon source for biosynthesis (Wise & Thompson 2010) and it has more recently been described as a part of the cancer cell's acid management system (Huang et al. 2013). The high rate of glycolysis allows cells to maintain biosynthetic fluxes during rapid proliferation but results in a high rate of lactate production which contributes in part to the consequent acidity in the tumour microenvironment (DeBerardinis et al. 2008).

The following section describes the above metabolic alterations, in particular glucose metabolism, in more detail to allow for a clearer understanding of the tumour landscape, as it relates to our current study.

1.4.1 Glycolysis and lactate metabolism

The role for glycolysis in normal cells is to synthesize of two molecules of pyruvate, two molecules of NADH, and a net production of two molecules of ATP. The pyruvate and NADH molecules are then transported to the mitochondria to be further processed for a greater ATP yield through aerobic respiration. Pyruvate is cycled through Tri-Carboxylic Acid (TCA) cycle for the synthesis of more high energy electron carriers, NADH and $FADH_2$, which together with the NADH molecules produced through glycolysis participate via the electron transport chain (oxidative phosphorylation) to yield thirty eight ATP per glucose molecule.

In most cancer cells, however, glycolysis and oxygen dependant mitochondrial respiration are uncoupled processes. This means that instead of the pyruvate (the glycolytic end product) being processed via the TCA cycle, it is instead converted into lactate by lactate dehydrogenases (LDH). The lactate is excreted into extracellular matrix. This is similar to what happens in normal cells in the absence of oxygen by a process of fermentative glycolysis. However this phenomenon occurs in cancers irrespective of oxygen availability, giving rise to the generally accepted 'cancer signature' termed the "Warburg effect" as Warburg was the first to describe this observation.

The Warburg effect yields a low net output of ATP per glucose molecule compared to that of oxidative phosphorylation and much debate and studies have been conducted to elucidate why cancer cells rely on uncoupled 'aerobic glycolysis'. One of the reasons suggested is that although the yield of ATP per glucose consumed is low, if the glycolytic flux is high enough, the percentage of cellular ATP produced from glycolysis can exceed that produced from oxidative phosphorylation (Pfeiffer et al. 2001; DeBerardinis et al. 2008). Therefore ATP production via glycolysis can outpace that of oxidative phosphorylation offering an advantage to cancer cells. In addition, the expression of glucose transporter, GLUT1 is often increased in cancers and conditions such as hypoxia in the tumour microenvironment activate and allow for the translocation of glucose transporters to the plasma membrane (Avril 2004), which augments the influx of glucose into cells, supporting the high glycolytic rate in these cells. Furthermore, glucose degradation via glycolysis provides cells with intermediates needed for biosynthetic pathways, including ribose sugars for nucleotides; glycerol and citrate for lipids; nonessential amino acids; and, through the oxidative pentose phosphate pathway, NADPH (DeBerardinis et al. 2008).

Lactate production and excretion by cancer cells as a result of the disconnection of glycolysis to mitochondrial respiration was initially thought to be a wasteful consequence of inefficient fermentative glucose metabolism. However several studies suggest that lactate secretion by cancer cells is not a random event. The emphasis upon cancer cell's increased glycolytic rate has unfortunately led to the idea that cancer cells subsist upon glucose alone with lactate being overlooked as a potential fuel, but instead identified only as an acidic promoter of metastasis (Nakajima & Van Houten 2013). Another layer of complexity in mapping tumour metabolism is added to classic understanding of the Warburg effect by the consideration of lactate as a metabolic fuel. Sonveaux et al. (2008) propose a model of 'metabolic symbiosis' amongst cells within the context of larger advanced-stage tumour environments and provide interesting interpretations on the function of different players in lactate metabolism. This idea reviewed by (Semenza 2008) and depicted in Figure 1.3 showing the lactate dehydrogenase enzymes and the lactate transporters monocarboxylate transporter (MCT) 1 and 4. When tumours outgrow their supporting vasculature, areas in the tumour mass that are less oxygenated emerge, giving rise to a heterogeneous metabolic profile in cells of the same tumour (Sonveaux et al. 2008), adapted specifically to their unique setting. The different cells in tumours harbour different properties or metabolic profiles that result from adaptive signalling in response to continued exposure to hypoxic environmental stress (Curry et al. 2013).

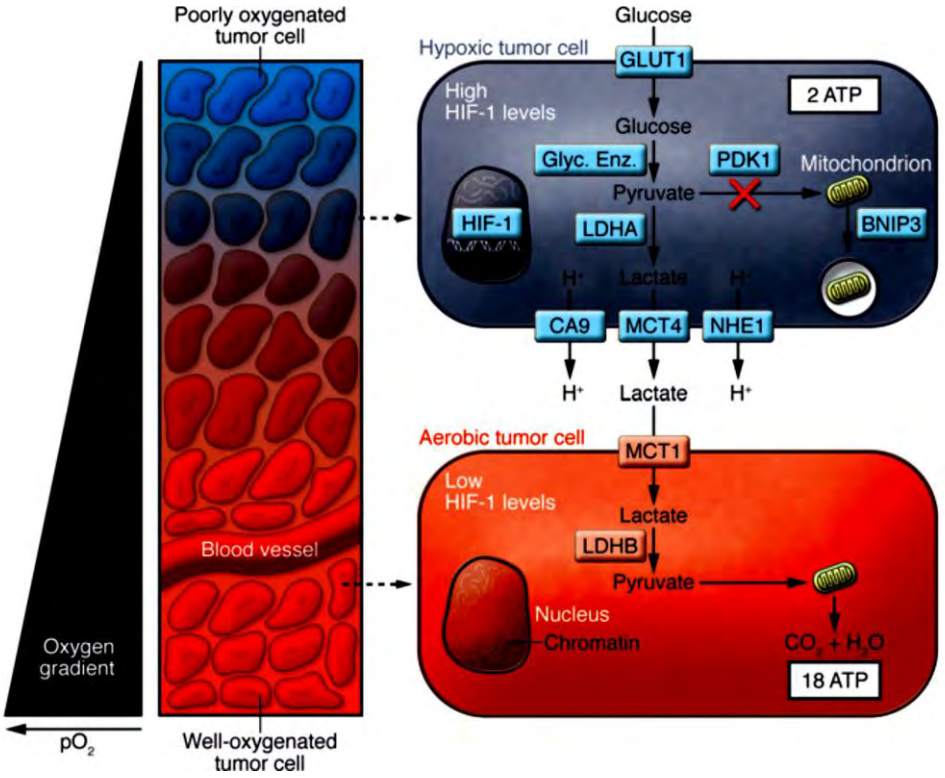

Figure 1.3. Intratumoral hypoxia and metabolic symbiosis. Tumours are characterized by gradients of O_2 levels, based on the distance of tumour cells from a functional blood vessel. Tumour cells surrounding the blood vessel are well oxygenated, whereas those more distant are poorly oxygenated and express high levels of HIF-1. HIF-1 induces the expression of proteins that increase: uptake of glucose (e.g., glucose transporter 1 [GLUT1]); conversion of glucose to pyruvate (e.g., glycolytic enzymes); generation of lactate and H+ (e.g., LDHA); and efflux of these molecules out of the cell (e.g., carbonic anhydrase IX [CA9], sodium-hydrogen exchanger 1 [NHE1], MCT4). Two moles of lactate are produced for each mole of glucose consumed by the hypoxic cell. This increase in glycolytic metabolism is associated with reduced substrate delivery to the mitochondria (through the action of pyruvate dehydrogenase kinase 1, PDK1) and reduced mitochondrial mass (as a result of autophagy triggered by BNIP3). Aerobic tumour cells express proteins that allow them to take up lactate (e.g., MCT1) and use it (e.g., Lactate dehydrogenase B), in the presence of O2, as their principal substrate for mitochondrial oxidative phosphorylation. From (Semenza 2013)

The idea of metabolic symbiosis between hypoxic and aerobic tumour cells is illustrated in Figure 1.3, where hypoxic tumour cells primarily use glucose for glycolytic energy production and release lactic acid, creating a lactate gradient that is in parallel with the oxygen gradient within the tumour (Sonveaux et al. 2008; Semenza 2008; Feron 2009). By contrast, in oxygenated tumour cells, lactate becomes the prominent substrate that fuels the oxidative

metabolism in these aerobic cells. This gives rise to symbiosis in which glycolytic and oxidative tumour cells mutually regulate their access to energy metabolites (Sonveaux et al. 2008; Semenza 2008; Feron 2009; Whitaker-Menezes et al. 2011; Curry et al. 2013).

Metabolic symbiosis is somewhat a controversial idea as it provides an alternative interpretation of Warburg's observation by considering the heterogeneity of tumours. The Warburg effect, as it is traditionally reflected and interpreted, does not account for the metabolic diversity that has been observed amongst cancer cells within a tumour, nor the influences that might direct such diversity (Nakajima & Van Houten 2013). Modern tools have shown that oncogenes, variable hypoxia levels, and the utilization of different carbon sources affect tumour evolution, while a more orthodox view on the Warburg effect points towards cancer cells displaying a single metabolic phenotype, which as discussed earlier is summed up as 'aerobic glycolysis'. The metabolic symbiosis concept makes a compelling case for another way of looking at tumour metabolism by considering the role of lactate and other metabolites in the tumour microenvironment, thereby suggesting that cells within the tumour may display diverse metabolic profiles.

1.4.2 Glycogen metabolism

Glycogen is a readily mobilized storage form of glucose. It is a very large, branched polymer of glucose residues (Figure 1.5) that can be broken down to yield glucose molecules when energy is needed. Most of the glucose residues in glycogen are linked by α-1,4-glycosidic bonds. Branches that occur at about every tenth residue are created by α-1,6-glycosidic bonds (Berg et al. 2002).

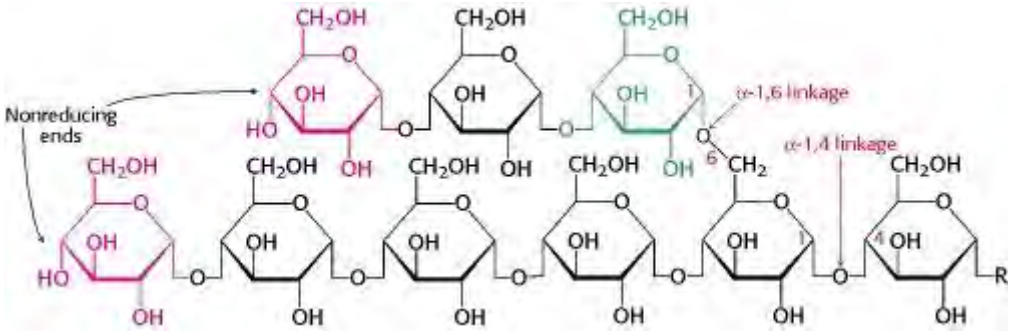

Figure 1.5. Structure of glycogen
The diagram shows of two outer branches of a glycogen molecule, the residues at the non-reducing ends are shown in pink and residue that starts a branch is shown in green. The rest of the glycogen molecule is represented by R. From (Berg et al. 2002)

The general physiological role of glycogen is to serve as a buffer for the maintenance of blood glucose levels. Glucose from glycogen is readily mobilized and thereby serves as a source of energy for sudden, strenuous activity. Unlike energy stored in fatty acids, the glucose released from glycogen can provide energy in the absence of oxygen and hence would be an ideal source during anaerobic conditions (Berg et al. 2002). The storage of glycogen is generally tissue specific, being isolated to liver, skeletal muscle tissue and brain tissue (Brown & Ransom 2007; Obel et al. 2012). Rousset and co-workers investigated glycogen storage in a panel of fifty eight human cancer cell lines and detected varying levels in a large majority of these cells (Rousset et al. 1981). While this discovery was made a while ago, only recently did the significance of glycogen accumulation in cancer cells become a subject for investigation.

Figure 1.6 depicts the key enzymes, substrates and regulatory components involved in glycogen breakdown and synthesis. Synthesis and breakdown of glycogen involves the activity of several enzymes and regulatory proteins. Among these, glycogen synthase (GS) and glycogen phosphorylase (GP) catalyse the key steps of synthesis and degradation, respectively (Berg et al. 2002).

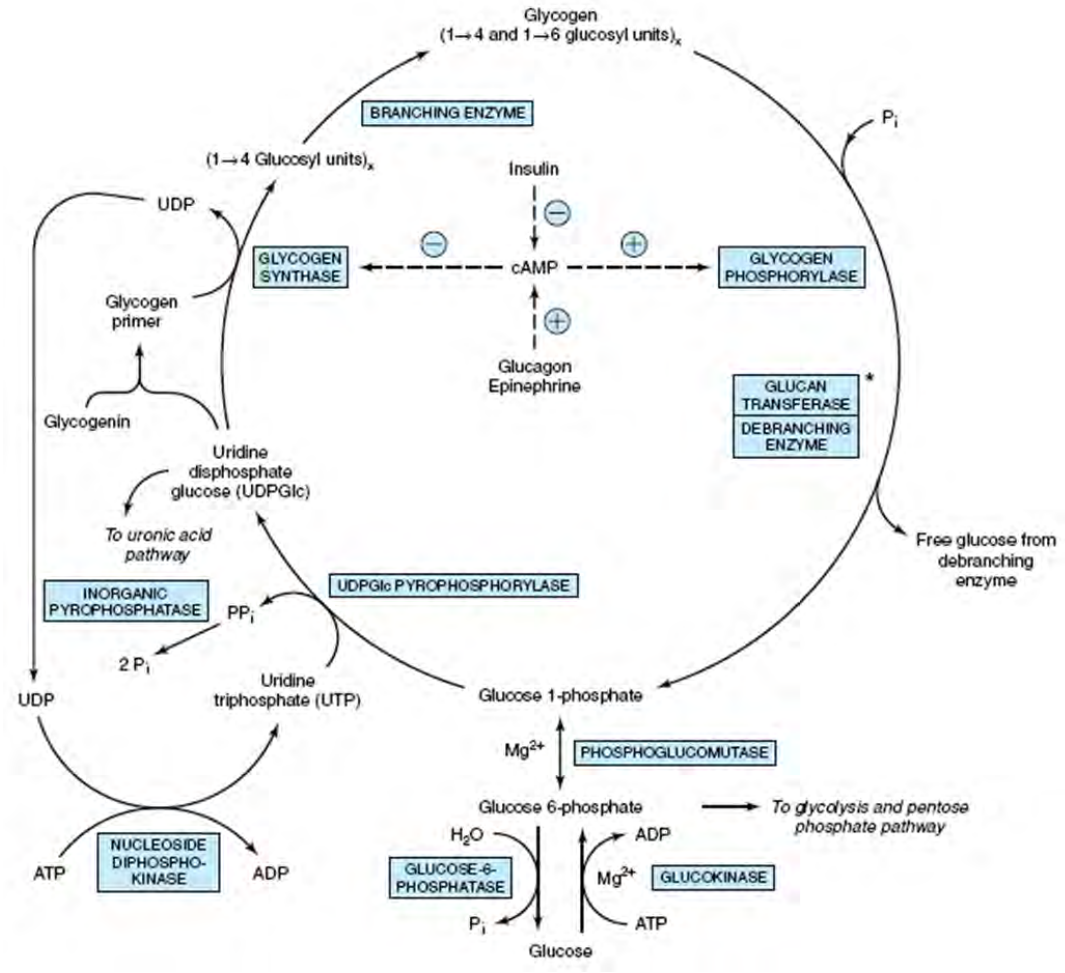

Figure 1.6. Schematic illustration of pathways in glycogen metabolism, in blue boxes; the enzymes involved in each reaction (represented as the black arrows) and the substrates, co-factors and products; in black writing. The main regulatory points for glycogen synthesis and breakdown are at the enzymes, glycogen synthase and glycogen phosphorylase respectively which are regulated by hormones; Insulin (which activates the synthesis of the glycogen macromolecule) and Glucagon and Epinephrine which stimulate the release of the glycogen stores in the form of glucose-1-phosphate (G1P) which gets converted to glucose-6-phosphate (G6P) by the action of Phosphoglucomutase 1 (PGM1). The G6P can then be channelled into the glycolytic pathway or pentose phosphate pathway or converted into glucose for gluconeogenesis in gluconeogenic tissues by the action of glucose-6-phosphatase.

The role of glycogen in cancer has been studied particularly as it relates to hypoxic tumour environments. Recent studies have shown that glycogen accumulation occurs in response to tumour stress environments such as treatment with anti-angiogenic therapies such as bevacizumab (a VEGF inhibitor that's routinely administered in the clinic to cut off tumour

blood supply and results in significantly reduced oxygen delivery to the tumour site), as well as exposure to hypoxia (Favaro et al. 2012; Pescador et al. 2010; Pelletier et al. 2012). Hypoxia leads to the overexpression of key enzymes that are involved in glycogen metabolism, promoting storage upon prolonged exposure. The detail regarding these mechanisms behind glycogen regulation as it relates to the cancer setting will be discussed further in Chapter 4.

1.4.3 The pentose phosphate pathway

Upon entry into cells, glucose is phosphorylated to form glucose-6-phosphate (G6P) by hexokinases. G6P then becomes a substrate for glycolysis, glycogen synthesis as well as the pentose-phosphate pathway (PPP). The PPP is essential for cancer cell survival because through a series of reactions in this pathway, ribose-5-phosphate (R5P) is generated. R5P is a precursor for nucleotide synthesis and the formation of the reducing equivalent NADPH, which is needed for cell proliferation, scavenging of ROS and lipid synthesis (Lu et al. 2013; Icard & Lincet 2012; Santos & Schulze 2012). Lipids are used for the construction of cell membranes and for energy storage, while nucleotides serve as substrates for continuous DNA replication.

The PPP has two branches, an oxidative and a non-oxidative arm and occurs exclusively in the cytoplasm (Figure 1.7). In the oxidative phase, G6P is converted to 6-phosphoglucono-δ-lactone by glucose- 6-phosphate dehydrogenase (G6PD). 6-phosphoglucono-δ-lactone is then hydrolysed to give rise to 6-phosphogluconate, which is then oxidatively decarboxylated by 6-phosphogluconate dehydrogenase (6PGD) to yield ribulose 5-phosphate (R5P). During the oxidative phase, NADP+ participates as the electron acceptor in the two oxidative reactions, which are the first and the last reactions. Hence, one molecule of glucose oxidized and

metabolized by the PPP can yield net output of two molecules of NADPH. NADPH plays a pivotal role in both reductive nucleotide biosynthesis and protecting cells from ROS, which are often the main cause of damage to macromolecules and ultimately leading to cell death (Jiang et al. 2014). The production of R5P, is generated from six-carbon glucose during the non-oxidative phase of the PPP. R5P can be reversibly converted into the glycolytic intermediates glyceraldehyde 3-phosphate (G3P) and F6P by TKT and transaldolase. Glycolysis and gluconeogenesis coordinate with the PPP to control the cellular production of NADPH and R5P and to determine which phase of the PPP is activated (Jiang et al. 2014).

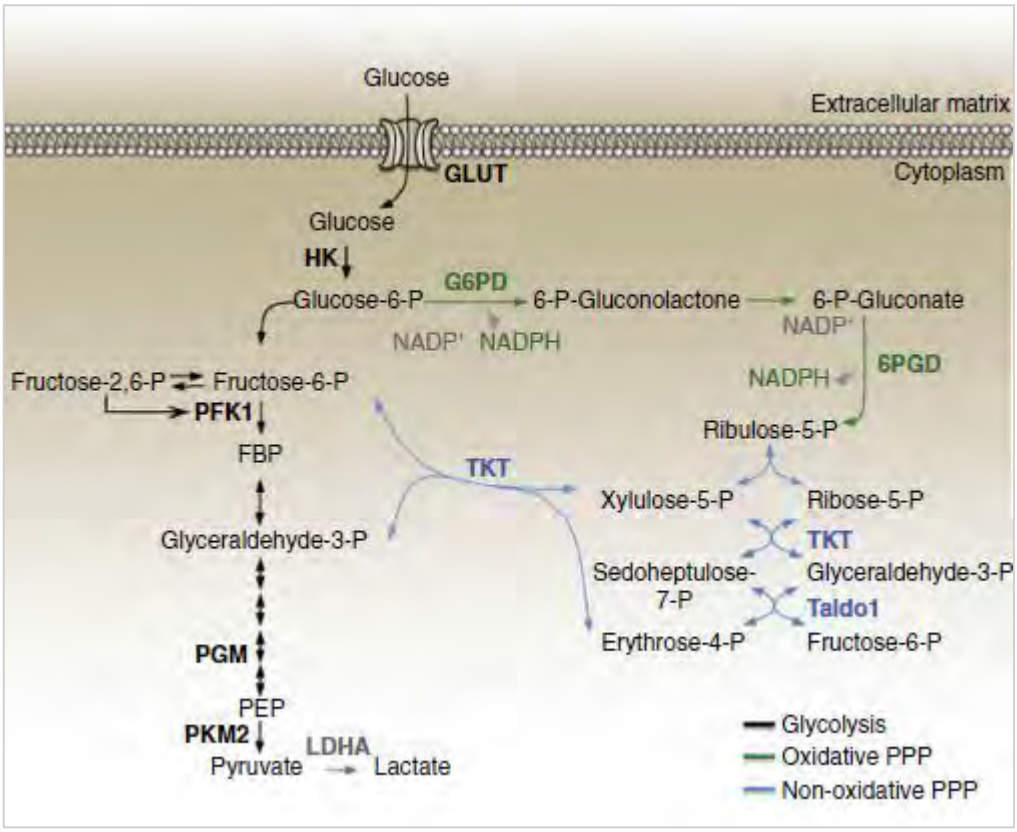

Figure 1.7. Schematic representation of the Pentose Phosphate Pathway and glycolysis is shown. The oxidative branch of the PPP yields NADPH that can be used in biosynthetic reactions for nucleotides, lipids and antioxidant defence. The reversible non-oxidative branch produces ribose-5-phosphate from the oxidative branch as well as glycolytic intermediates. Solid black arrows represent glycolytic flux, green arrows represent the oxidative branch of the PPP, and light blue arrows represent the multi-step processes of the non-oxidative branch of the PPP. For clarity, each component of the metabolic process has been abbreviated. PPP, pentose phosphate pathway; G6PD, glucose- 6-phosphate dehydrogenase; 6PGD, 6-phosphogluconate dehydrogenase; TKT, transketolase; Taldo1 (TAL), transaldolase; HK, hexokinase; GLUT, glucose transporters; PFK1, phosphofructokinse-1; PGM, Phosphoglycerate mutase; PKM2, pyruvate kinase (PK)-M2; LDHA, lactate dehydrogenase A; FBP, fructose-1,6-bisphosphate; PEP, phosphoenolpyruvate. From (Jiang et al. 2014)

In cancer, the PPP has received considerable attention in research efforts of recent years. Ongoing studies suggest that the PPP is tightly and meticulously regulated in cells and that its abnormal regulation leads to uncontrolled biosynthesis (Jiang et al. 2014). As the first and rate-limiting enzyme and control site in the oxidative branch of the PPP, G6PD has recently received much interest. The activity of G6PD is mediated by various signals, and it acts as a

sensor of cellular NADP+ levels. Increased NADP+ activates G6PD by competing with NADPH for binding to this enzyme. Therefore, changes in the cellular NADP+/NADPH ratio by oxidative stress or other metabolic reprogramming can be expected to impact the PPP flux through G6PD (Jiang et al. 2014). G6PD plays an important role in supporting cancer growth by supplying NADPH for maintenance of the intracellular redox status of cancer cells. Studies have also shown that aberrant transcription factor activity influence G6PD expression and activity. Tumour suppressors such as p53 have been shown to inhibit both expression and activity of G6PD, and as p53 is one of the most frequently mutated tumour suppressors, in many cancers, G6PD function is consequently enhanced (Jiang 2011). Interestingly, G6PD has also been shown to be up-regulated by hypoxia in some cancer cells (Gao et al. 2004).

The non-oxidative pentose phosphate pathway, which allows six-carbon glucose conversion to five-carbon ribose for DNA or RNA synthesis, is of utmost importance for the proliferation process and accounts for more than 85% of the ribose recovered in tumour nucleic acids (Liu et al. 2010). The two enzymes, transketolase (TKT) and transaldolase are the main regulatory points in this branch of the PPP. Three human transketolase genes have been identified, namely: TKT, transketolase-like 1 gene (TKTL1) and TKTL2 (Langbein et al. 2006; Földi et al. 2007). TKTL1, a mutated transketolase and not TKT and TKTL2 was shown to be overexpressed in a number of cancers. Some examples are; in urothelial, colorectal and non-small cell lung cancers where TKTL1 overexpression has been associated with poor patient outcomes (Langbein et al. 2006). The Transaldolase (TAL) enzyme on the other hand, has been shown to be overexpressed in colorectal cancer (Ma et al. 2009) and was also found to associate with metastatic hepatocellular carcinoma (Wang et al. 2011). The overexpression of both TKTL1 and TAL yields high levels of R5P in cancer cells and interestingly, R5P has been identified in metabolic profiling of cancer cells as one of the most strongly up-regulated metabolites in

hypoxia (Frezza et al. 2011; Masson & Ratcliffe 2014). The correlation between overexpression of these PPP enzymes and their association with tumour aggressiveness points to their role in supporting carcinogenesis.

1.5 Oncogenes and transcription factors that drive metabolic reprogramming

The different hallmark capabilities of cancer cells are all hypothesized to depend upon uncontrolled transcription, and deregulated cellular energetics is no exception (Darnell 2002). The altered metabolic processes of these cells are a result of oncogene driven mechanisms and dysregulation of transcription factors that may direct and promote cell proliferation. Oncogenes have also been shown to promote glycolysis in the tumour microenvironment (Zeng et al. 2014). The majority of glycolytic enzymes contain evolutionarily conserved, consensus Myc-binding sites within their regulatory DNA sequences. The Myc oncogene is known to transactivate the expression of LDH-A, which converts pyruvate to lactate thereby promoting glycolysis under aerobic conditions (Shim et al. 1997; Feron 2009). On the other hand the serine/threonine kinase AKT which falls into the category of oncogenes that promote cancer cell survival has been shown to exert direct effects on cancer cell metabolism rendering cells to be reliant on aerobic glycolysis for survival, independent of HIF activities (Elstrom et al. 2004).

The tumour suppressor, p53 has previously been shown to negatively regulate the expression of Phosphoglycerate Mutase, one of the enzymes required for glycolysis (Kondoh et al. 2005). p53 was shown to also influence glycolytic flux by repressing the expression of glucose transporters; GLUT1 and GLUT4, limiting the entry of glucose into cells (Puzio-Kuter 2011). As discussed previously, p53 inactivates the enzyme G6PD and thereby inhibits the pentose

phosphate pathway, adversely affecting the cells' ability to cope with oxidative stress. In cancer however, the p53 function is often inhibited and or the protein itself mutated (Muller et al. 2011) allowing cancer cells to escape this negative regulation.

The above represent only a few examples of oncogenes and transcription factors known to play a role in promoting and/or preventing carcinogenesis via metabolic reprogramming.

Recently the E2F transcription factors have been associated with changes in metabolic regulation (Clem & Chesney 2012; Blanchet et al. 2013). The E2F family of transcription factors has been known to play a key role in the control of the cell cycle as well as DNA replication in association with the retinoblastoma (RB) tumour suppressor (Giacinti & Giordano 2006; Macaluso et al. 2005).

1.5.1 The role of hypoxia and HIF in the regulation of cancer cell metabolism

An underlying theme that emerges from investigations and discussions on reprogrammed cancer cell metabolism is the role played by tumour hypoxia. The unique biological architecture of solid tumours and the tumour microenvironment indicates the diverse range of metabolic properties of different cells within the tumour landscape. The disparity in the oxygen distribution across the tumour mass, due to insufficient and impaired tumour vasculature often gives rise to hypoxic regions within the tumour. Cancer cells in these regions have been known to present a clinical challenge because they are often more resistant to radiotherapy and many chemotherapeutic drugs than cancer cells in normoxic regions (Wilson & Hay 2011; Horsman et al. 2012; Tong et al. 2013; Zhao et al. 2013). Hypoxic cancer cells are therefore thought to increase the probability of tumour recurrence and this is possibly a result of their altered metabolic prolife (Flamant et al. 2012). Hypoxia-induced

metabolic changes can be largely attributed to the function of the transcription factor called Hypoxia-Inducible factor, HIF. HIF plays a major role in multiple aspects of cellular metabolism (Figure 1.8).

HIF is a key regulator in the intracellular response to tumour hypoxia, and to date, this transcription factor been shown to regulate more than a hundred downstream targets that have been shown to participate tumour metastasis, angiogenesis, energy metabolism, cell differentiation and apoptosis (Liu et al. 2012; Liao et al. 2009).

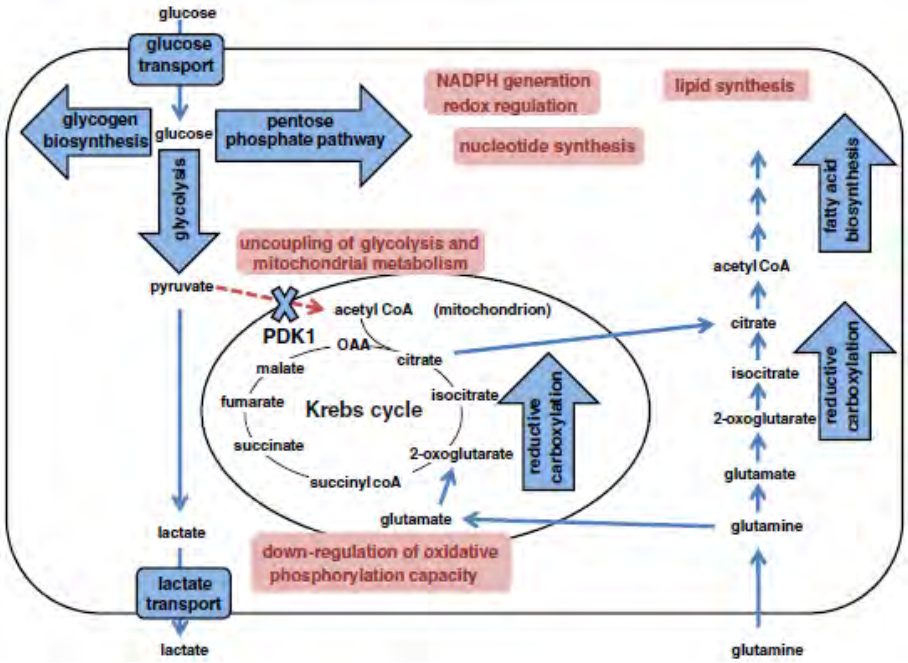

Figure 1.8. Schematic illustrating the action of HIF on multiple aspects of cellular metabolism. HIF plays a major role in glucose metabolism, facilitating glucose uptake in cancer cells while also enhancing the activity of glycolytic enzymes and thereby promoting lactate production. On the other hand HIF also influences glycogen biosynthesis by regulating the major enzymes involved glycogen metabolism. HIF promotes nucleotide synthesis and redox regulation through the functions of the PPP by positively regulating the expression of G6PD in hypoxia. The uncoupling of glycolysis to mitochondrial respiration is due to the actions of PDK1, a HIF target gene, represented by the red-dashed arrow. (Icard & Lincet 2012). HIF function is generally associated with macromolecular biosynthesis (like lipid biosynthesis) to support proliferation under hypoxic conditions. The blue arrows represent flux of the metabolic processes stimulated by HIF function i.e. glucose metabolism and flux (glycolysis, glycogen synthesis, the PPP for redox balance in the cells), glutaminolysis which supports macromolecular synthesis (Fatty acid synthesis for the biosynthesis of lipids). From (Masson & Ratcliffe 2014)

1.6 Identifying targets in cancer metabolism

Analysis of gene expression patterns together with the biological characterization of differentially expressed genes that drive carcinogenesis may provide a means to identify druggable targets, where the 'druggability' of a molecular target e.g. protein refers to its potential to be modulated by small and deliverable, drug-like molecules. In the same way as antibiotics target the biosynthetic processes that are unique to microorganisms, the possibility of selectively targeting the biosynthetic and energy generating processes of cancer cells holds promise as a strategy for improving cancer therapy (Vander Heiden 2011). The therapeutic potential of targeting metabolic adaptation in tumours, stems from the understanding that altered metabolism is a key consequence of important genetic drivers of cancer. However, the molecular mechanisms by which targeting metabolism could impair chemo-resistance are not fully understood and warrant further investigation (Zhao et al. 2013).

Earlier in section 1.2, the usefulness of targeting cancer molecular capabilities (hallmarks) to halt or abolish uncontrolled proliferation was discussed. Traditional approaches involving the treatment of cancer cells based on a singular druggable entity has seen limited success. Understanding the molecular changes cancer undergoes has led to approaches using drugs that target different cellular pathways. Targeting multiple pathways is discussed by (Tang et al. 2013) who states that, "a recent trend in drug development is to identify drug combinations or multi-target agents that effectively modify multiple nodes of disease-associated networks". Hanahan (2014), on 'rethinking the war on cancer' makes a compelling case for a combined onslaught on multiple hallmarks and also argues that strategically co-targeting interdependent hallmarks could for example look like co-inhibiting tumour angiogenesis, together with preventing invasion and metastasis or coupled to disruption of

cancer energetics and metabolism. Another option could be to target proliferative signalling along with the reactivation of disabled mechanisms for programmed cell death and growth suppression, as well as disruption of cancer-cell metabolism (Hanahan 2014). Hanahan (2014), also notes that interim steps more realistically will involve even fewer (pairwise) combinatorial attacks to test the value and feasibility of such treatment methods.

Combining current chemotherapeutic agents with targeted disruption of deregulated cellular metabolism represents a promising strategy to overcome drug resistance and improve the efficacy of current chemotherapeutic agents in cancer patients (Zhao et al. 2013). This will require a thorough understanding of cancer cell metabolism in order to select the most preferential combinations with minimum toxicity.

1.6.1 Phosphoglucomutase 1 (PGM 1) in cancer

A microarray study performed in our laboratory using RNA isolated from a cohort of non-cancerous and advanced-stage cervical cancer patients revealed a group of genes involved in glucose metabolism as differentially expressed (van der Watt, PhD thesis, 2009), within the group of metabolic enzymes shown to have altered expression in cancer patient tissue, Phosphoglucomutase 1 (PGM1) was identified. PGM1 is an evolutionarily conserved enzyme that regulates one of the key metabolic carbohydrate trafficking points in prokaryotic and eukaryotic organisms (Gururaj et al. 2004). PGM1 belongs to a family of phosphohexose mutases. Several phosphoglucomutase isoforms have been identified where PGM1 accounts for more than 90% of total PGM activity (Ravazzolo et al. 1985). While PGM2 is known to function mainly as a phosphopentose mutase, PGM3 was found to play a role in the

regulation of sulforphane (SFN)-induced apoptosis in prostate cancer cells and showed potential as a molecular target for prostate cancer therapy (Lee et al. 2010).

As a phosphotransferase, PGM1 catalyses the reversible isomerization of glucose-1-phosphate to glucose-6-phosphate (with magnesium as a co-factor). G6P becomes a precursor for glycolysis and the pentose phosphate pathway, thereby placing PGM1 at crossroads of metabolic processes that have been shown to have increased utility in cancer; glycolysis, glycogen metabolism and the pentose phosphate pathway.

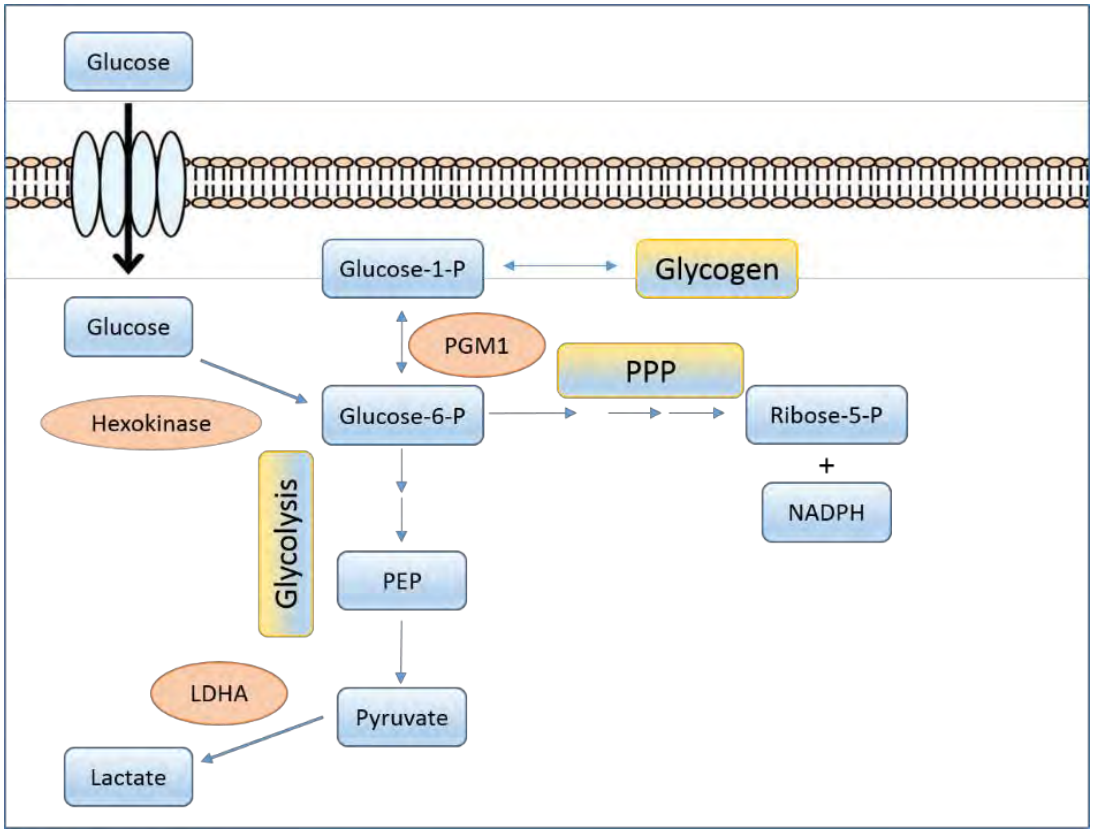

Figure 1.9. PGM1 in relation to the pathways involved in glucose metabolism. PGM1 sits at the crossroads of three metabolic pathways, namely: glycolysis, the pentose phosphate pathway and glycogen metabolism. The arrows represent direction of glucose conversion to different substrates in the different pathways. In glycolysis, glucose is converted to pyruvate then to lactate, in glycogen metabolism G6P is converted to G1P, a precursor in glycogen synthesis and in the pentose phosphate pathway G6P is converted to R5P, a precursor for nucleotide synthesis and NADPH, the intracellular antioxidant.

The p21 protein (Cdc42/RAC)-activated kinase-1 (PAK-1) has been shown to phosphorylate and regulate the enzymatic activation of PGM1 in breast cancer cells (Gururaj et al. 2004) and recently (Bae et al. 2014) showed that the C-terminal threonine residues of PGM1 are critical for its stability and activity. Research in recent years has shown that PGM1 expression is significantly increased in response to hypoxia (Pelletier et al. 2012), however the mechanisms that lead to this response are not clear.

The deficiency of PGM1 was shown to present in a rare disease classified under glycogen storage disorders and designated as glycogenosis type XIV (Stojkovic et al. 2009; Lee et al. 2014; Ondruskova et al. 2014). Recent evidence has shown PGM1 deficiency as a mixed-type congenital disorder of protein N- glycosylation which is characterized by the presence of a bifid uvula at birth and may serve an early clinical clue to the presence of the syndrome (Tegtmeyer et al. 2015). No studies to date have described the effects of PGM1 overexpression although association of PGM1 with cancer has surfaced in recent work. Little is known about its expression and functional relevance in cancer. This study seeks to investigate PGM1 expression, regulation and role in cancer biology.

1.7 Project aims

This study aimed to determine the role of PGM1 in cancer. The objectives were:

1. To investigate PGM1 expression of in cancer, transformed and non-cancer cells
2. To investigate transcriptional regulatory mechanisms associated with PGM1 expression in cancer cells.
3. To determine the functional significance of PGM1 in cancer by inhibiting its expression and investigating effects on cancer biology and metabolism.

CHAPTER 2

PGM1 EXPRESSION IN CANCER AND TRANSFORMED CELLS

2.1 INTRODUCTION

Carcinogenesis results from a multi-step process that is often driven by inherent and acquired changes to the expression profile of genes in signalling pathways (Emmert-Streib & Glazko 2011). The analysis of gene expression patterns in cancer research is routinely and extensively used in the mining for novel therapeutic targets and diagnostic markers. This approach employs various and diverse techniques ranging from characterising single genes to high-throughput methods that constitute multiple gene analysis of transcriptional and proteomic changes that take place across different cohorts of cells, tissue types and disease states. Data from these techniques is used to provide insight into mechanisms and pathways that underpin cancer development and sustain progression. The main objective therefore in investigating gene expression patterns is to identify and exploit an underlying finger-print in cancer cohorts that is unique to cancer cells and distinctly different from the normal phenotype, to aid in the discovery of novel selective treatment strategies for cancer.

Previously, gene profiling studies to investigate changes that associate with cervical cancer development in a cohort of advanced-stage cervical cancer patient specimens compared to normal cervical epithelial biopsies was conducted. The data revealed different functional groups of genes to have altered expression in cancer including; nuclear transport, cell cycle, proteasomal degradation, MAPK signalling pathways, cell adhesion and cytoskeletal organization, as well as metabolism (van der Watt 2009; Ward et al. 2011). Amongst these functional groups that were investigated, several genes involved in cellular metabolism were found to have elevated expression in the cancer patients (van der Watt, PhD thesis, 2009).

Pyruvate kinase M2 (PKM2) which catalyses the dephosphorylation of Phosphoenol pyruvate (PEP) to produce pyruvate and ATP showed increased mRNA expression in the microarray data. PKM2 is specifically overexpressed in cancer cells and its characterization has led to investigating the potential of small molecule inhibitors and activators, targeted at this enzyme as cancer therapeutics (Wong et al. 2013). Other glycolytic genes such as Phosphoglucose isomerase (PGI), Enolase 1 (ENO 1), Phosphoglycerate kinase 1 (PGK1) and Lactate dehydrogenase A (LDHA) were also identified with elevated expression and have previously been shown to have increased expression in cancer cells and tissues (Tsutsumi et al. 2009; Capello et al. 2011; Chen et al. 2003; Ahmad et al. 2013; Billiard et al. 2013). Studies have gone further to investigate the potential of these enzymes in the selective targeting of cancer cells as well as assisting in the development of novel prognostic and diagnostic tools against cancer (Wong et al. 2013; Song et al. 2014; Chen et al. 2003; Miao et al. 2013).

Genes involved in glucose metabolism although not directly participating in glycolysis that showed altered expression by microarray analysis include Glycogen Phosphorylase, muscle isoform (PYGL) and Phosphoglucomutase 1 (PGM1). PYGL has been shown to have increased expression in cancer and is the main enzyme required for glycogen breakdown or mobilization in cells (Favaro et al. 2012). While there are multiple studies that have focussed on the association of some of the above mentioned metabolic enzymes with cancer, very little is known regarding PGM1 in cancer.

PGM1 catalyses the preliminary step in glycogen synthesis producing glucose-1-phosphate (G1p) from glucose-6-phophate (G6P) which may be processed further for the synthesis of the large glycogen polymer. PGM1 also catalyses the last step in the glycogen breakdown

process which involves the conversion of G1P into G6P, an intermediate that can be channelled to the glycolytic as well as the pentose phosphate pathways.

In this study we aimed to investigate PGM1 expression levels in cervical cancer patient material and cancer cell lines of different tissue origin.

2.2 RESULTS

2.2.1 Expression of metabolic enzymes PGK1, ENO1 and PGM1 in cancer patient tissue.

With most high throughput methods, single target analysis is required to confirm and validate the accuracy of the general, high-throughput screening (Rajeevan et al. 2001; Allison et al. 2006; Morey et al. 2006). To validate a subset of genes involved in glucose management that showed upregulation by microarray analysis (van der Watt et al, PhD thesis, 2009) quantitative real time PCR was used. qRTPCR results confirmed a significant increase in the expression of the glycolytic genes ENO 1, PGK1 (Figure 2.1 A and B) as well as upregulation of PGM1 expression (Figure 2.1 C). As much research has been done on ENO1 and PGK1 in cancer and very little is known on PGM1, our study focussed on PGM1 as a potential novel metabolic gene, with altered expression and regulation in cancer.

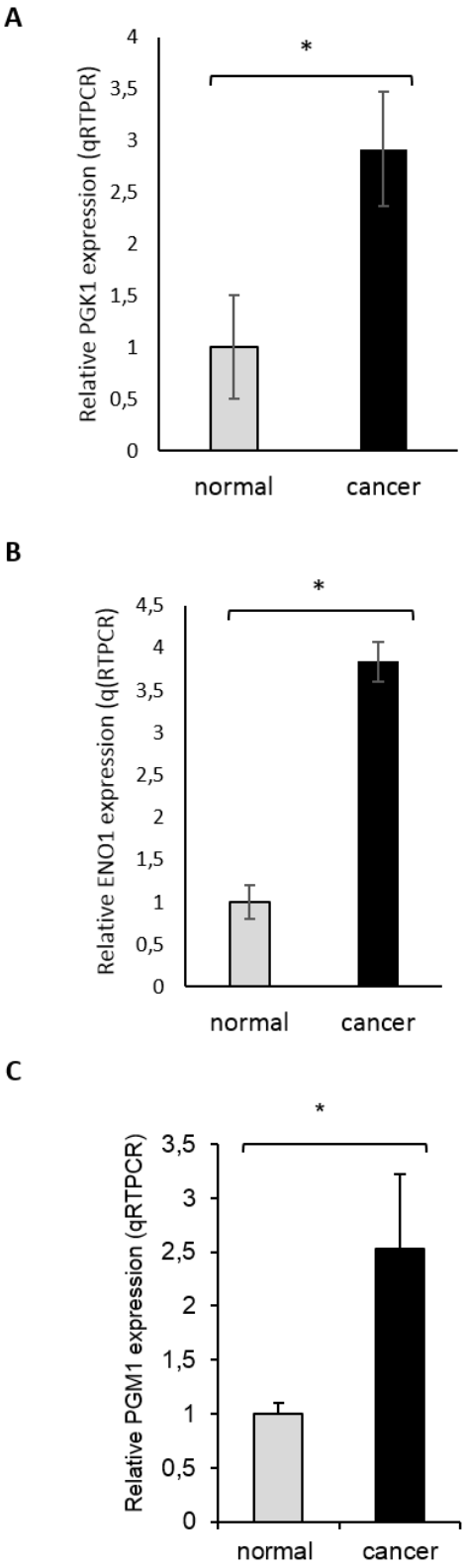

Figure 2.2. PGK1, Enolase 1 and PGM1 mRNA are differentially expressed in cervical cancer. qRT-PCR data showing **A.** PGK1, **B.** Enolase 1 and **C.** PGM1 to be significantly increased in cervical cancer tissue compared to non-cancerous patient tissue. Data, normalized to β-Glucuronidase (Gus B) and Cyclophilin D as housekeeping genes, analysed using the $2^{-\Delta\Delta Ct}$ Method, non-cancers, n=8, cancer, n=13. * $p<0.05$.

2.2.2 PGM1 protein expression in cancer cell lines of different tissue origin

Having established that PGM1 mRNA expression was elevated in cervical cancer patient material, we next investigated its protein expression by western blot analysis using a panel of cervical cancer cell lines (HPV positive, CaSki, HeLa, Me180, SiHa, MS751 and HPV negative C33A cells) and a normal primary epithelial cervical cell line (HCX). Our results show higher levels of PGM1 protein in the majority of cervical cancer cells compared to HCX cells (Figure 2.2A and B).

To investigate whether high PGM1 expression was unique to cervical cancer or a feature of cancer of different origins, we used western blot analysis and immunofluorescence to evaluate PGM1 expression in cancer cell lines of different tissue origins including; breast and oesophageal cancer cell lines. PGM1 protein levels were found to be higher in four of the six oesophageal squamous cell carcinomas cell lines compared to the immortalized normal oesophageal epithelial cell line (EPC2) (Figure 2.3 A and B). Similarly, higher PGM1 expression was observed in (MCF7 and MDA-MB-231 breast cancer cells) compared to the non-tumourigenic breast epithelial cell line (MCF12A) (Figure 2.3 C and D).

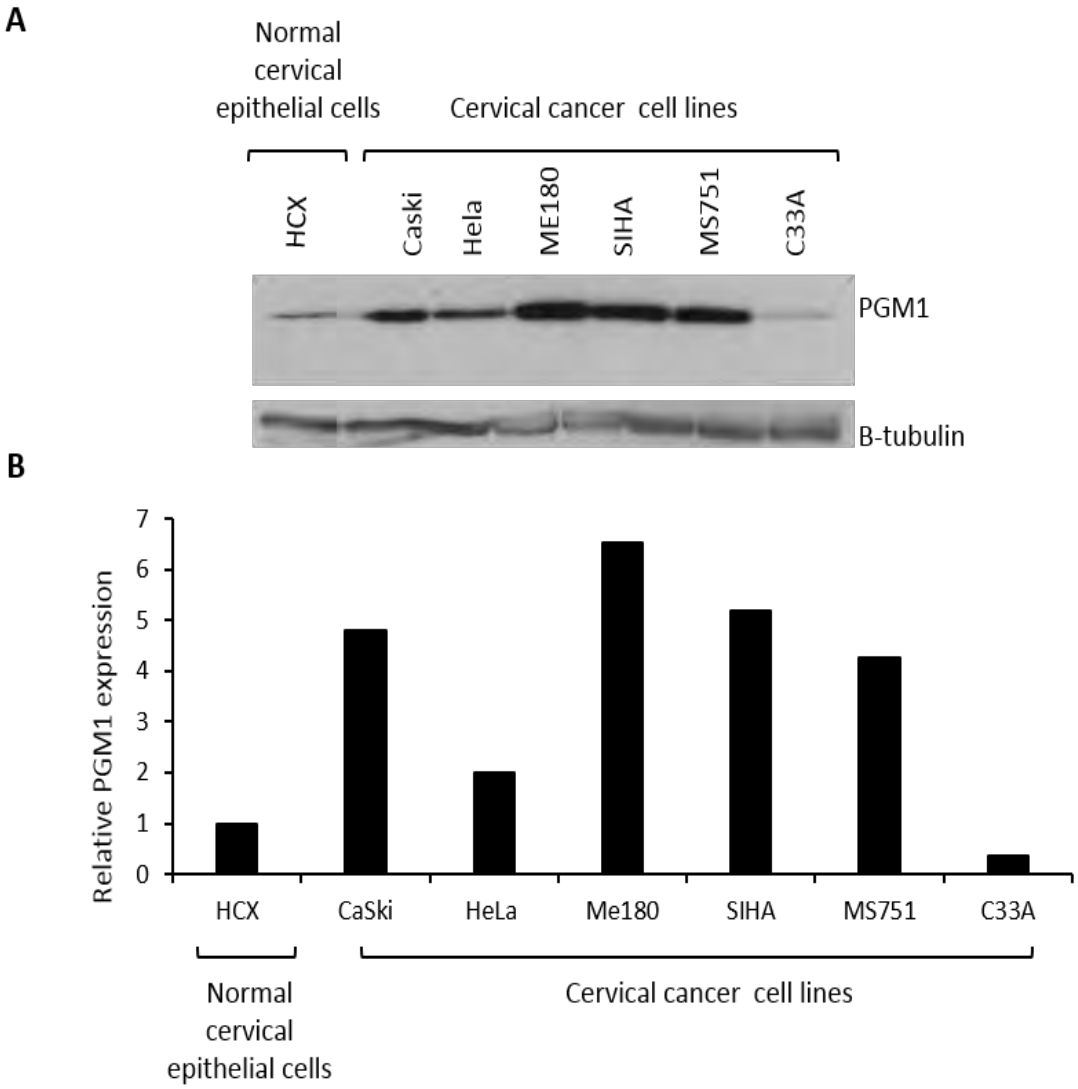

Figure 2.2. Increased PGM1 protein expression in cervical cancer cell lines. **A.** Western blot for PGM1 protein expression in normal cervical epithelial cells (HCX) and a panel of six cervical cancer cell lines, CaSki, HeLa, ME180, SIHA, MS751 and C33A. β-tubulin was used as a loading control. **B.** The histogram is a quantitative representation of PGM1 protein expression relative to β-tubulin using Image J Software. Results shown are representative of experiments done at least two independent times.

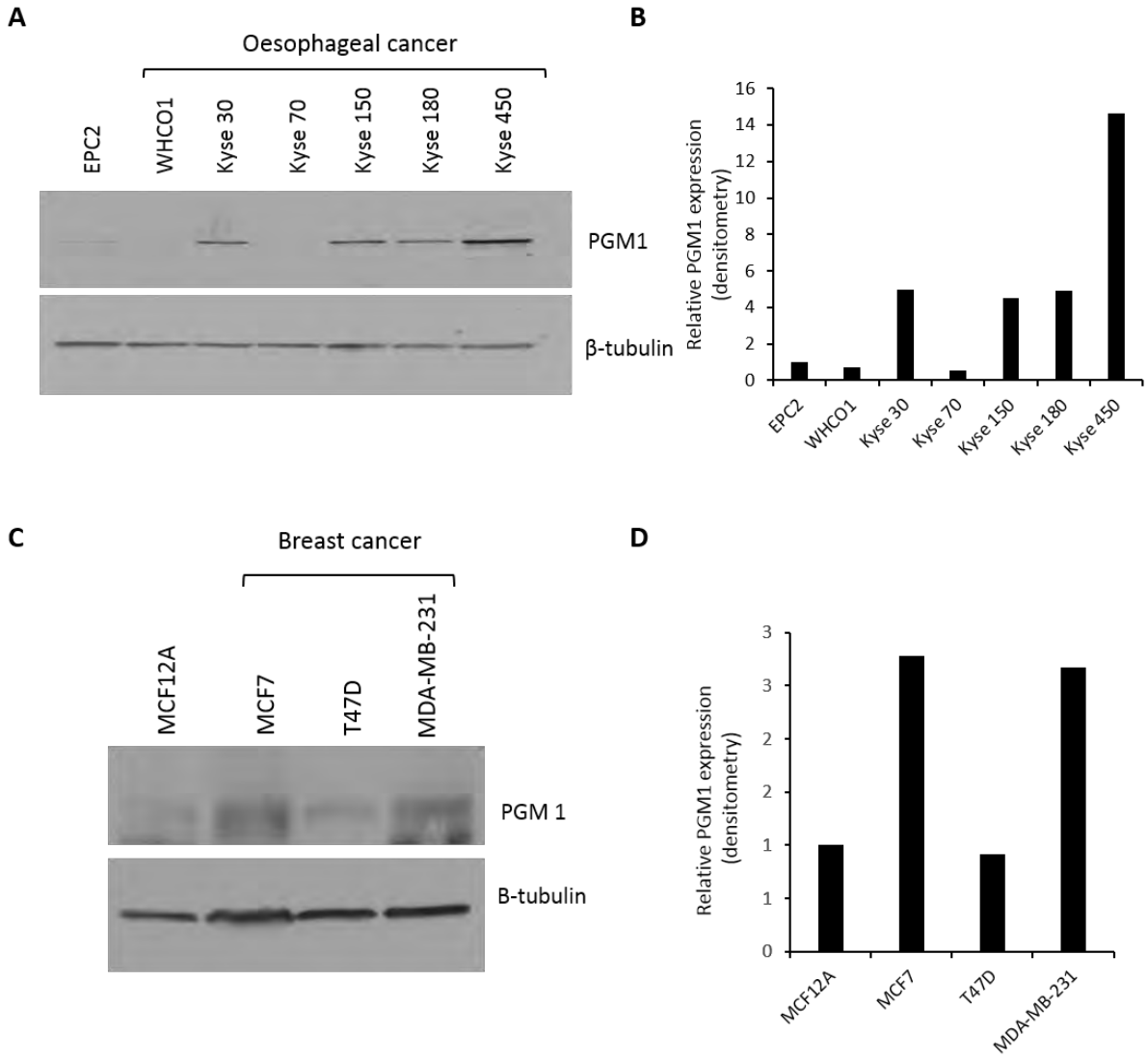

Figure 2.3. PGM1 protein expression in oesophageal and breast cancer cell lines. **A.** Western blot analysis showing PGM1 protein levels in oesophageal cancer cell lines in relation to the normal immortalized oesophageal cells, EPC2. **B.** Quantification of band intensity relative to β-tubulin, showing PGM1 protein expression in oesophageal cancer cells. **C.** PGM1 expression in breast cancer cell lines (MCF7, T47D and MDA-123) compared to the non-tumourigenic breast epithelial cells, MCF12A. **D.** Quantification of band intensity relative to β-tubulin, showing PGM1 protein expression in breast cancer cells. Results shown are representative of experiments performed in duplicate.

2.2.3 PGM1 protein expression in normal versus transformed cells

We also investigated whether PGM1 expression associated with cellular transformation. This was explored by comparing PGM1 expression in normal and transformed fibroblasts. Our results show higher expression in the SVW138 transformed cells compared to its normal counterpart, WI38 (Figure 2.4 A). Higher expression was observed in the CaSki and the HepG2 cancer cell lines (Figure 2.4 A and B). HepG2 cells were included for their liver origin and thereby consequently high metabolic activity.

A lower band was observed in W138 cells compared to the transformed and cancer cells lines. To investigate whether or not the lower band observed in WI38 cells on Western blot was PGM1 or non-specific, these cells were treated with PGM1 targeted siRNA. The top band was lost suggesting that the bottom band was a non-specific interaction with the antibody (data not shown).

In addition to western blot analysis, we performed immunofluorescent analysis for PGM1 expression in normal W138, transformed SVWI38 and cancer cell lines, CaSki and HepG2. These results confirm higher PGM1 expression in the cancer cell lines (Figure 2.5A). Together the results presented here showed high PGM1 expression in cervical cancer patient material as well as high levels in cell lines of cervical, oesophageal and breast cancer origin.

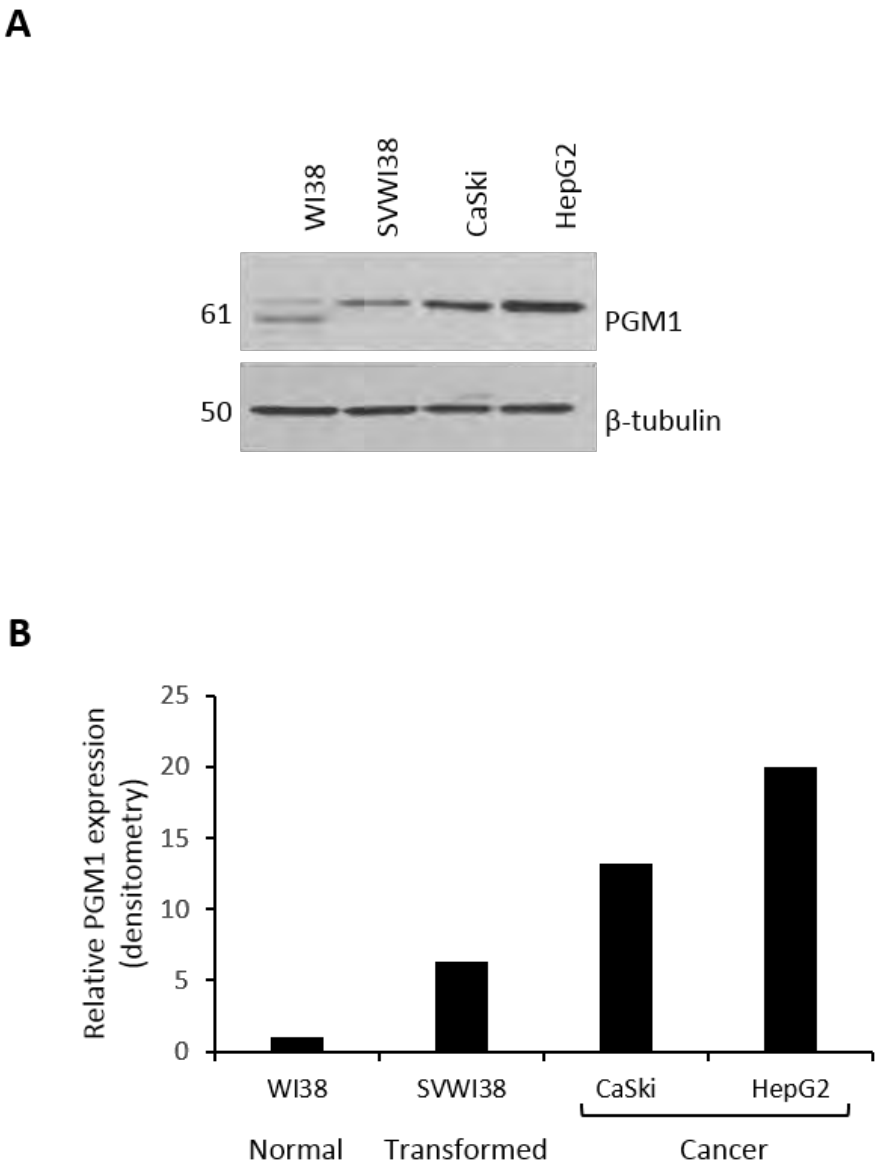

Figure 2.4. PGM1 Protein expression in normal, transformed fibroblasts and cancer cells. A. Western blot analysis showed higher PGM1 protein expression in the transformed lung fibroblasts (SVWI38) and cervical (CaSki) and liver (HepG2) cancer cell lines compared to the normal lung fibroblast cells (WI38), β-tubulin was used as a loading control. **B.** Quantification of PGM1 levels relative to β-tubulin done by densitometric analysis. Results shown are representative of experiments performed in duplicate.

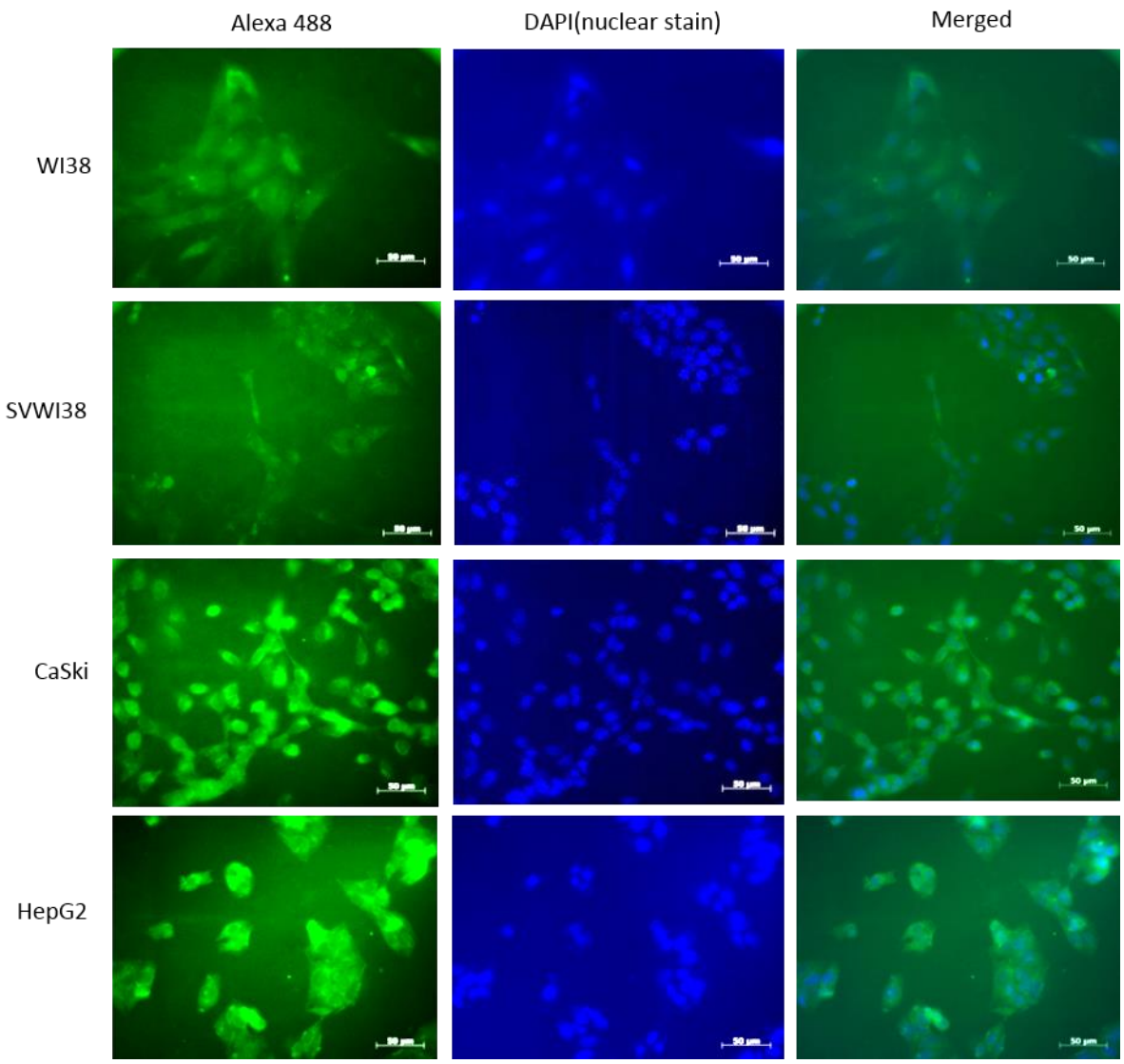

Figure 2.5. PGM1 Protein expression in normal, transformed fibroblasts and cancer cells by Immunofluorescence. PGM1 expression levels are shown to be higher in the CaSki and HepG2 cancer cells compared to the normal fibroblast cells.

2.3 DISCUSSION

The increased expression of genes involved in glucose metabolism, in particular glycolysis, is a characteristic that has been described previously and in the last decade more data has been generated supporting the 'Warburg effect'. Warburg described that cancer cells showed an increased dependence on glycolysis as their major energy source to meet energy demands, as opposed to relying on the more energy efficient Krebs and Oxidative Phosphorylation processes irrespective of oxygen availability (Warburg 1956; Upadhyay et al. 2013).

Over the years the Warburg effect has generated much debate on its significance as a characteristic displayed by cancer cells, with different reasons put forward as to why it is that some cancer cells rely on aerobic glycolysis for their energy needs and survival. Current consensus is that both glucose uptake and glycolysis are heightened processes in cancer and this has led to the acceptance of these changes in cellular energetics as a cancer hallmark (Hanahan & Weinberg 2011). There is growing evidence that genes involved in glucose metabolism are differentially expressed in cancer compared to normal. Data generated in our laboratory supports the Warburg hypothesis in that, glycolytic genes showed elevated expression in the cohort of advance-stage cervical cancers (van der Watt, PhD thesis, 2009).

Of the genes validated in this study, Enolase 1 which encodes α-enolase (ENO A), an isoform found in most adult tissues was confirmed as differentially expressed by qRT-PCR. ENO A catalyses the dehydration of 2-phospho-d-glycerate to phosphoenolpyruvate in the second half of the glycolytic pathway and has been previously shown to be overexpressed in cervical cancer (Capello et al. 2011; Altenberg & Greulich 2004; Bae et al. 2006). ENO A is expressed on the cell surface (Moscato et al. 2000) and by acting as a plasminogen receptor it has been shown to promote cell migration and cancer metastasis. Phosphoglycerate Kinase 1 (PGK1),

also validated in this study, is an ATP-generating enzyme of the glycolytic pathway catalysing the conversion of 1,3-diphosphoglycerate to 3-phosphoglycerate. PGK1 has been shown to be overexpressed in colon cancer and this increased expression has been linked to metastasis (Ahmad et al. 2013). Our data showing PGM1 expression to be increased in cervical cancer compared to non-cancerous cervical tissue is a first to our knowledge. PGM1 functions to reversibly convert G1P to G6P and can therefore influence the pentose phosphate pathway, glycolysis and glycogen synthesis.

Studies such as those done by (Favaro et al. 2012) and (Pelletier et al. 2012) show elevated PGM1 expression in response to specific biological stimulants such as treatment with Bevacizumab, an anti-angiogenic drug and hypoxic stress. Our data shows that even outside of external stimuli PGM1 expression levels were higher in cancer cells and transformed cells compared to normal. High PGM1 expression appears not to be unique to cervical cancer cells as other cancer cell lines that we investigated such as breast and oesophageal cancers also show high PGM1 levels. We observed the high PGM1 protein levels in the liver cancer cell line, HepG2. The high expression in HepG2 cells is likely a result of the inherent function of liver tissue as the body's metabolic centre and in particular its role in maintaining blood-sugar homeostasis through monitoring glucose metabolism and regulation. A transformed cell line SVWI38 showed higher PGM1 expression levels compared to the normal WI38 cell line suggesting that PGM1 up-regulation associates with the transformed phenotype and could possibly be an early event in cancer development.

Elevated PGM1 expression in the cervical cancer cell lines was more pronounced in the HPV positive cell lines as opposed to the HPV negative, C33A cell line, implying a possible involvement of the activity of HPV oncoproteins in altered PGM1 expression in cervical

cancer. HPV oncoproteins have been directly and indirectly implicated in changes in metabolism and the expression of metabolic enzymes (Mclaughlin-drubin & Münger 2010). For example, the HPV 16 E7 protein has been shown to associate with and alter the activity of the pyruvate kinase (PK) one of the glycolytic enzymes. HPV 16 E7 transformed cells have been shown to exhibit high Pyruvate Kinase (PK) expression which leads to an increased glycolytic activity (Zwerschke & Mazurek 1999). This oncoprotein has been shown to allosterically activate α-glucosidase, an enzyme involved in glycogen catabolism (Zwerschke et al. 2000; Chakrabarti & Krishna 2003). PGM1 expression was also increased in cancer cell lines that are not necessarily associated with HPV infection. The HPV oncoprotein E7 is reported to be responsible for the loss of the retinoblastoma (Rb) tumour suppressor function in HPV-induced cancers. HPV E7 leads to the rapid ubiquitination and consequent degradation of Rb in HPV infected cells. This results in a release of a block on genes regulated by RB. Non-HPV associated cancers cells, Rb 'loss of function' can occur as a result of deactivating mutations or deletions of the gene that encodes this protein (Liu et al. 2004; Giacinti & Giordano 2006). Loss of Rb would associates with the uncontrolled expression of genes that were normally held at bay by its inhibitory functions. The transcriptional regulation of PGM1 expression in cancer cells will be further investigated in Chapter 3 of this thesis.

CHAPTER 3

TRANSCRIPTIONAL REGULATION OF PGM1 EXPRESSION IN TRANSFORMED AND CANCER CELLS

3.1 INTRODUCTION

The classic enzymology of PGM1 has been extensively reported while the regulation of its expression in cancer has seen limited investigation (Bae et al. 2014). Phosphorylation of serine 108 of PGM1 has been shown to act as a phosphoryl group donor to producing G-1,6-BP (Pouysségur et al. 1977), and p21-activated kinase 1 (Pak1) was shown to phosphorylate threonine 466 of PGM1 and enhance its enzymatic activity (Gururaj et al. 2004). PAK 1 has been shown to be upregulated in a number of cancers including breast, lymph, bladder and ovarian cancer (Balasenthil et al. 2004). PAK 1 was also shown to be expressed in cervical cancer and its functions include promoting cell proliferation and inhibiting apoptosis (Tsin-Wah 2013). To date there have been no published reports on the transcriptional regulation of PGM1 expression in cancer cells.

A bioinformatics search for putative transcription factor (TF) binding sites in the region 2kb upstream and 101 bp downstream of PGM1's transcription start site (TSS) was performed. A number of TFs that potentially bind to this regulatory region of the PGM1 promoter were identified. Of these factors that could potentially bind to the PGM1 gene, E2F and HIF proteins were of particular interest, as these TFs commonly associate with cancer development (Lum et al. 2007; DeBerardinis et al. 2008; Dang et al. 2008; Porporato et al. 2011; Masson &

Ratcliffe 2014; Nevins 2001; van der Watt et al. 2011; Ward et al. 2011; DeGregori & Johnson 2006).

A number of studies have demonstrated that E2F proteins are involved in the control of the expression of genes important for DNA replication as well as promoting cell cycle progression and consequently proliferation (Nevins 1998; Dyson 1998; Ishida et al. 2001). The retinoblastoma protein (pRB) and other pocket binding proteins on the other hand suppress E2F-mediated transcription in cells during progression through the early G1 phase, ascribing tumour suppressive functions to these proteins (Choi et al. 2014). pRB and E2F are often described as opposing molecules that control the G1/S-phase transition. The mechanisms involved in their interactions however, are far more complex, involving different family members that form complexes which can either activate or repress promoter activities (Dyson 1998). Few studies have demonstrated a direct association of E2F proteins to metabolic function, despite an intuitive extrapolation that high proliferative rates of cancer cells may require a proportionate quantity of cellular components (Blanchet et al. 2013; Clem & Chesney 2012). For example, the pre-cursors of DNA replication and substrates of nucleotide synthesis produced by pathways such as the pentose phosphate pathway, a pathway that can be influenced by PGM1.

The transcription factor, hypoxia-inducible factor-1 (HIF-1) is the main regulator responsible for inducing the expression of genes that facilitate adaptation and survival of cells from normoxia (approximately 21% oxygen) to hypoxia (approximately 1% oxygen) (Wang et al. 1995; Ke & Costa 2006). Diminishing oxygen gradient in tumours often occurs as a result of impaired or inadequate vasculature which consequently induces HIF. HIF functions as a heterodimer consisting of HIF-1α and HIF-1β (also called the aryl hydrocarbon receptor

nuclear translocator [ARNT]) in most cells (Keith et al. 2001; Hu et al. 2003). The oxygen regulated α subunit has three isoforms: HIF-1α, HIF-2α, and HIF-3α while the constitutively expressed β subunit has only two isoforms HIF-1β and HIF-2β (Wang et al. 1995; Semenza 2009). The α-subunit is transported into the nucleus and dimerizes with the β subunit when oxygen concentrations are below 6% (Jiang et al. 1996). Under normoxic conditions, HIF-1α is synthesized and hydroxylated by prolyl hydroxylase domain (PHD) proteins to facilitate binding to the von Hippel-Lindau protein (pVHL), which targets HIF-1α for ubiquitination and ultimately marks the protein for degradation by the 26S Proteasome. In hypoxia this cascade is inhibited allowing the HIF heterodimers to bind to their target genes (Salceda & Caro 1997). HIF has been shown to promote a glycolytic phenotype in cancer, with recent evidence showing an association with glycogen accumulation and enhanced expression of genes involved in glycogen metabolism.

The objective in this study was, to investigate transcriptional regulatory mechanisms that may account for the high levels of PGM1 expression in cancer cells, with particular focus on the roles of E2F an HIF1. The cell culture models used in the following experiments were mostly the HPV positive HeLa and CaSki cells (which in some instances, HeLa cells were selected over the CaSki due to difficulties with transfection efficiencies) and C33A, HPV negative cervical cancer cells for comparative HPV related observations.

3.2 RESULTS

3.2.1 Cloning of the PGM1 promoter and bioinformatics search for transcription factor binding sites

To determine transcriptional regulatory mechanisms that associate with elevated PGM1 expression in cancer cells, a bioinformatics analysis of the region -2Kb upstream of the transcription start site and +101 downstream was searched for putative transcription factor binding sites. The *in silico* search was done using the MatInspector software programme (https://www.genomatix.de/). Search outputs identified seven potential E2F sites at various positions and one hypoxia responsive element (HRE) for HIF 1 binding (Figure 3.1).

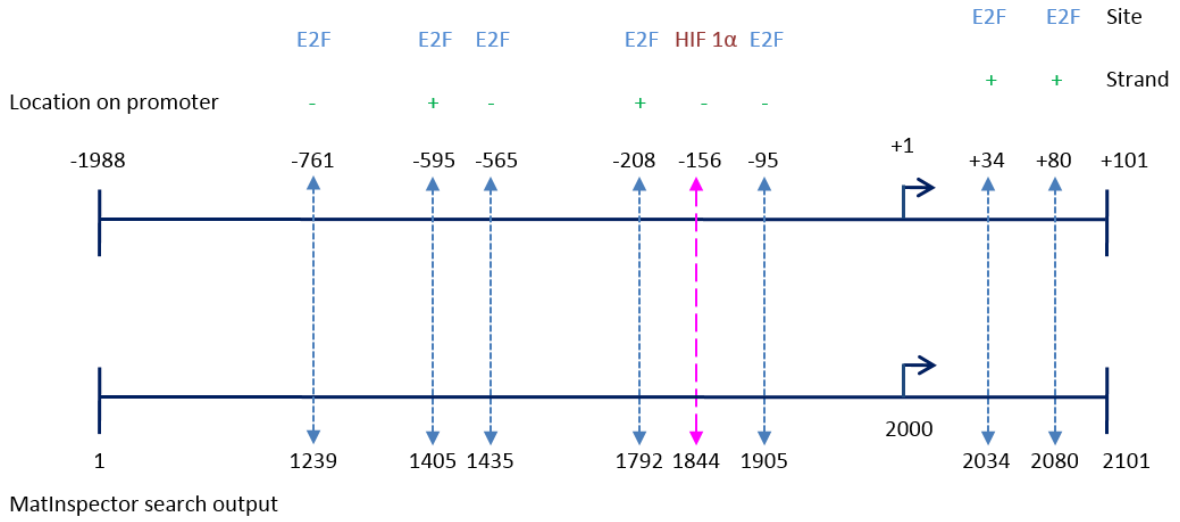

Figure 3.1. Human PGM1 promoter map. Schematic representation of data from a MatInspector search for transcription factor binding sites in the (-2000 to +101) region of the PGM1 promoter, using the genomatix (MatInspector) software suite. The map shows the co-ordinates of putative binding sites for the three transcription factors, E2F and HIF 1, as denoted in search output and their corresponding location on the PGM1 promoter. Only the position of the first base of the potential binding site is indicated in the schematic.

Primers for PCR were designed to span the region of approximately 2 Kb upstream of the transcription start site (TSS) of the PGM1 gene, together with approximately 100 bp of the 5' untranslated regions (downstream from the TSS). This region was PCR amplified and subcloned into pGEM-T-Easy. After screening and confirming correct inserts by sequencing, the (-1988 to +101) PGM1 promoter insert was released by double digesting plasmids with NheI and HindIII restriction enzymes. The (-1988 to +101) fragment was then cloned into the pGL3-Basic vector upstream of a luciferase reporter construct (Figure 3.2A), allowing for quantitative analysis of PGM1 promoter activity in cells. The PGM1 promoter fragment cloned into pGL3-basic was checked by restriction enzyme digestion (Figure 3.2A ii). The pGL3-pPGM1 (-1988/+101) promoter construct was transfected into CaSki cells and luciferase activity as a measure of promoter activity showed 10-fold higher activity with the (-1988 to +101) promoter containing construct compared to the empty vector control (Figure 3.2B).

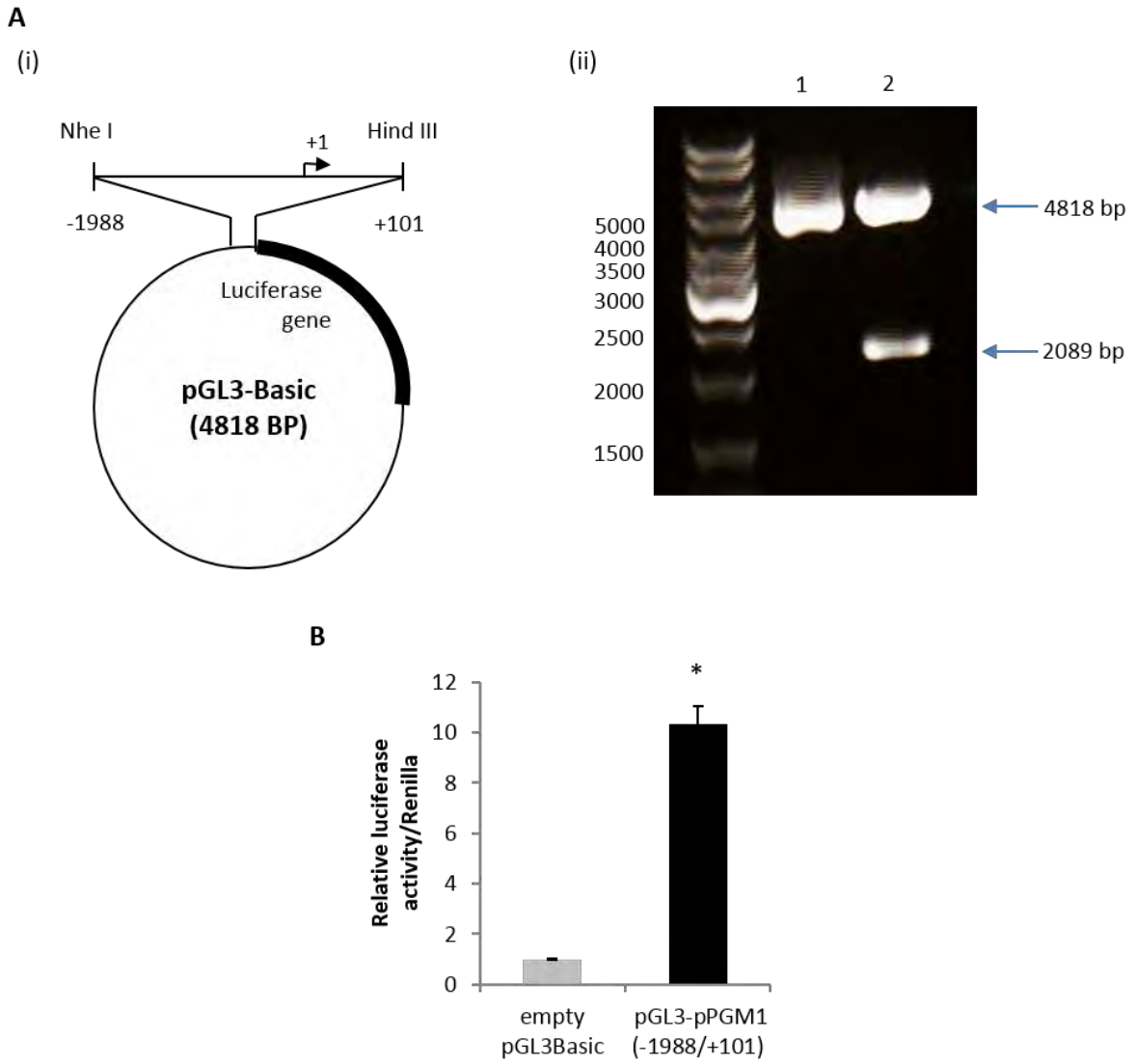

Figure 3.2. Promoter activity of human PGM1 (-1988 to + 101) cloned into pGL3- Basic reporter vector. A. (i) Schematic illustration of the cloned PGM1 promoter (-1988 to +101) in pGL3-Basic. The promoter fragment was cloned upstream of the luciferase reporter gene using Nhe l and Hind III restriction sites in the vector's multiple cloning site. **(ii)** Restriction enzyme digest of the pGl3- Basic vector (lane 1) and the vector containing insert (pGL3-pPGM1 -1988/+101) (lane 2) with Nhe1 and Hind III to release the promoter fragment. Digests were electrophoresed on a 1% agarose gel and visualized accordingly, the release of a 2089 bp DNA fragment indicated successful cloning of the PGM1 promoter into pGL3-Basic. **B.** The empty vector and pGL3-pPGM1 were transfected into CaSki cells and luciferase activity measured. Results show significant promoter activity in the PGM1 (-1988 to +101) construct compared to the empty vector (*$p < 0.05$). The Renilla reporter was used as an internal control for transfection efficiency. Results shown are the mean ± SEM of experiments performed in triplicate and repeated at least two independent times.

3.2.2 PGM1 protein expression in transformed and cancer cells in relation to PGM1 promoter activity.

PGM1 protein expression was shown to be increased in the cancer and transformed cells when compared to the normal cell lines. FGo, CCD1068-SK and WI38 normal fibroblast cells showed relatively lower endogenous PGM1 protein expression compared to transformed (SVWI38, CT1) and cancer cell lines (CaSki and HeLa) (Figure 3.3 A and B). As WI38 and CCD1068-SK cells proved difficult to transfect, promoter assays were done in FGo cells as a representative normal cell line. The pGL3-pPGM1 (-1988/+101) promoter construct was transfected into FGo, SVWI38, CaSki and HeLa cell lines and dual-luciferase assays used to compare PGM1 promoter activity. Results showed significantly higher (-1988/+101) PGM1 promoter activity in the SVWI38 transformed cells and in CaSki and HeLa cancer cell lines compared to normal FGo cells (Figure 3.3 C).

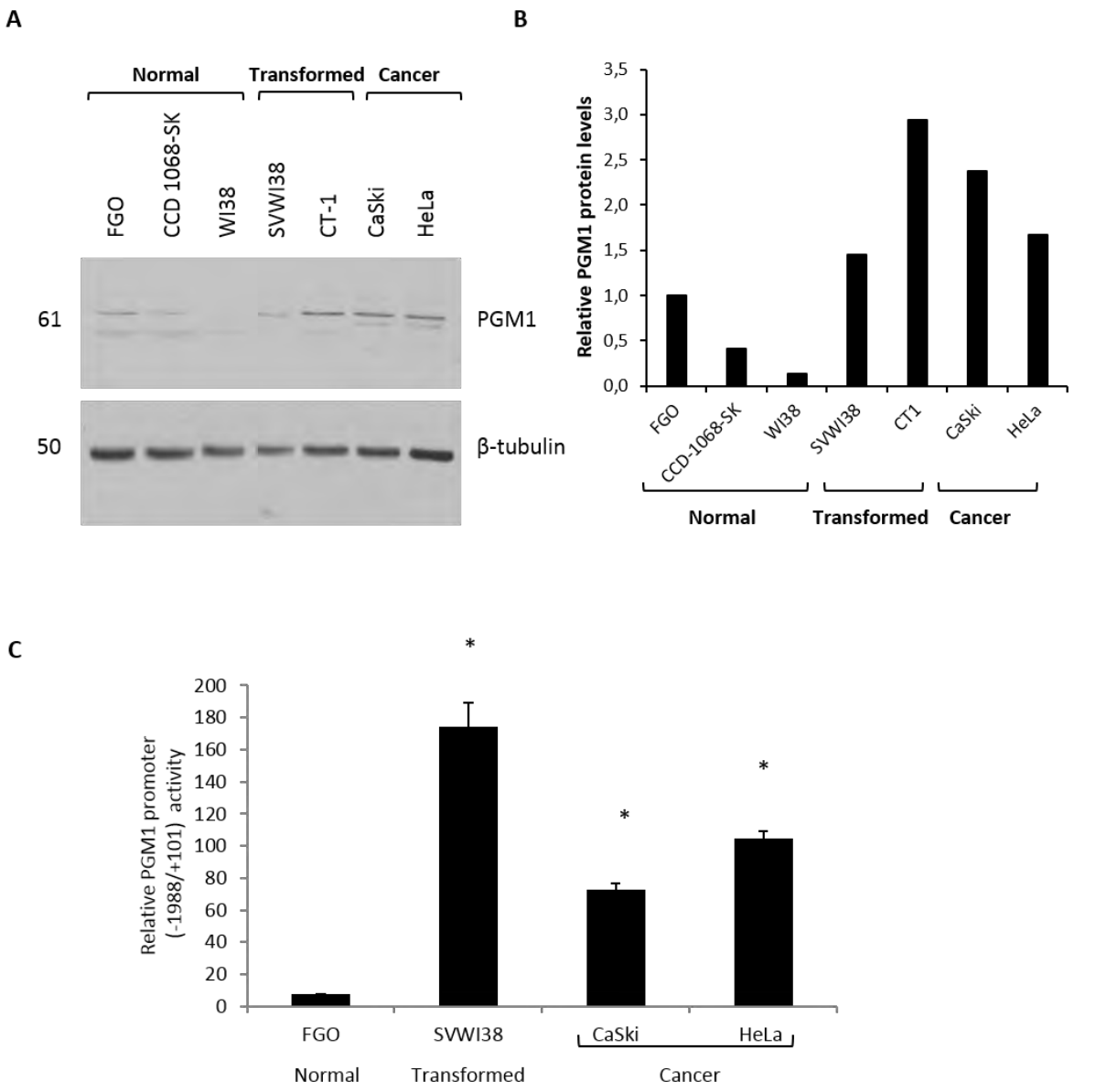

Figure 3.3. -1988 to +101 PGM1 promoter activity in normal, transformed and cancer cells correlates with endogenous protein levels. **A**. PGM1 Protein expression in by western blot analysis shows higher expression in transformed fibroblasts (SVWI38 and CT-1) and cervical cancer cells (CaSki and HeLa) compared to the normal fibroblasts (FGO, CCD1068-SK and WI38). **B.** Quantification of PGM1 protein expression relative to β-tubulin. Results are representative of experiments performed at least two independent times **C.** PGM1 promoter activity in normal and transformed fibroblasts and cancer cells transfected with the pGL3-pPGM1 (-1988/+101) for 48 hours, a Dual luciferase assay was used and luciferase activity normalized to pTK-renilla. Results show higher expression in the transformed cell line (SVWI38) and cancer cell line CaSki and HeLa and compared to FGo normal fibroblasts. Results show are the mean ± SEM of experiments performed in triplicate and repeated at least two independent times.

3.2.3 The effect of E2F/DP1, E7 Inhibition and RB overexpression on PGM1 expression and promoter activity in cervical cancer cells

E2F family members function as heterodimers of an E2F member with a DP family member. DP1 dimerizes with E2F to enhances both DNA binding and transactivation activities (Zaragoza et al. 2010). Recent studies have implicated the E2F/RB axis in the control of metabolic function, a limited number of which have linked E2F family members with glycolytic control (Blanchet et al. 2013; Clem & Chesney 2012). One such study showed that E2F1 acts as a switch between the glycolytic mode during proliferation and the oxidative phosphorylation under dormant or stressful conditions (Yeo et al. 2011). The genes associated with this E2F regulated switch are not known and currently under investigation.

In order to determine whether E2F influences the expression and activity of PGM1 in cancer, we inhibited the expression of its binding partner DP1 using siRNA. DP1 was silenced instead of directly targeting individual E2F family members because DP1 is essential for the function of all the different E2F proteins, thereby allowing for simultaneously inhibition as opposed to requiring different siRNA's for all nine different E2F proteins. Western blot analysis showed a reduction in PGM1 protein levels in CaSki cells treated with a DP1 targeting siRNA which inhibits the function of most E2F members (Figure 3.4 A). Since E2F activity in cervical cancer cells associates with the HPV E7 onco-protein, we investigated whether inhibiting HPV16 E7 would have an effect on PGM1 protein expression. HPV E7 is known to cause the phosphorylation of the retinoblastoma protein (pRb), which targets Rb protein for degradation thereby freeing E2F to bind to its downstream target genes. Our results show that E7 inhibition resulted in a reduction in phosphorylated-Rb levels which associates with a consequent decrease PGM1 protein expression (Figure 3.4 B). By inference, a decrease in

phosphorylated Rb suggests that functional Rb can bind and inhibit E2F and thereby interfere with PGM1 expression. Overexpressed Rb in HPV positive and negative cervical cancer cell lines, HeLa and C33A also resulted in a reduction in PGM1 promoter activity (Figure 3.4 C (i) and (ii)). These results suggest a role for E2F in the regulation of PGM1 protein expression and promoter activity.

3.2.4 E2F/DP1 binds regions within the PGM1 promoter

To determine whether the E2F/DP1 heterodimers could directly bind to the PGM1 promoter at the regions containing putative E2F binding sites (with the consensus sequence 5'-TTTSSCGS-3'; where S denotes either C or G), Chromatin Immunoprecipitation (ChIP) assays were performed using chromatin prepared from CaSki cells. ChIP primers spanned the PGM1 promoter regions from (-784 to -579), (-257 to -77) and (-110 to +77) (Figure 3.5A). Our results show E2F/DP1 binding to all three regions in the PGM1 promoter (Figure 3.5 B, C and D).

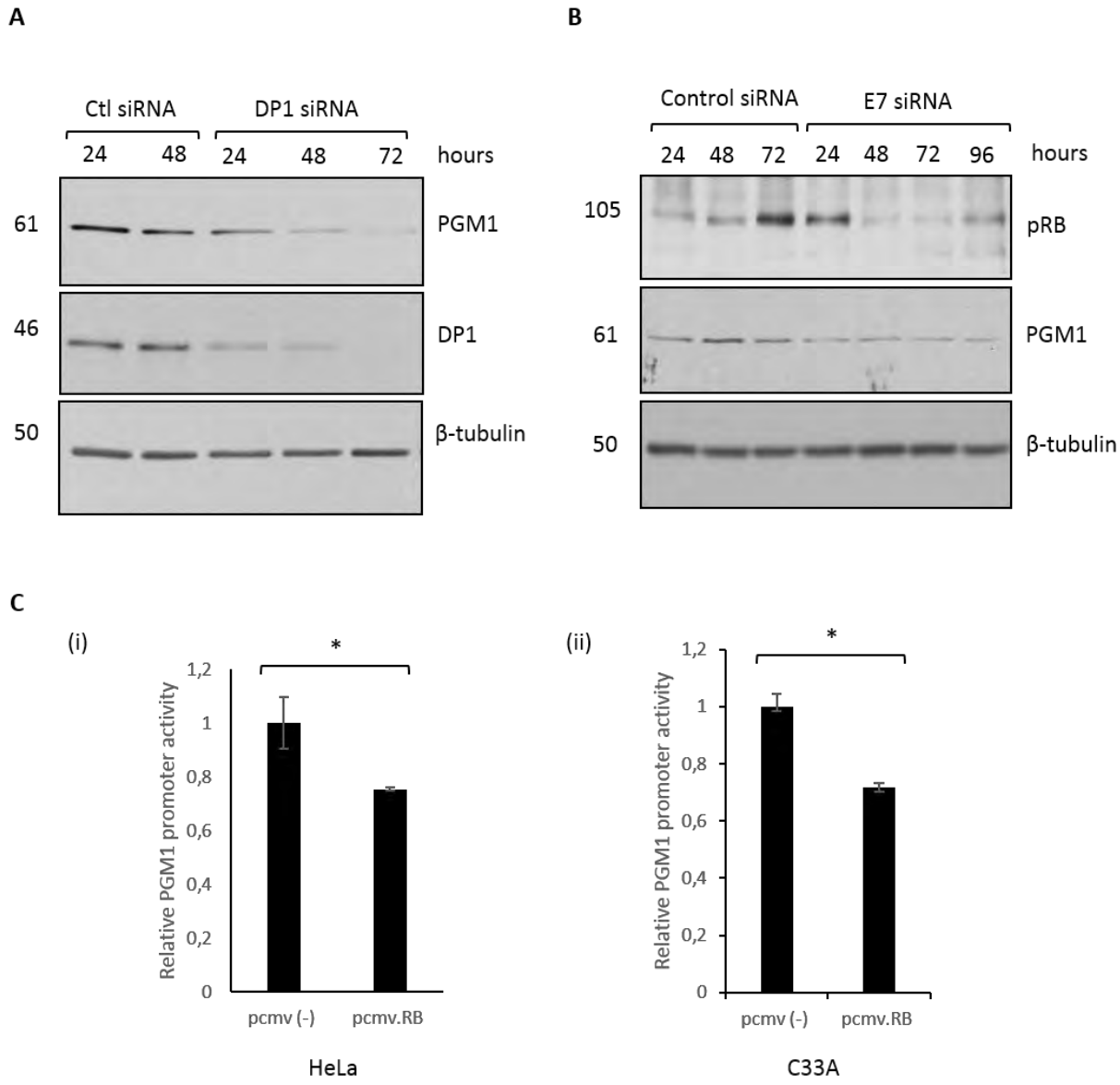

Figure 3.4. DP1 and E7 inhibition and RB overexpression in cervical cancer cells decreases PGM1 protein expression and promoter activity. A. Western blots showing PGM1 protein levels after DP1 inhibition using siRNA in CaSki cells. **B.** HPV16 E7 siRNA was used to inhibit E7 expression in CaSki cells and a significant reduction in phosphorylated Rb was observed and correlated to reduction PGM1 protein expression **C.** Rb overexpression in cervical cancer cells (i) HeLa and (ii) C33A and (-1988 to +101) PGM1 promoter activity was investigated by a dual luciferase assay. Renilla was used as an internal control. Results shown are the mean ± SD of experiments performed in triplicate at least two independent times, * $p < 0.05$.

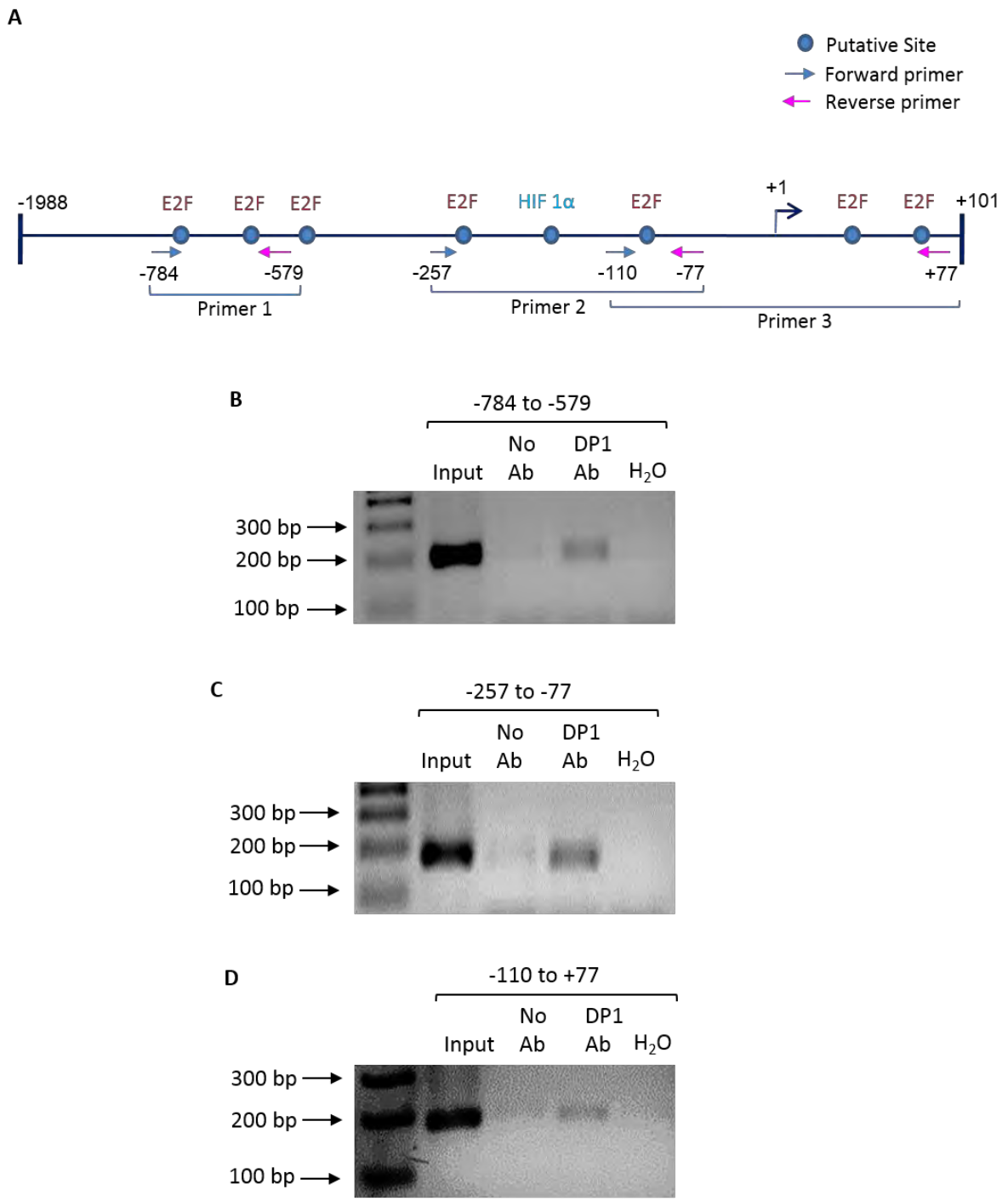

Figure 3.5. Binding of E2F/DP1 to the PGM1 promoter in the regions -784 to -579 and -257 to -77. **A** Schematic representation of the location of the primers used for the ChIP assay. Samples of sonicated chromatin from CaSki cells, immunoprecipitated with a DP1 antibody as indicated. DNA Isolated from the immunoprecipitated material was amplified by PCR using primers 1, 2 and 3 spanning the regions containing the different putative E2F sites. Amplified fragments were analysed by electrophoresis on a 2% agarose gel. Results show direct binding of E2F/DPI in the regions: **B** -784 to -579, **C** -257 to -77 as well as **D** -110 to +77 of the PGM1 promoter.

3.2.5 Analysis of PGM1 promoter activity through promoter deletion constructs

Having established binding of the E2F/DP1 complex at different sites within the (-1988 to +101) PGM1 promoter fragment, we sought to determine the regions necessary for E2F activation of the PGM1 promoter in cancer cells. A series of deletion constructs were thus synthesized using forward primers designed to incorporate a Nhe l restriction sites such that promoter deletion constructs spanning (-587 to +101) and (-135 to +101) could be synthesized. All constructs were confirmed by restriction digestion analysis using Nhe I and Hind III (data not shown) and transfected into CaSki, HeLa and C33A cells. Results in all cell lines indicate that the shortest promoter fragment (-135 to +101) retained promoter activity (Figure 3.6). Interestingly deletion of the -1988 to -135 regions resulted in small but significant increase in promoter activity suggesting the presence of possible repressor elements in this region and/or activator elements in the (-135 to +101) region.

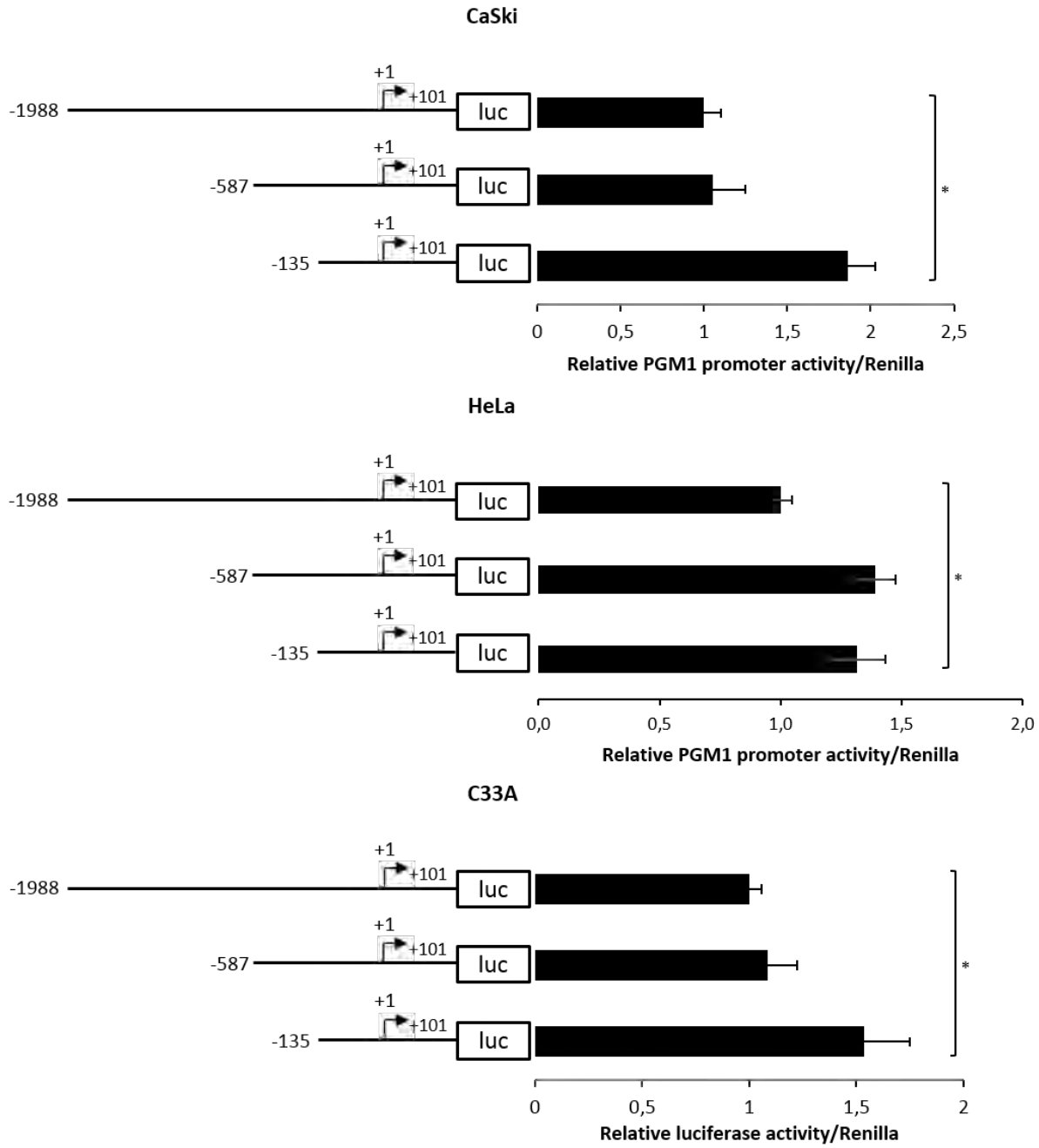

Figure 3.6. Activity of PGM1 promoter deletion constructs in CaSki HeLa and C33A cells. Luciferase reporter constructs containing deleted fragments of the human PGM1 promoter were transfected transiently into CaSki, HeLa and C33A cells, respectively. TK-Renilla-Luc was used as an internal control for transfection efficiency. Results shown are the mean ± SEM of experiments performed in triplicate and repeated at least two independent times, (*$p < 0.05$).

3.2.6 The effect of HPV E7 inhibition on PGM1 promoter activity

To further investigate the functional significance of (-135 to +101) region of the PGM1 promoter, HPV16 E7 was inhibited using siRNA in CaSki as a means to release the block on Rb and hence result in E2F inhibition. A reduction in (-135 to +101) PGM1 promoter activity was observed when E7 was inhibited (Figure 3.7). This data further suggests that E2F family members have a regulatory role in PGM1 expression.

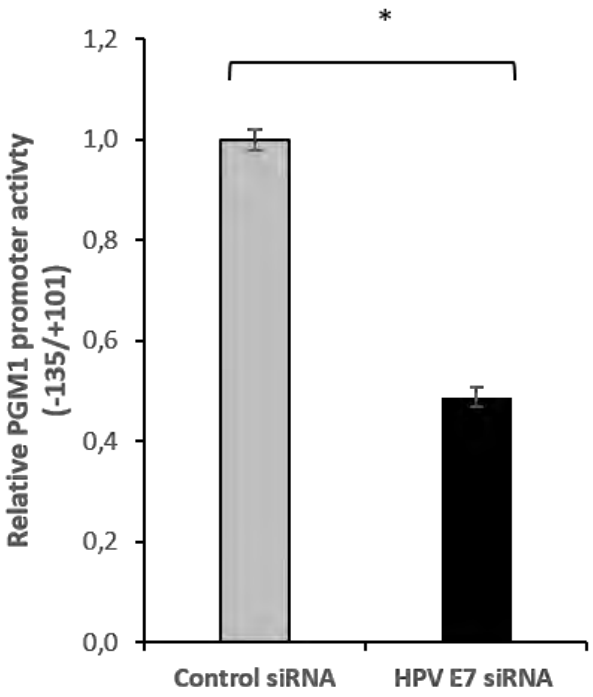

Figure 3.7. HPV E7 Inhibition influences PGM1 promoter activity in the short -135/+101 promoter fragment. Luciferase reporter constructs containing the (-135/+101) region of the human PGM1 promoter were transfected transiently into CaSki cells, simultaneously with HPV E7 siRNA used to inhibit E7 expression in CaSki cells. Inhibition of E7 in cells transfected with the (-135 to +101) PGM1 promoter fragment showed a significant reduction in promoter activity (*$p < 0.05$). Total protein was used as an internal control. Results shown are the mean ± SEM of experiments performed in triplicate and repeated at least two times.

3.2.7 Site directed mutagenesis of putative E2F/DP1 binding sites in the (-135 to +101) PGM1 promoter region.

Using siRNA against E2F/DP1 and *in vivo* ChIP assays we have identified E2F/DP1 as a potential regulator of PGM1 expression. Our promoter deletion assays showed that the (-135 to+101) region of the PGM1 gene contained elements sufficient for promoter activity. The bioinformatics search for putative transcription factors within this region revealed three putative E2F/DP1 binding sites at positions (-95 to -88), (+34 to +42) and (+80 to +87). These three sites were mutated to investigate their requirement for PGM1 promoter activity. The site mutations were done according to published sequence conversion to a NheI restriction site (van der Watt et al. 2011) with the exception of the (-95 to -88) (E2Fa) site which was converted to a Xho I site due to difficulties with primer design in this region (Figure 3.8A). In all instances, mutagenic sites were verified by submitting the sequence to MatInspector (https://www.genomatix.de/) to check for the absence of the E2F binding site after mutation. Our data showed that mutating each of the three putative E2F/DP1 binding sites had no effect on PGM1 promoter activity in comparison to the wild-type promoter construct (Figure 3.8 A and B). This suggests that E2F/DP1 regulation of the PGM1 promoter may be at regions not recognized as classic E2F binding sites or that E2F regulates PGM1 expression in an indirect manner.

A

Mutation	Primer sequence	Restriction site introduced (underlined)
PGM1 E2Fa - WT	5' CACTTAGGGGAGGAGTTGCGGGCCTCTTTTTACAGTG 3'	
PGM1 E2Fa - mut	5' CACTTAGGGGAGGAGTctCGaGCCTCTTTTTACAGTG 3'	Xho I
PGM1 E2Fb - WT	5' CTGCCAGGAGGTGGGCTGGCGCGGAGGGAGGGCCCTG 3'	
PGM1 E2Fb - mut	5' CTGCCAGGAGGTGGGCgctaGCGGAGGGAGGGCCCTG 3'	Nhe I
PGM1 E2Fc - WT	5' CCCTGTCCCTTTAAGGAGGAGGGCCAAACGCCGGCCTAGAG 3'	
PGM1 E2Fc - mut	5' CCCTGTCCCTTTAAGGAGGAGGGCtAgcCGCCGGCCTAGAG 3'	Nhe I

B

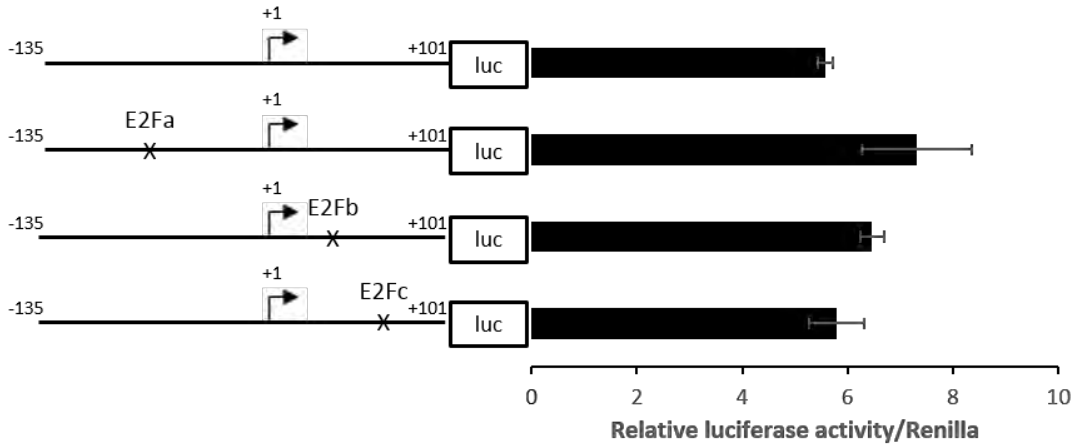

Figure 3.8. Site-directed mutagenesis of the E2F sites in the -135 to +101 PGM1 promoter fragment shows no change in activity. Mutations of the putative E2F binding site were synthesised using the PGM1 (-135 to +101) promoter construct at positions (-95 to -88), (+34 to +42) and (+80 to +87) positions (marked as E2F a, b and c respectively). **A**. The respective consensus sites are in red, with the bases chosen for mutation in green and the mutated bases in lower case bold. Restriction sites were introduced and are underlined. Only the sense mutagenic primer is indicated (antisense primers are described in Chapter 6). Mutagenesis was performed to eliminate the putative E2F. **B**. Effect of putative E2F binding site mutations on PGM1 (-135 to +101) promoter activity in CaSki cells. Wild type and mutated constructs were transfected into CaSki cells and luciferase activity determined. No significant changes in luciferase activity we observed between wild-type and mutated sequences (*$p < 0.05$). Results shown are representative of experiments performed in triplicate, at least two independent times.

3.2.8 PGM1 expression and promoter activity under conditions of hypoxia

The transcription factor, HIF 1, when activated has been shown to promote the expression and activation of many enzymes involved in glycolytic metabolism (Semenza 2010). We identified a putative hypoxia-responsive-element (HRE) at position (-156 to -152) in the bioinformatics search for potential TF binding sites within the PGM1 promoter, where the HIF heterodimers may bind to the consensus sequence 5'-NCGTG-3', where N represents an A or G.

Since HIF1 is responsive to hypoxia we sought to investigate whether hypoxia influenced PGM1 expression in cancer cells and whether this response was dependent on HIF1 function. Nickel (II) sulphate ($NiSO_4$) and cobalt (II) chloride ($CoCl_2$) are known to mimic hypoxia in part by inhibiting the function of prolyl hydroxylase domain-containing enzymes (PHDs), thereby stabilizing HIF (Nardinocchi et al. 2009; Rohwer & Cramer 2011; Stenger et al. 2011). HIF, upon PHD inhibition is then free to bind to the promoters of its target genes and regulate their expression. Our results show that both hypoxia mimics $CoCl_2$ and $NiSO_4$ stimulated the expression of HIF1α in CaSki and HeLa cells at a concentration of 0.5 mM. The increase in HIF1α levels associated with an increase in PGM1 levels (Figure 3.9 A and B). Similar to data observed with protein expression, 0.5 mM $NiSO_4$ treatment resulted in a significant increase in PGM1 mRNA levels (Figure 3.10 A).

To determine whether the change in PGM1 mRNA expression in response to hypoxia was due to transcriptional events or stabilization of the mRNA, cells were treated with Actinomycin D, which acts by interfering with *de novo* mRNA synthesis, prior to treatment with the hypoxia mimicking agent, $NiSO_4$. The induction of PGM1 mRNA was inhibited by actinomycin D

treatment (Figure 3.10 B), suggesting that hypoxia affected its transcription rather than its stability.

To further determine whether hypoxia inducing agents regulated PGM1 expression, we monitored its effects on (-1988 to +101) PGM1 promoter activity. Both 0.5 mM $NiSO_4$ and $CoCl_2$ at 0.5 mM treatment resulted in a significant increase in (-1988/+101) PGM1 promoter activity (Figure 3.11 A and B). Together these results show that hypoxia mimicking agents induce HIF1 stabilization that associates with elevated PGM1 promoter activity, mRNA and protein levels.

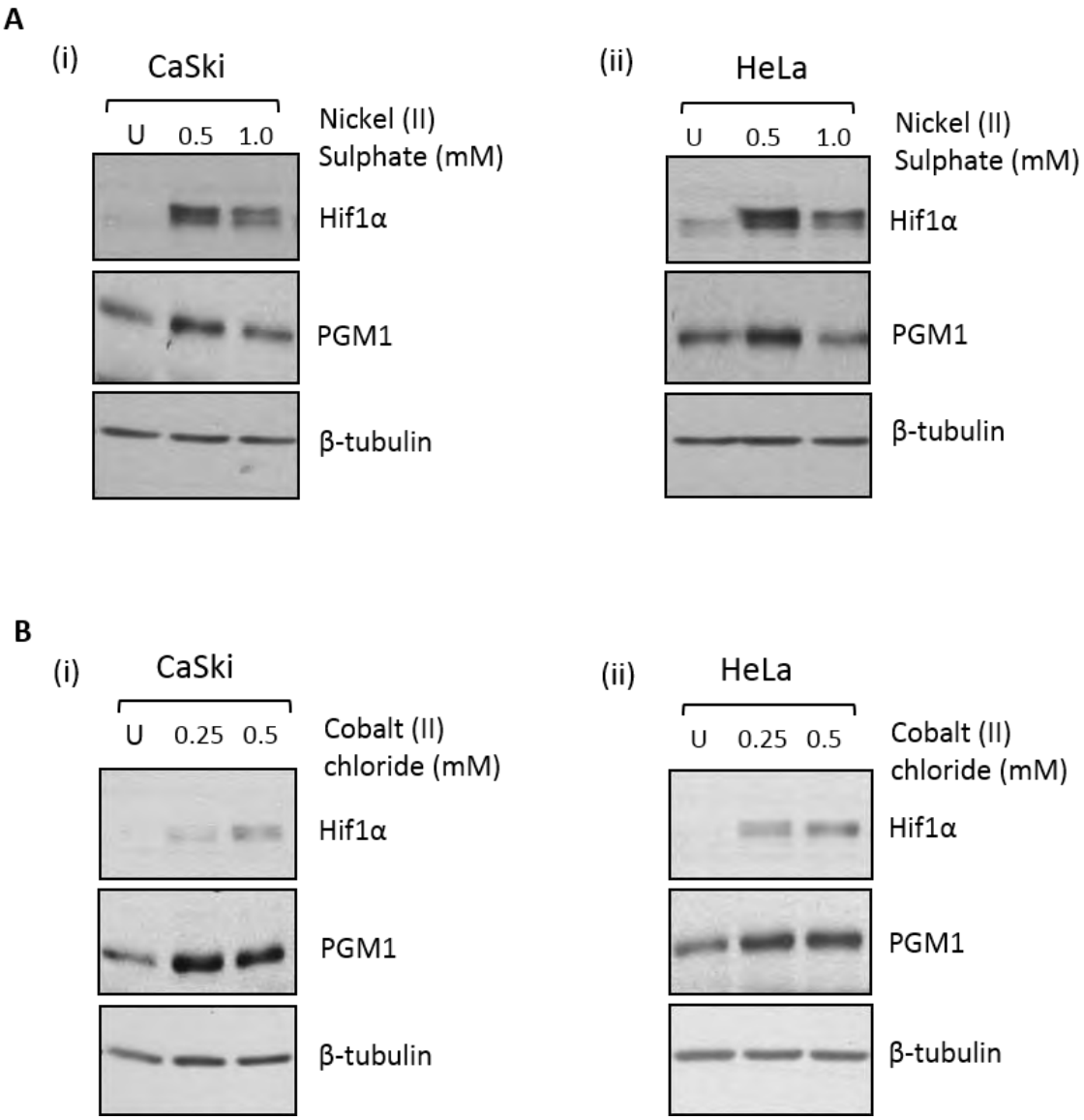

Figure 3.9. Effect of hypoxia mimics A. CoCl2 and B. NiSO4 on PGM1 protein expression CaSki and HeLa cells were grown until approximately 80% confluent, then treated with 0, 0.25 and 0.5mM $CoCl_2$ and 0, 0.5 and 1 mM $NiSO_4$ respectively. Whole cell lysates were harvested after 24 hrs post treatment and subjected to western blot analysis to detect HIF1 α and PGM1 protein expression. β-tubulin was used as a loading control. HIF1 α induction was observed in both cell lines with a simultaneous increase in PGM1 expression observed at concentrations of 0.25 and 0.5 mM of $CoCl_2$ and 0.5 mM of Nickel Sulphate respectively.

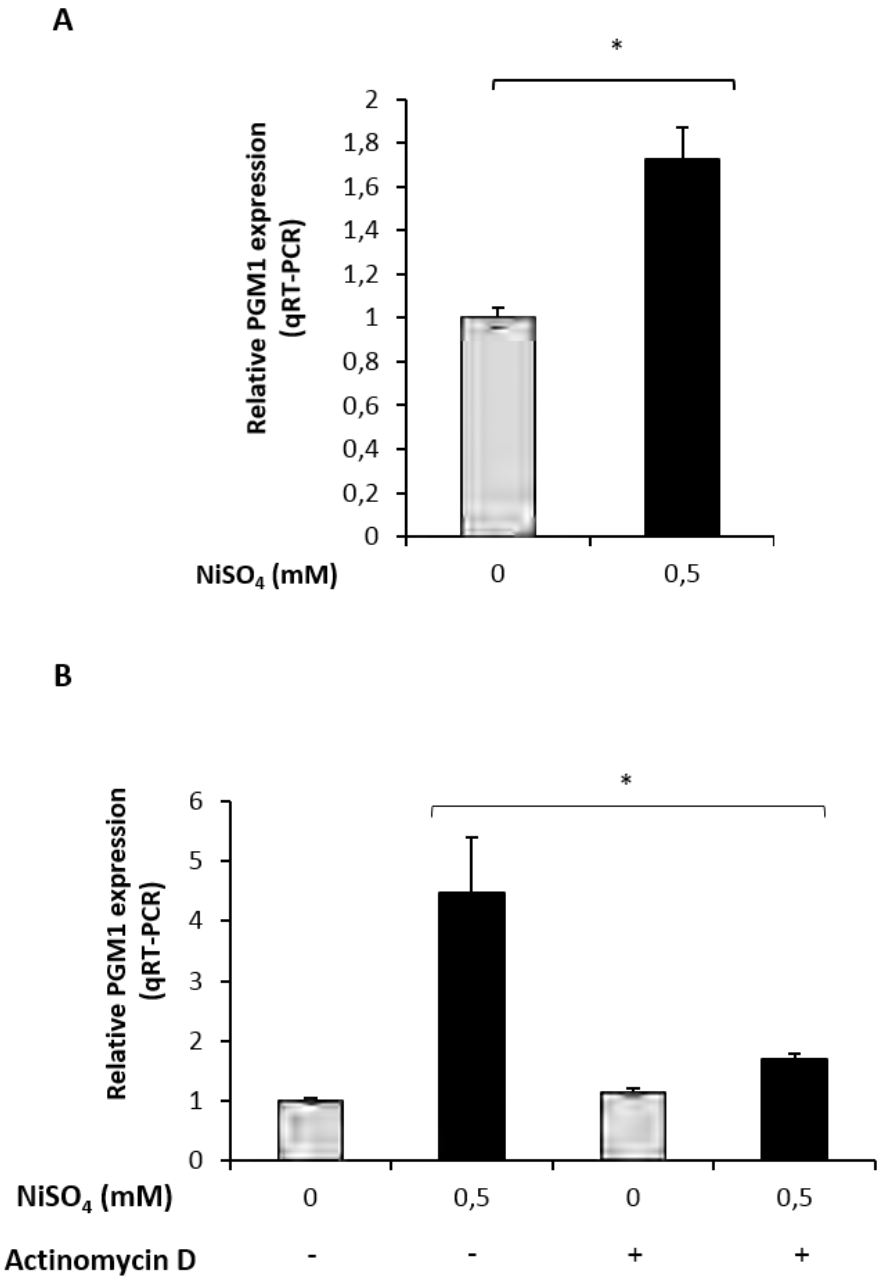

Figure 3.10. Hypoxia mimicking agents induce PGM1 mRNA expression and Actinomycin D inhibits hypoxia-induced PGM1 mRNA expression. A. RNA was extracted from HeLa cells treated with 0.5 mM $NiSO_4$ and qRT-PCR performed with data normalized to B-actin, experiment was repeated twice in triplicate, * $p < 0.05$ **B**. HeLa cells were cultured in 25mM glucose containing media, then treated with 1µg/ml Actinomycin D for 30 min, the Act D was removed then cells subjected to 0.5 mM Nickel sulphate overnight. The data shown is the mean ± SEM of experiments performed in triplicate and repeated at least two times, * $p < 0.05$. Hypoxia induced PGM1 mRNA expression and the hypoxia-induced PGM1 expression was blocked by Actinomycin D.

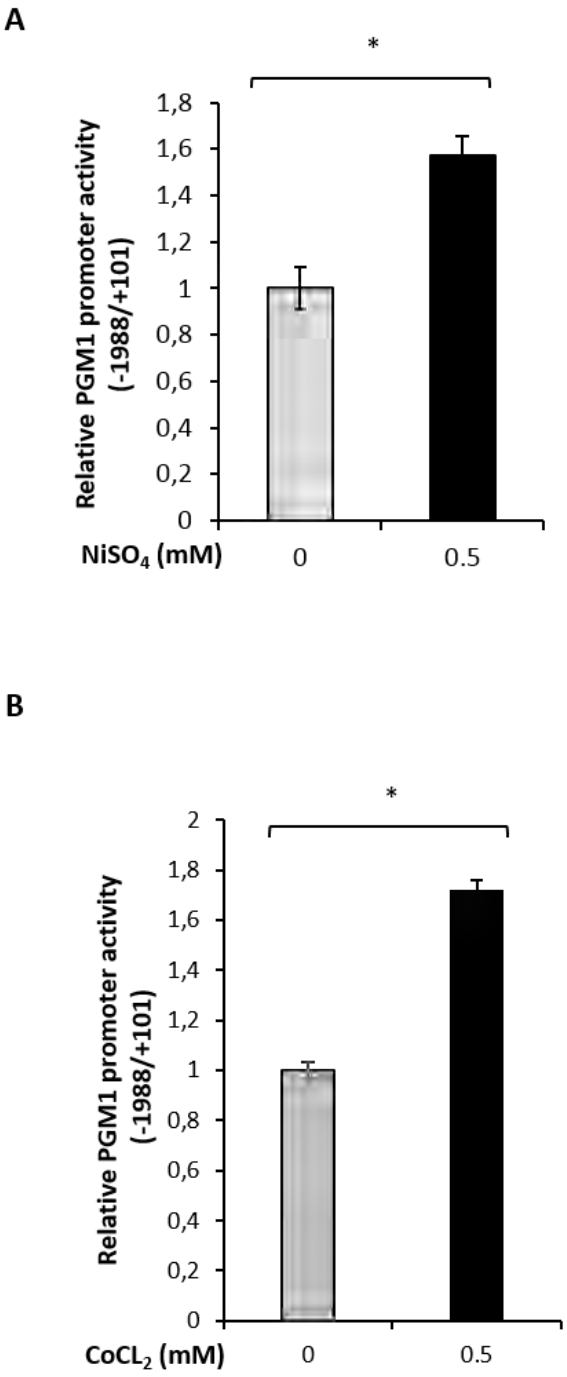

Figure 3.11: Hypoxia mimicking agents, $NiSO_4$ and $CoCl_2$ induce PGM1 promoter activity in cervical cancer cells. HeLa cells were cultured in 25 mM glucose and transfected with the -1988 to +101 PGM1 promoter constructed overnight then treated with 0.5 mM **A.** $NiSO_4$ and **B.** $CoCl_2$ for 24hrs. All data was normalized to total protein. Results shown are the mean ± SEM of experiments performed in triplicate and repeated at least two independent times. *$p < 0.05$

3.2.9 *In vivo* binding of HIF1α to the PGM1 promoter

A bioinformatics search for TF binding sites identified a potential hypoxia-responsive element (HRE) at position (-156 to -152) on the PGM1 promoter (Figure 3.12 A). To investigate whether HIF1α bound to this region, ChIP assays with chromatin prepared from HeLa cells in normoxia and cells treated with 0.5 mM $NiSO_4$ to mimic hypoxia, were performed using primers that spanning the region (-257 to -77). Results show no change between the negative control and the HIF1α antibody pulldown in conditions of normoxia (Figure 3.12B). An increase in HIF1α pulldown relative to the negative control was observed in hypoxia mimicked conditions (Figure 3.12C), suggesting that HIF1α binds to the PGM1 promoter.

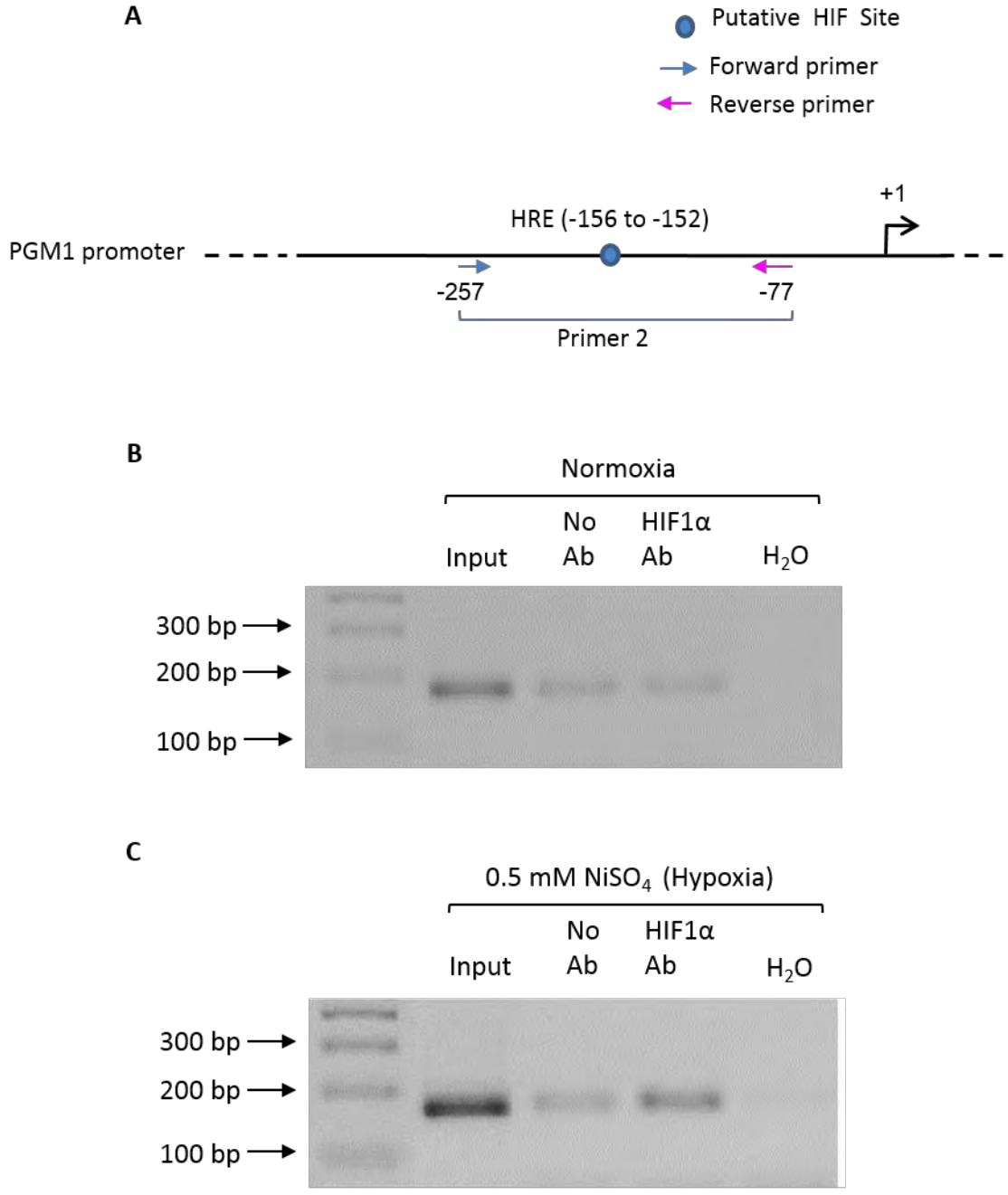

Figure 3.12. **HIF 1 a binds the (-257 to -77) region of the PGM1 promoter.** DNA Isolated from control and HIF1α immunoprecipitated material was amplified by **A.** PCR using primers spanning the putative HIF 1 site at -257 to -77 region of the PGM1 promoter. Samples of sonicated chromatin from HeLa cells either in **B.** normoxia or subjected to **C.** treatment with 0.5 mM $NiSO_4$ to mimic hypoxia, then immunoprecipitated with a HIF1 α antibody as indicated. Amplified fragments were analysed by electrophoresis on a 2% gel.

3.2.10 Analysis of hypoxia-induced PGM1 promoter activity

Mutation of the putative HIF1α binding site was carried out in order to determine whether this region contained a true Hypoxia Responsive Element (HRE) or HIF1α binding site. This was done by site directed mutagenesis in which three bases of the consensus site were converted into a BamHI restriction enzyme site (Figure 3.13A). The mutations were checked by both restriction enzyme digestion and sequence analysis. Hypoxia-induced promoter activity from the mutant construct was compared to that of the wild-type PGM1 (-1988 to +101) construct in HeLa and SVWI38. Results show in both cell lines that mutating the putative HIF1α binding site did not inhibit hypoxia induced activation (Figure 3.13 B and C). The possibility of an HRE in other locations within the -1988 to +101 promoter was thus investigated.

PGM1 promoter deletion constructs were transfected into HeLa cells, and cells were exposed to hypoxia mimicking agents. This was done order to determine the HIF responsive regions and ascertain whether the shortest deletion constructs (which excludes the (-156 to -152) region, but contains the highly conserved (+19 to +23) region) would respond to hypoxia. Our result show that all constructs including the shortest (-135 to +101) PGM1 promoter fragment, showed enhanced promoter activity in response to the treatment with hypoxia mimicking reagents (Figure 3.14), suggesting that a hypoxia-responsive element could be present in the (-135 to +101) region.

Sequence alignment of the PGM1 promoter region across multiple species and manual search revealed another potential HRE which appeared to be highly conserved at (+19 to +23) position of the PGM1 promoter (Figure 3.15 boxed in green).

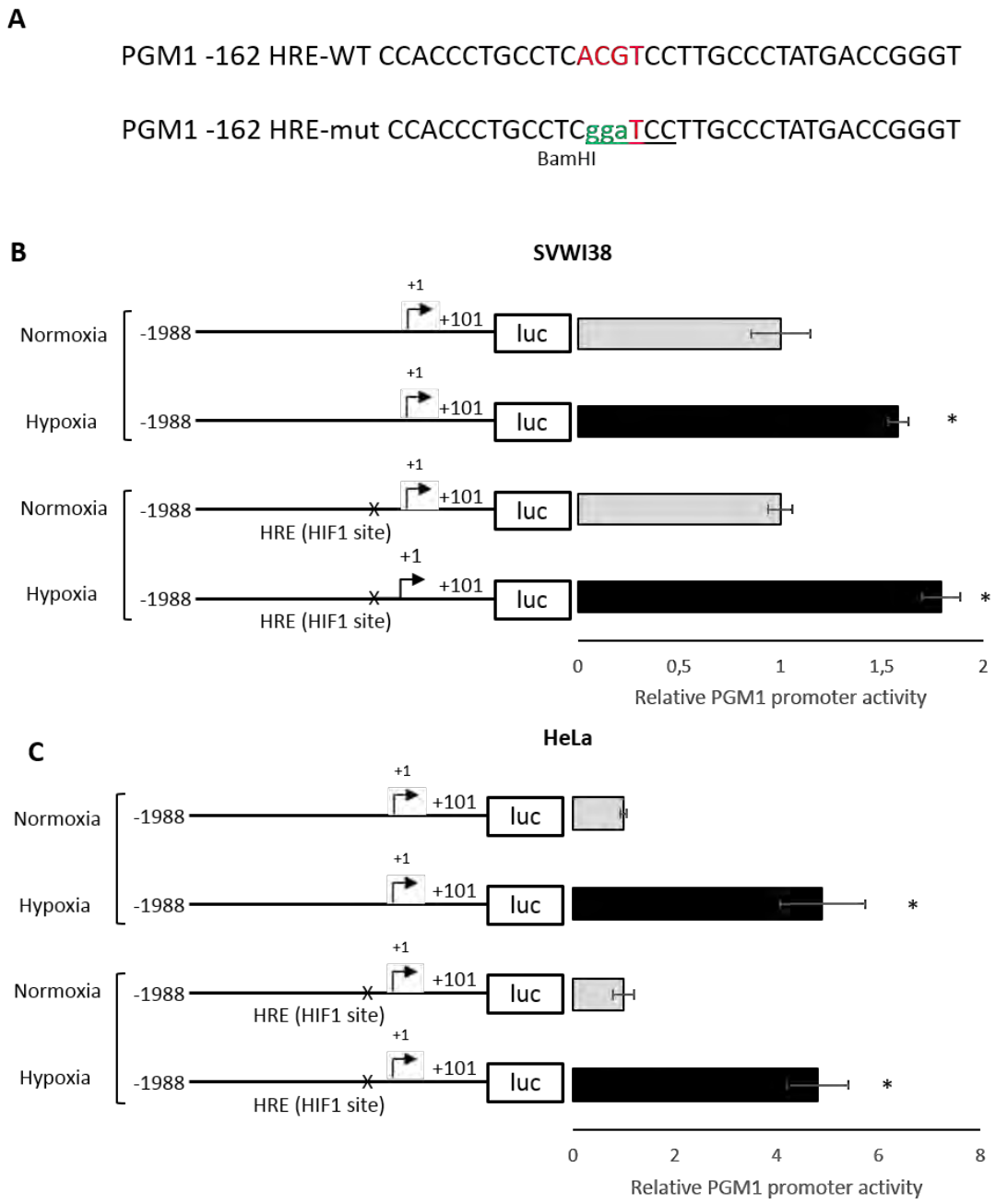

Figure 3.13: Site-directed mutagenesis of the (-156 to -152) putative hypoxia responsive element (HRE) in the PGM1 (-1988 to +101) promoter. A. Mutation of the HRE for HIF1 binding was carried out by site-directed mutagenesis using mutagenic primers, with the PGM1 (-1988 to +101) promoter construct as a template. The consensus HRE is in red, with bases chosen for mutation in green. Mutations in the HRE are marked by lower-case bold type. A BamHI restriction site was introduced and is underlined. The sense mutagenic primer is depicted. **B. and C.** Mutation of the HRE has no effect on the PGM1 (-1988 to +101) promoter activity in response to hypoxia (treatment with 0.5 mM $NiSO_4$) in SVWI38 (B) and HeLa (C) cell lines. Data was normalized to total protein. Experiments are shown as the mean ± SD of experiments in triplicate and performed at least two times (* $p < 0.05$).

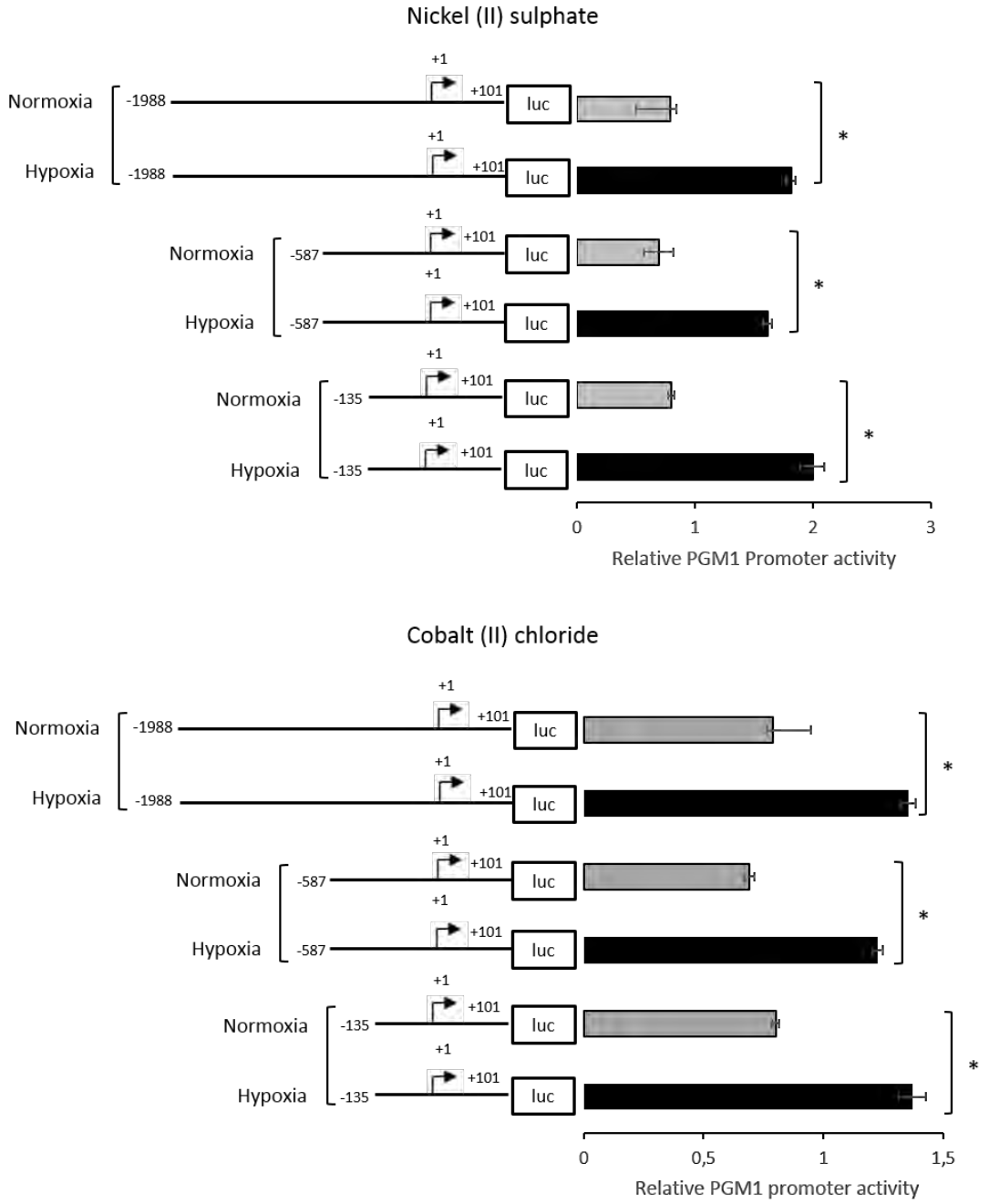

Figure 3.14: Activity of PGM1 promoter deletion constructs in response to hypoxia. Luciferase reporter constructs containing deleted fragments of the human PGM1 promoter were transfected transiently into HeLa cells then treated with 0.5 mM NiSO4 for 24 hrs to mimic hypoxia in cells. Protein concentration was used to normalize data. All PGM1 promoter fragments showed a significant increase activity in response hypoxia as well as the (-135 to +101) fragment (*$p < 0.05$). Results shown are the mean ± SEM of experiments performed in triplicate at least two independent times.

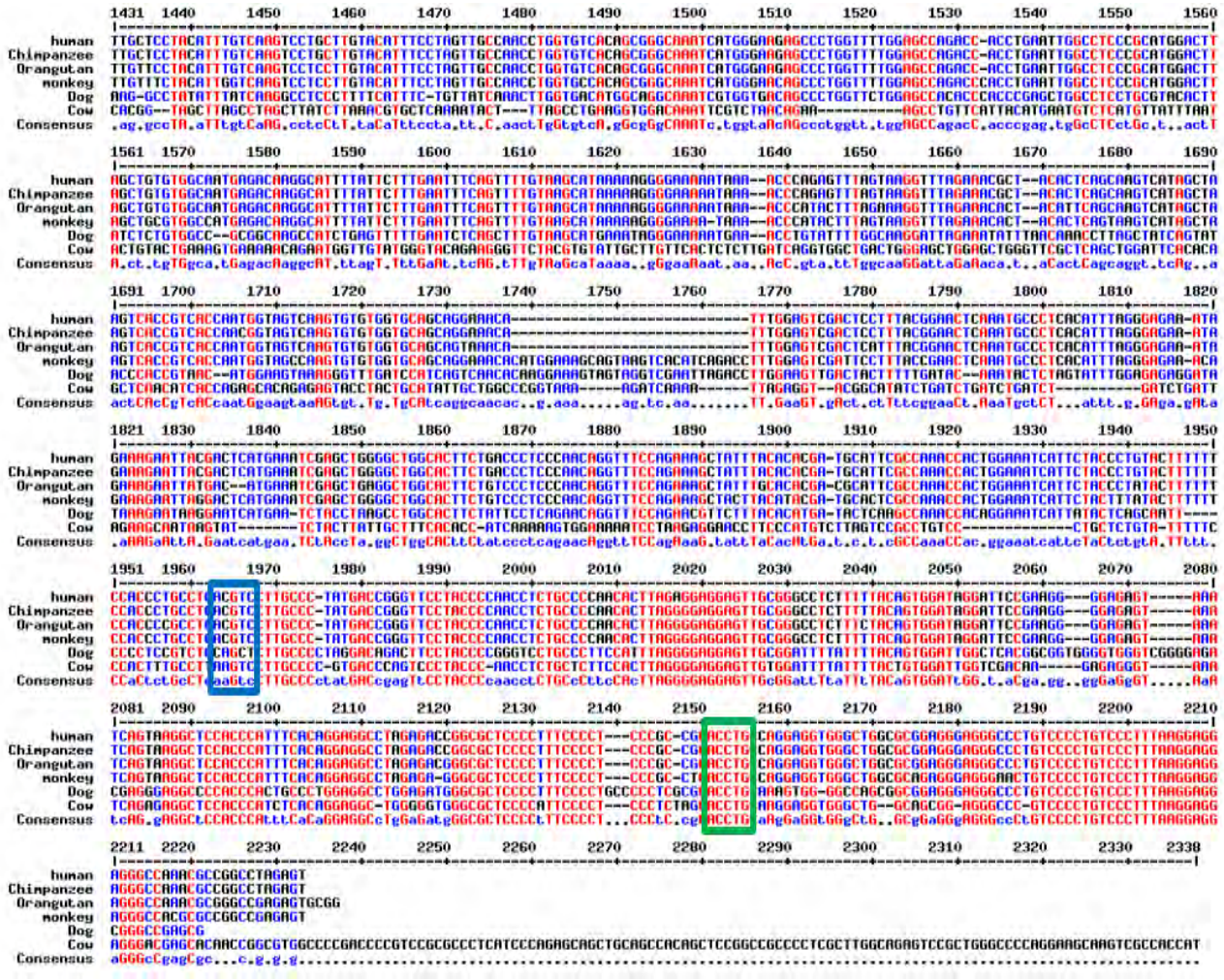

Figure 3.15: Sequence alignment showing HRE at -162 and another putative and conserved HRE at +19. Schematic representation of data from Multalin, the programme used to align wild-type (-2000 to +101) regions of the PGM1 promoter across different species. The position of the putative (-156 to -152) HRE was identified using from MatInspector (indicated in the blue box) and manually identified (+19 to +23) HRE conserved across species (indicated in the green box).

The potential HRE site located in the (+19 to +23) region was then mutated by site directed mutagenesis and the mutated promoter analysed for transcriptional activation under normoxia and hypoxic conditions. Our data shows that the response of the mutant -135 to +101 PGM1 promoter fragment behaved in similar fashion to the wild-type promoter (Figure 3.16) suggesting that the sequences around the (+19 to +23) region are not involved in HIF1α regulation of the PGM1 promoter.

A

PGM1 +19 HRE-WT CTTTCCCCTCCCGCCGGACCTGCCAGGAGGTGGGCTGG
PGM1 +19 HRE-Mut CTTTCCCCTCCCGCCGGAtCcGCCAGGAGGTGGGCTGG
BamHI

B

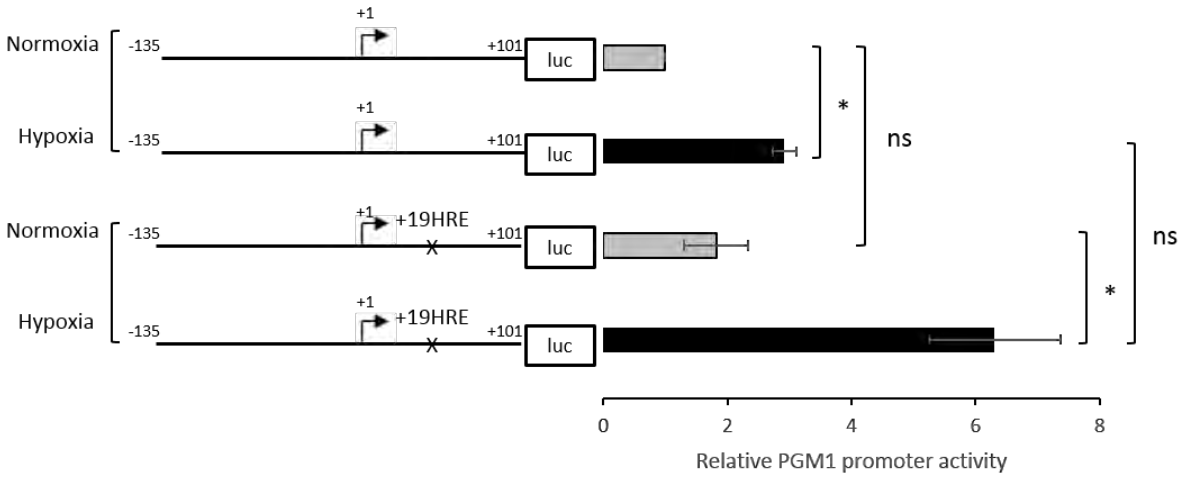

Figure 3.16: Site-directed mutagenesis of the (+19 to +23) region of the PGM1 promoter. Mutation of the (+19 to +23) region by site-directed mutagenesis using mutagenic primers, with the PGM1 (-135 to +101) promoter construct as a template. **A.** The consensus HRE is shown in red, with bases chosen for mutation in green. Mutations in the HRE are marked by lower-case bold type. A BamHI restriction site was introduced and is shown **B.** Mutation of the HRE does not reduces PGM1 (-135 to +101) promoter activity as measured by luciferase assays in response to hypoxia (treatment with 0.5 mM $NiSO_4$) in the HeLa cell line. Total protein was used to normalize all data. Results shown are the mean ± SEM of three independent experiments each performed in triplicate (*$p < 0.05$), ns = not significant.

3.3 DISCUSSION

Differential expression patterns in genes encoding enzymes involved in metabolism have been observed in a number of cancers, and deregulation of some of these genes has been linked to specific clinical outcomes in cancers (Cavalieri et al. 2007; Chaika et al. 2012). Alterations in genes involved in glucose metabolism has also been described and associated with cell survival in pancreatic cancer (Gapstur et al. 2007). Investigating transcriptional regulatory mechanisms that underpin these differential patterns in gene expression to account for the altered metabolic profile of cancer cells can assist in providing insight into processes and pathways that drive and sustain carcinogenesis.

Here we cloned the PGM1 promoter in order to investigate the transcriptional mechanisms responsible for the high expression of PGM1 seen in cervical cancer cells. We show here that changes in PGM1 gene expression in cancer compared to normal are likely, associate with the transcription factor activities of E2F and HIF as endogenous levels of PGM1 expression responded to alteration in the presence of these transcription factors.

Rb has been shown to suppress the transcription of the metabolic enzymes such as; thymidine kinase (TK) and dihydrofolate reductase (DHFR), which are both required for the synthesis of nucleotides. Rb's negative effect on metabolic enzymes occurs through physical interaction with E2F proteins which result in the suppression of energetic and anabolic functions in metabolism (Clem & Chesney 2012). In our study, we show that when E2F function is inhibited via DP1 siRNA treatment or overexpression of RB or through HPV16 oncoprotein E7 siRNA targeting, endogenous PGM1 levels are inhibited, suggesting that E2F/DP1 regulates PGM1

expression. We also show direct binding of DP1 (suggesting E2F/DP1 complexes) to the PGM1 promoter via ChIP assay.

The region of the PGM1 promoter necessary for E2F/DP1 regulation of PGM1 expression was assessed via generation of deletion constructs of the PGM1 promoter. Our results showed that although binding of the DP1 protein was observed using ChIP assays in the areas spanning the putative E2F sites across the (-1988 to +101) promoter, the region (-135 to +101) was sufficient for maintaining high PGM1 promoter activity. We also observed that E7 inhibition significantly decreased PGM1 promoter activity in this region. Mutation of the three putative E2F sites (a, b and c) in the (-135 to +101) region by site directed mutagenesis however, had no effect on the activity of the promoter construct. These findings using artificial promoter constructs did not reconcile with what was observed on endogenous PGM1 levels. It is possible that there are other factors complexed with DP1 that could bind to the PGM1 promoter in -135 to +101 region and contribute the high PGM1 expression observed. DP1 has been reported to have other binding partners apart from E2F (Harbour & Dean 2000; De La Luna et al. 1999). Studies have shown p53 to compete with E2F1 for DP1 binding and mutational analysis to define within DP-1 a C-terminal region required for the interaction with p53, thereby providing an alternative mechanism through which p53 can regulate cell proliferation (Sørensen et al. 1996). A recent study also proposed novel functions of DP1 in which transcriptional activities were independent of E2F proteins to co-ordinate the Wnt/β-catenin signalling (Kim et al. 2012). There is also a chance that the obstruction of only one site at a time would not be sufficient to eliminate all promoter activity and therefore future work could possibly look at investigating the effects of a “triple mutant” in which all three sites within the (-135 to +101) region are removed.

Several studies have implicated hypoxia as a promoter of the expression of genes involved in glucose metabolism (Lum et al. 2007; DeBerardinis et al. 2008; Brahimi-Horn et al. 2011). More recently, PGM1 protein expression was shown to increase in response to hypoxic environments, such as seen when cancer cells were treated with anti-angiogenic agents (Favaro et al. 2012; Pelletier et al. 2012). To mimic hypoxia we treated cells with hypoxia mimicking agents which inhibit the function of PHDs thereby stabilizing HIF and allowing for investigations on the effects of HIF activation on PGM1 expression. We showed that PGM1 protein, mRNA and promoter activity was increased in response to hypoxia thereby validating these recent observation in our current context.

An *in silico* search for potential HIF responsive elements identified a putative HRE at position (-156 to -152) in the PGM1 promoter, and ChIP assays showed binding of HIF-1α within the region surrounding the putative HRE. Artificially mutating the (-156 to -152) region of the PGM1 promoter had no effect on PGM1 promoter activity in response to hypoxia. Transient transfection of PGM1 promoter deletion constructs found a hypoxia response to still occur within the (-135 to +101) region of PGM1 promoter. A manual search for potential HRE sequences within this region identified another potential HRE, located at (+19 to +23). Mutagenesis of this region however, showed no abrogation of PGM1 promoter activity in response to hypoxia. This suggests indirect effects of hypoxia and the hypoxia-mimicking agents (nickel II sulphate and cobalt II chloride) on PGM1 promoter activity, possibly through the binding of other transcription factors which may or may not be HIF-target genes such as metal-regulatory transcription factor 1 (MTF-1) or otherwise termed the metal-responsive-element (MRE) binding transcription factor. MTF-1 is a pluripotent transcriptional regulator

involved in cellular adaptation to various stress conditions, primarily exposure to heavy metals but also to hypoxia or oxidative stress (Günther et al. 2012; Saydam et al. 2002). MTF-1 has been shown to promote the cadmium-induced expression of N-myc downstream regulated gene (NDRG1). The exact molecular function of NDGR1 is unknown, however it has been shown to respond to several stress conditions and is often overexpressed in many types of cancer and the hypoxia-induced expression NDGR-1 has been established to be HIF1-dependent (Bracher 2009). It is therefore likely that a similar mechanism could be applicable to the regulation of PGM1 under stress conditions, by both hypoxia and metal-induced stress which in our experimental model may obscure isolated hypoxic events.

Together our data suggests that PGM1 expression is regulated by transcription factors such as E2F/DP1 and HIF1α. This regulation was observed in endogenous protein expression and at a transcriptional level as seen by alterations in mRNA expression and promoter activity. The regions in the PGM1 promoter responsible for E2F/DP1 and HIF1α regulation is however not clear at present as mutations of the putative binding sites had no effect on PGM1 promoter activity. Further investigations are required to identify the exact regions involved.

CHAPTER 4

THE EFFECT OF PGM1 INHIBITION ON CANCER CELL METABOLISM AND BIOLOGY

4.1 INTRODUCTION

The immortalization and transformation of cells to attain a malignant phenotype is mostly driven by altered or abnormal gene expression patterns that consequently influence metabolic process in order to sustain tumour growth, viability and spread (Liu et al. 2010). Cancer cells are subject to fluctuations in extracellular conditions that often include periods of inadequate supply of energy sources such as glucose and glutamine, as well as oxygen. Nutrient availability is dependent upon an adequate blood supply to and within the growing tumour mass. In advanced solid tumours, oxygen delivery to the neoplastic and stromal cells is often reduced or even abolished by a diminishing diffusion gradient, structural abnormalities of tumour microvessels, and resultant disturbed microcirculation (Vaupel et al. 1989). Irregularity in oxygen distribution causes changes in metabolic processes often driven by the activation of the transcription factor, HIF which promotes cancer cell survival and continued proliferation.

The uptake, trafficking and conversion of glucose into energy, forms an integral part of the cancer's response to the tumour microenvironment and these processes in cancer create a very unique metabolic profile directed by aberrant transcription factor activity.

Recent studies have revealed a number of metabolic enzymes that show elevated expression and activity in cancer. Some of these enzymes have gained attention in the last decade as

potential therapeutic targets, with drugs targeting these enzymes being either under preclinical investigations or approved for clinical use (Vander Heiden 2011). Vander Heiden, (2011) makes a case for chemotherapy designed based on either targeting nucleotide, protein or lipid synthesis, amino acid, fatty acid, NAD or mitochondrial metabolism, glycolysis and the TCA cycle.

In addition to the potential of individually targeting key molecules in metabolic pathways for cancer therapy, co-targeting metabolism along with traditional treatment regimens may help to overcome resistance to other cytotoxic agents by persistent cancer cells still stands. To exploit cancer metabolism and more rationally select complementary target combinations would require a thorough understanding of pathway biochemistry and metabolic regulation in cancer (Vander Heiden 2011). The basis of our investigations on the role PGM1 in cancer metabolism stem from its positioning in glucose metabolism. Much ambiguity still surrounds which pathways are preferentially supported by PGM1 activity due to the reversible nature of the enzyme. Our goal was to determine the following; which pathways; glycolysis, pentose phosphate pathway or glycogen synthesis are enhanced by PGM1 function and preferred by cancer cells when subjected to stresses commonly found in tumour settings such as hypoglycaemia and hypoxia. Secondly, to determine the biological significance of elevated PGM1 expression in cancer.

As G6P, a direct product of PGM1 function in one direction, is a substrate for glycolysis, we investigate the effect of inhibiting PGM1 on glycolysis. Inhibition of glycolysis has been shown to effectively kill colon cancer cells and lymphoma cells in hypoxic environments in which the cancer cells exhibit high glycolytic activity and decreased sensitivity to common anticancer

agents (Xu et al. 2005). Furthermore, depletion of ATP through inhibition of glycolysis has also been shown to potently induce apoptosis in multidrug-resistant cells (Xu et al. 2005).

G6P is also a substrate of the pentose phosphate pathway, a process that produces NADPH which is believed to contribute towards protecting cells from oxidative damage by scavenging ROS. This is particularly true for cancer cells where intracellular ROS levels may be higher due to excessively high proliferative rates (Tsouko et al. 2014). NADPH is also required for lipogenesis supporting de novo synthesis of cell membranes (Perl et al. 2012). Somatic mutations resulting in oncogene activation and tumour suppressor inactivation are in part due to ROS produced as by-products of metabolism (Dang 2012).

Glycogen is thought to provide an alternative source of energy for cancer cells under conditions of metabolic stress such as hypoxic and/or glucose depletion (Lee et al. 2004; Pescador et al. 2010; Pelletier et al. 2012; Favaro et al. 2012). We sought to determine whether PGM1 inhibition would influence the cells' glycogen content, as excess G6P (that may accumulate via the action of hexokinases) can be converted to G1P by PGM1, after which, through a number of modifications, the modified UDP-glucose units are then linked up to construct glycogen polymer through the action of glycogen synthase 1 (GYS1). The synthesized glycogen can later be mobilized for energy in the event of a deficit in glucose entry from the extracellular environment.

Jones & Thompson, (2009) stated that; "Growing tumours face two major metabolic challenges— how to meet the bioenergetic and biosynthetic demands of increased cell proliferation, and how to survive environmental fluctuations in external nutrient and oxygen availability when their growth outpaces the delivery capabilities of the existing vasculature". The chronic and optimized use of glucose by cancer cells is thought to be means to tackle both

challenges. As a carbon source, glucose through accelerated glycolysis can provide the ATP needed to sustain cellular functions and biosynthetic precursors to support cancer cell proliferation (Moreno-Sánchez et al. 2007; Sonveaux et al. 2012; Bao et al. 2013). Converting excess glucose into glycogen can also be an alternative source of energy in periods of prolonged nutrient deprivation. The metabolic fate of glucose involves three pathways, glycolysis, glycogen synthesis and the pentose phosphate pathway (Figure 4.0). PGM1 is located at a significant traffic point of glucose metabolism.

In addition to monitoring metabolic pathways, whose function may be altered following PGM1 overexpression in cancer, the work done in this chapter also aimed to determine whether PGM1 inhibition affects cancer cell viability in the presence and absence of metabolic stress conditions.

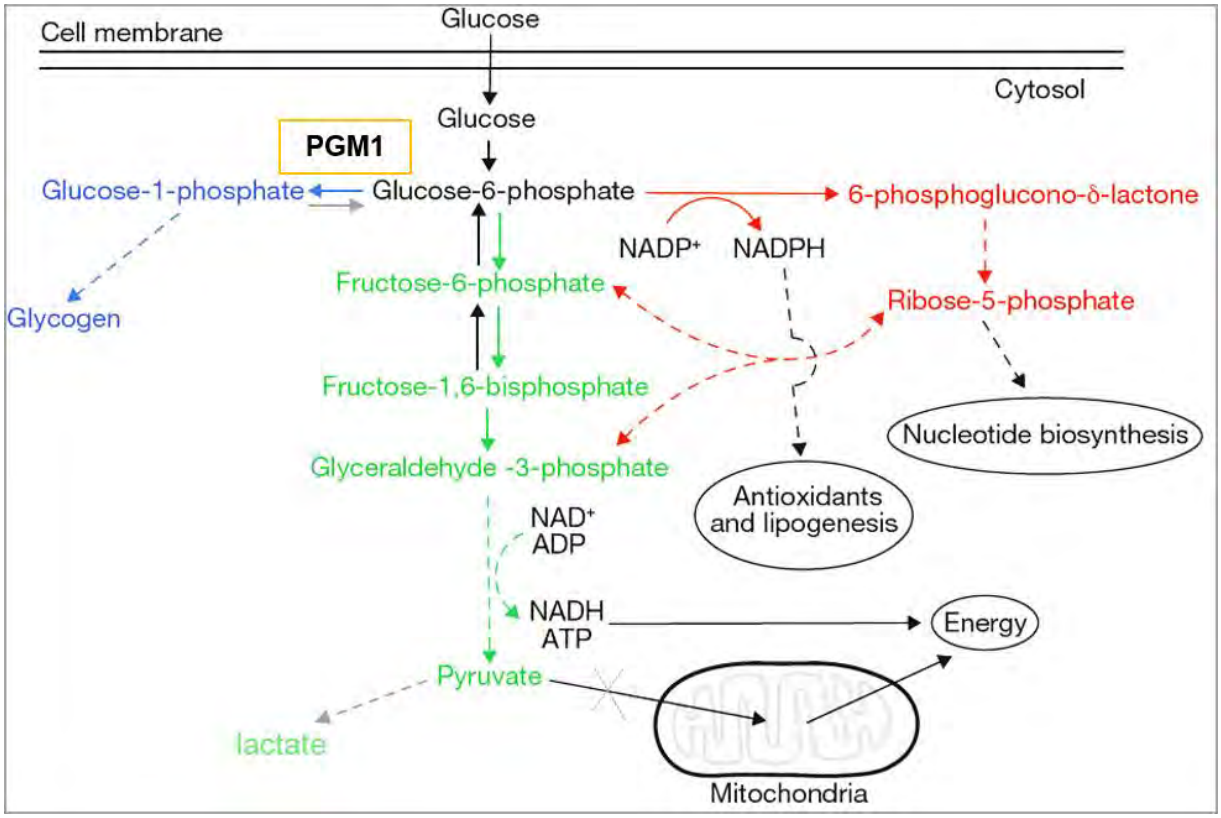

Figure 4.0. The Fate of glucose through glycolysis, the pentose phosphate pathway and glycogen synthesis. PGM1 sits at a three-way of glucose metabolic pathways; glycolysis, the pentose phosphate pathway and glycogen metabolism. The arrows represent direction of glucose conversion through the different pathways to the metabolic outputs (indicated in black circles). In glycolysis (shown in green), glucose is converted to pyruvate through to lactate for energy, the entry of pyruvate into the mitochondrial to produce energy is often limited in cancer cells. In glycogen metabolism (shown in blue) G6P is converted to G1P, a precursor in glycogen synthesis, a product whose use is more pronounced when there is a deficit in extracellular glucose entry. In the pentose phosphate pathway (shown in red) G6P is converted to R5P, a precursor for nucleotide synthesis and NADPH used as an intracellular antioxidant or in lipogenesis supporting cell proliferation. Adapted From (Gottlieb, 2011)

4.2 RESULTS

4.2.1 The effect of PGM1 inhibition on glycogen content and glycolysis in cancer cells

Our earlier results showed that PGM1 expression was high in cancer compared to normal cells in culture, and this was evident under both normoxic and hypoxic conditions. Here we aim to decipher the functional relevance of PGM1 in cancer cells by inhibiting its expression using siRNA. Western blot analysis shows successful and sustained inhibition of PGM1 in CaSki cells for up to four days post transection with targeted PGM1 siRNA in standard culture conditions of 25 mM glucose and normoxia (Figure 4.1). We performed a Periodic-Acid Schiff (PAS) stain for the presence of glycogen, where a pink stain indicated glycogen. Glycogen deposits were assayed in CaSki and HepG2 cells. Our results show that the inhibition of PGM1 in both cell lines causes a reduction in glycogen deposits in both cell lines (Figure 4.2). Accompanying western blots shows PGM1 knockdown at the same time points used to assay glycogen deposits. Glycogen content was assayed in HepG2 liver cancer cells as this cell line serves as a control for cells that should contain high glycogen levels as livers cell typically metabolize glucose into glycogen. These results were supported by the glycogen titration assay for quantitative analysis of glycogen stores. Our results show a significant reduction in glycogen content when PGM1 was inhibited in CaSki and HeLa cervical cancer cell lines (Figure 4.3). These observations were made in normal ambient culture conditions where oxygen availability and glucose are in excess, suggesting a role for PGM1 in glycogen metabolism in normoxia, in the absence of environmental stresses.

Considering the role played by glycolysis in cancer cell survival and proliferation, we sought to investigate the effect of inhibiting PGM1 expression on glycolytic output by assaying lactate production, as lactate is a well-established end product of glycolysis in cancer cells (Holroyde

et al. 1979; Kennedy & Dewhirst 2010). PGM1 converts G1P to G6P, and G6P through a series of reactions is converted to pyruvate which is then dehydrogenated to form lactate, and lactate is then secreted out of the cells into the extracellular environment where can be calorimetrically assayed.

We inhibited PGM1 expression in cancer cells and investigated whether glycolysis would be affected in high (25mM, a concentration typically used for the culturing of most cancer cell lines) (Zhuang et al. 2014) and low glucose conditions (2.5 mM glucose which is approximately half of the physiological serum concentration of glucose) by assaying lactate levels. The rationale behind examining lactate production in hypoglycaemic conditions being that; mobilizing glycogen stores may be necessary to provide energy in the cells grown under conditions of extracellular glucose insufficiency and therefore PGM1 may be required to provide the G6P that is necessary for glycolysis in this context. Our results indicate that lactate production was significantly lower in CaSki cells cultured in low glucose (2.5 mM) compared to high glucose (25mM) (Figure 4.4). PGM1 inhibition resulted in a slight, but not significant decrease in lactate production in both conditions of glucose sufficiency (25 mM) and deprivation (2.5 mM). The control cells and PGM1 knockdown cells displayed similar glycolytic output suggesting that PGM1, although participating in glycogen synthesis, it is not required for glycolysis.

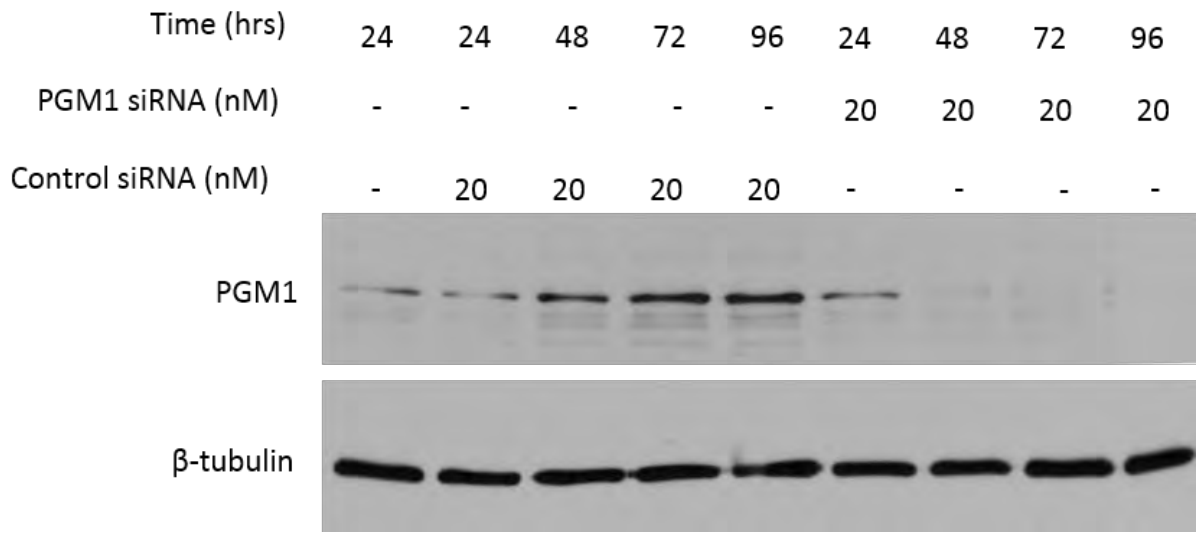

Figure 4.1. Inhibition of PGM1 expression by targeted siRNA. CaSki cells were transfected with 20 nM control or PGM1 targeted siRNA and protein was harvested at 24, 48, 72 and 96 hrs post transfection. Western Blot analysis showed significant reduction in PGM1 protein expression upon siRNA treatment. The scrambled (control) siRNA had no effect on PGM1 protein levels. Western Blots shown are representative of experiments performed two independent times.

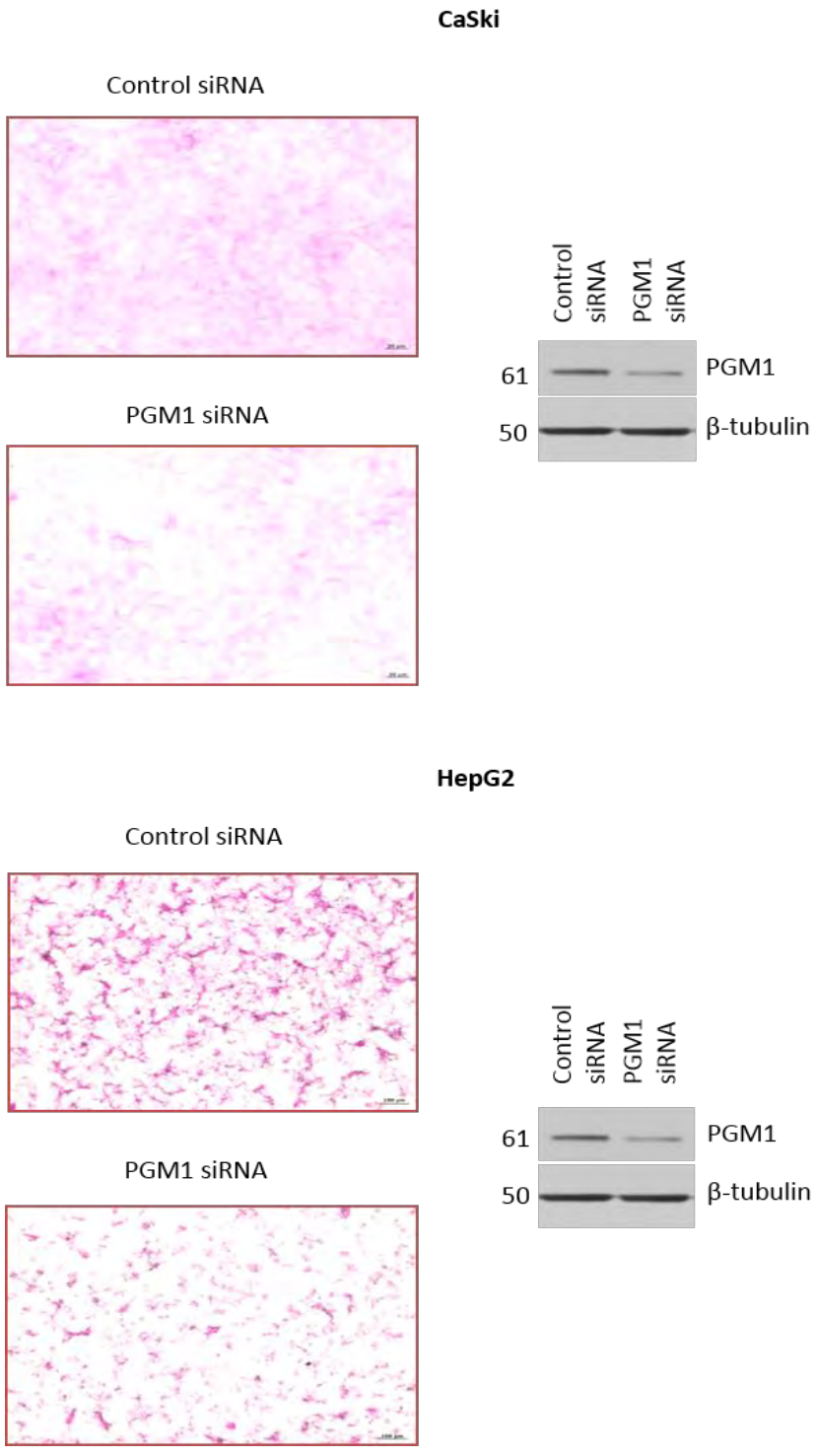

Figure 4.2. PGM1 inhibition results in decreased glycogen content in cancer cells.
Cells were cultured in media containing 25 mM glucose and transfected with scrambled Control siRNA and PGM1 siRNA over 96 hours then stained for glycogen using periodic acid and Schiff's reagent. Accompanying western blots show PGM1 inhibition at the 96hr time point.

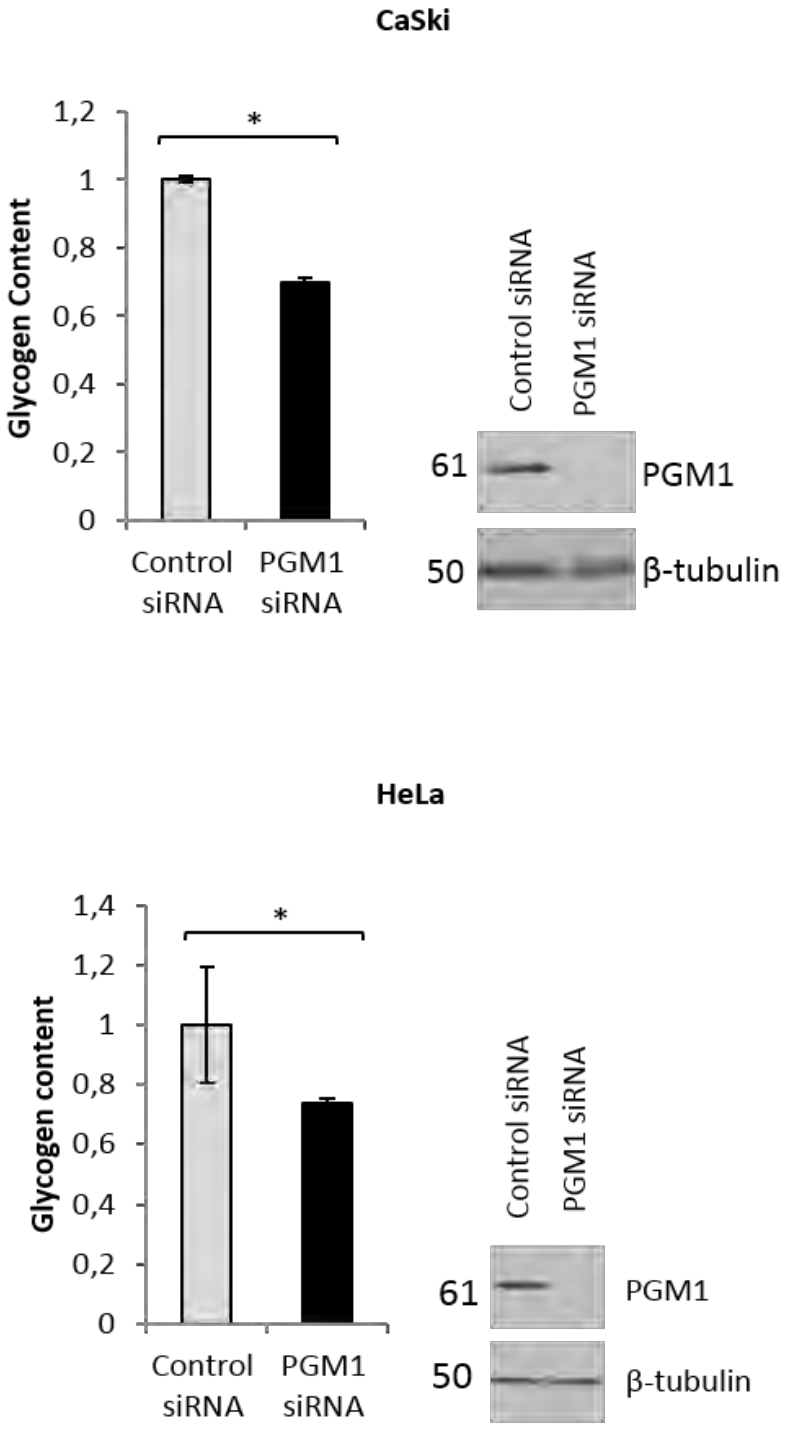

Figure 4.3 Glycogen titration assay in CaSki and HeLa. Cells were cultured in media containing 25 mM glucose and transfected with control siRNA and PGM1 siRNA for 96 hours followed by glycogen was extraction for assays. Experiments shown are the mean ± SD of experiments performed in triplicate and performed two independent times (* $p < 0.05$). Accompanying western blot analysis show inhibition of PGM1 at the assay time point.

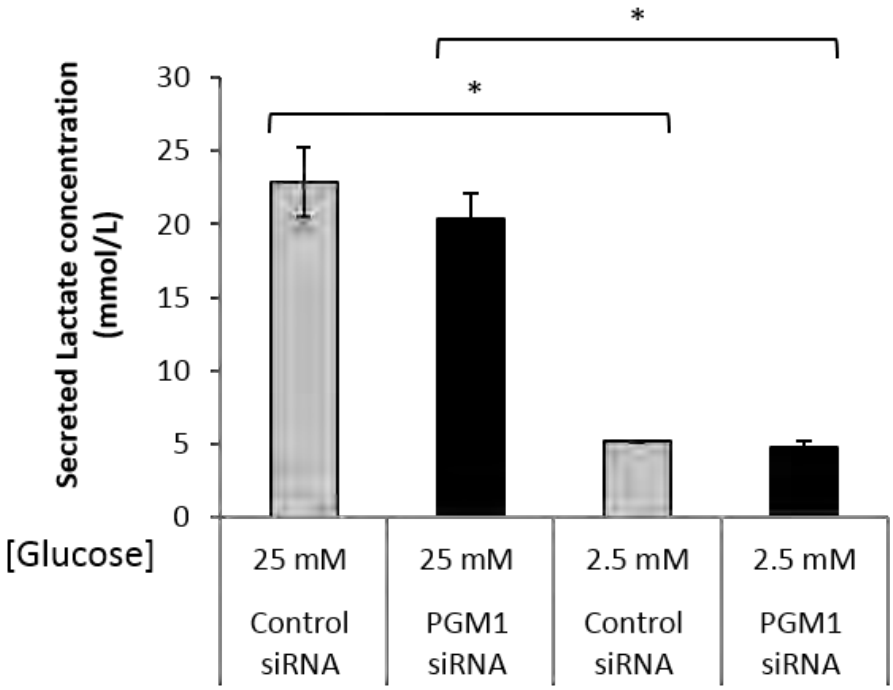

Figure 4.4. Inhibition of PGM1 expression does not affect secreted lactate levels in high and low glucose. CaSki cells were plated in High (25 mM) and Low (2.5) glucose media, then treated with PGM1 siRNA for 72hrs, media was then collected from the cells and assayed for lactate. The glucose concentration influenced lactate output significantly, where the cells cultured low glucose showed reduced concentrations of lactate. Data shown are the mean ±SD from three independent experiments *$p < 0.05$.

4.2.2 The effect of Inhibiting PGM1 expression in cancer cells on NADPH production, and intracellular ROS levels under ambient and metabolic stress conditions

Evidence from previous studies comparing the production of ROS in cancer and normal cells suggests that cancer cells in general are under increased oxidative stress compared to normal cells (Szatrowski & Nathan 1991). Other studies have also gone further to show that neoplastic transformation is associated with increased basal oxidant stress (Trachootham et al. 2006). Cancer cells also have increased accumulation of ROS-mediated reaction products as well as the over-expression of antioxidant enzymes in response to oxidative stress (Pelicano et al. 2004), implying that the degree of oxidative stress in a cell hinges on the delicate the balance between the rate of ROS generation and the activity of scavenging systems that detoxify them (Schumacker 2006). NAPDH produced from the pentose-phosphate pathway proposed to have a role a one of detoxifying systems against ROS in cancer cells. As G6P (a product of PGM1 function), is as a substrate to the NADPH producing reaction catalysed by G6PDH, we assayed NADPH levels in control and PGM1 knockdown cells. We hypothesized that inhibiting PGM1 would result in a decrease in G6P and hence a decrease in NAPDH levels. Surprisingly, we observed an in increase NADPH in PGM1 knockdown cells grown in both high (Figure 4.5A) and low (Figure 4.5 B) glucose conditions. The difference was marginal in high glucose and was more pronounced under conditions of hypoglycaemic stress (Figure 4.5B).

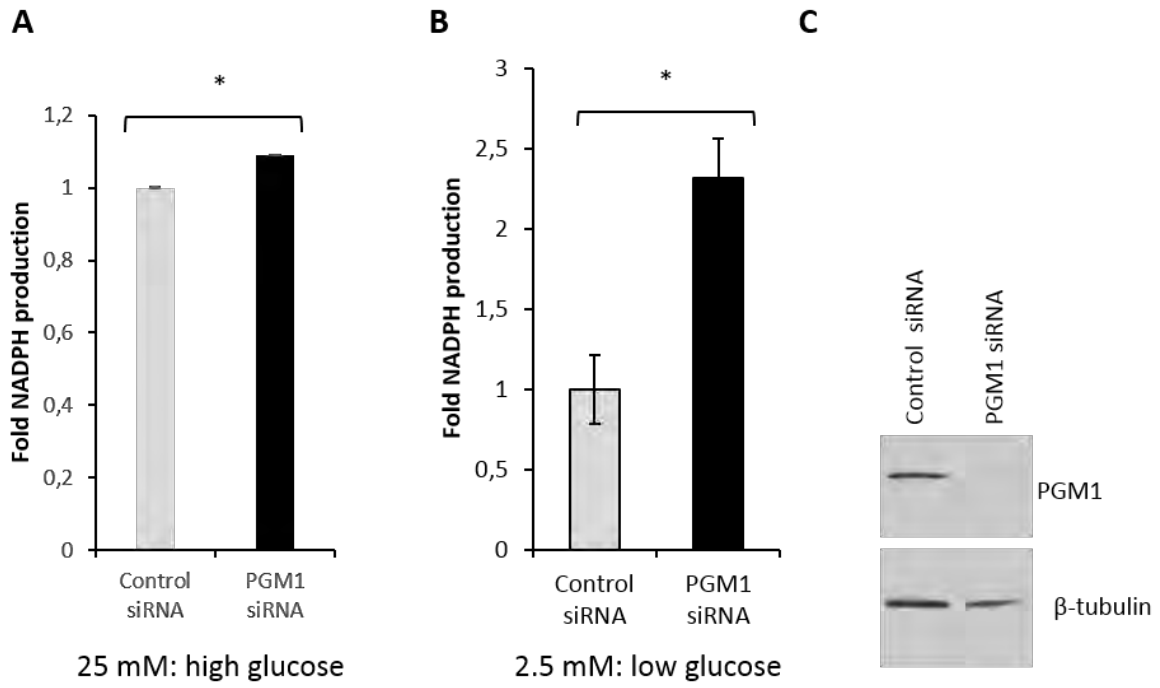

Figure 4.5. PGM1 inhibition significantly increased NADPH levels CaSki cells were cultured in **A.** 25 mM glucose and **B.** 2.5 mM glucose then transiently transfected with PGM1 siRNA and levels of NADPH were investigated 72 hrs post transfection using the NADPH assay (Abcam). A significant increase in NADPH levels when PGM1 was inhibited was observed. **C.** Western blots showing PGM1 inhibition, β-tubulin used as a loading control. Results the mean ± SEM of experiments performed in triplicate and repeated at least two independent times. * $p<0.05$

Since changes in NADPH levels influence general oxidative state of cells, we assayed global ROS levels in control and PGM1 knockdown cells. Inhibiting PGM1 had no effect on ROS production in conditions of low and high glucose (Figures 4.6 A and B). Interestingly, when cells were exposed to hypoxia (1% oxygen in a hypoxic chamber), we observed hypoxia-induced ROS production in both high and low glucose conditions (Figure 4.7 A), which is a documented result of exposure to oxygen deprivation (Kondoh et al. 2013). Despite these changes in ROS following hypoxic treatment, PGM1 knockdown did not influence the global ROS levels. The accompanying western blots show reduction in PGM1 expression PGM1 siRNA in all the conditions in cells tested (Figure 4.7 B). These results suggest that while PGM1 influences NADPH levels these changes are not sufficient to lead to changes in ROS production.

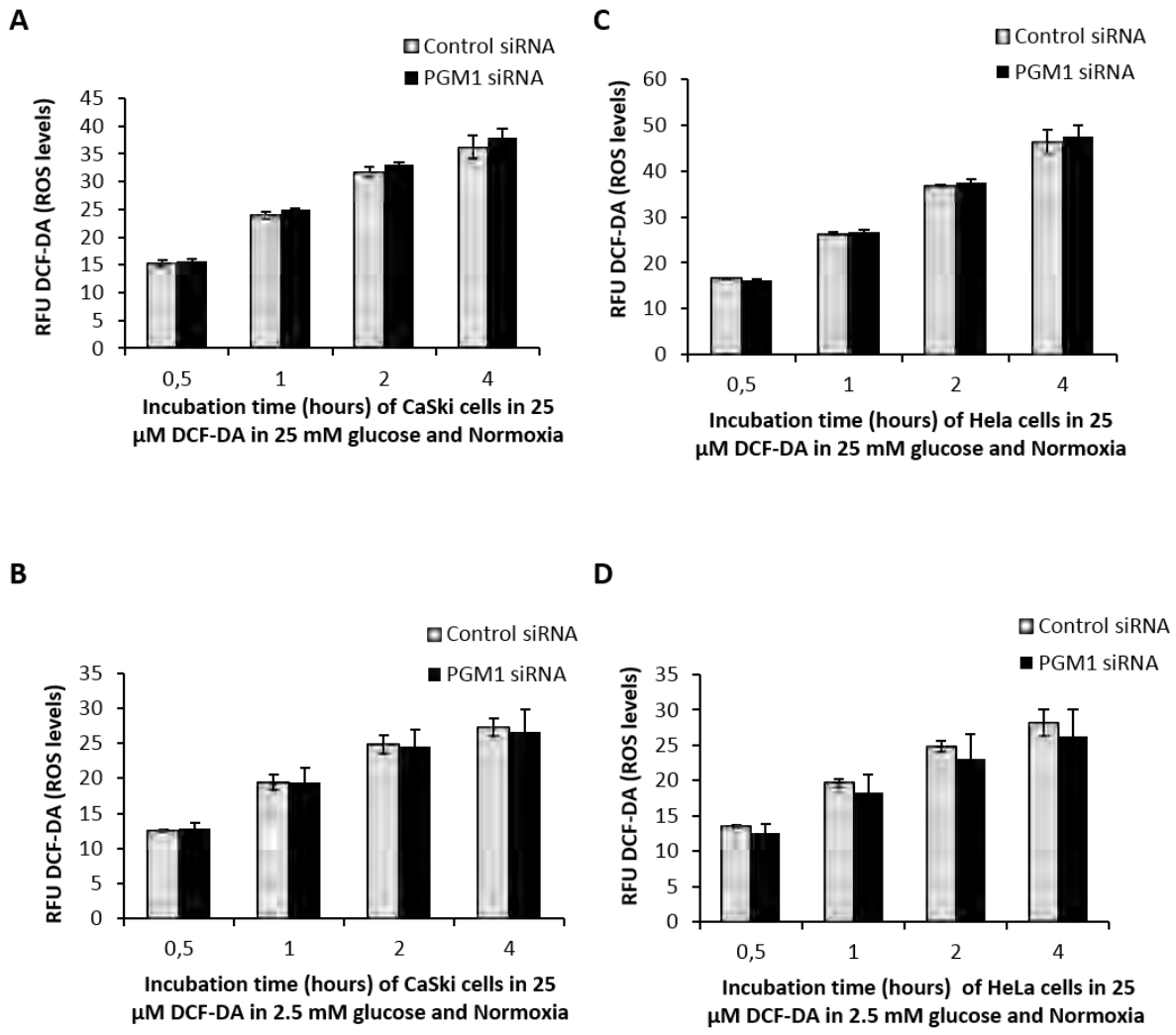

Figure 4.6. PGM1 function does not influence the oxidative state of cancer cells. **A. and B.** CaSki and **C. and D.** HeLa cells grown in 25 mM (A and C) and 2.5 mM (B and D) glucose containing DMEM respectively and transiently transfected with control and PGM1 siRNA. All cells were then incubated with 25 µM DCF-DA for 30 min at 37°C after fluorescence was measured every hour. ROS generation was measured by oxidation of DCF-DA. Western blot analysis was performed to verify inhibition of PGM1 expression in the experiment. No difference in ROS was observed in all conditions in response to PGM1 inhibition. Histograms represent the mean ± SD of experiments samples and are representative of three independent experiments.

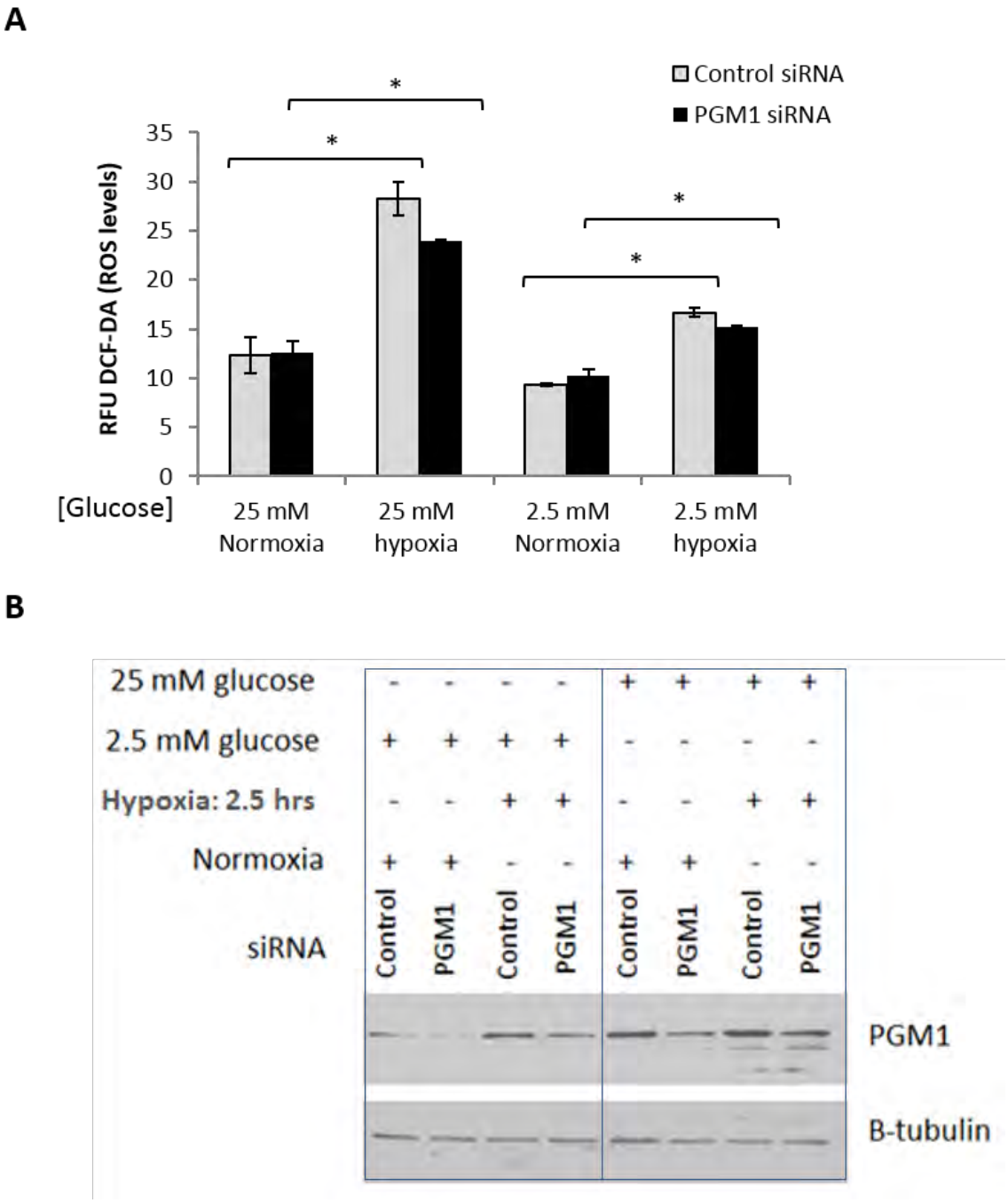

Figure 4.7. PGM1 has no effect on hypoxia-induced ROS generation. **A.** CaSki cells were transfected with control and PGM1 siRNA for 72 hours, then incubated with 25 µM DCF-DA for 30 min after which cells were subjected to 1% oxygen for 2h30 min then assayed for ROS generation as a function of DCF-DA fluorescence. Results shown are the mean ±SD of experiments done in triplicate and performed at least two independent times, *$p<0.05$ comparing normoxia and hypoxia. **B.** Protein lysates were harvested in parallel and run on a western blot to detect PGM1 expression, β-tubulin was used as a loading control.

4.2.3 The effect of inhibiting PGM1 on cancer cell proliferation

The effect of PGM1 inhibition on cancer cell proliferation was investigated by transiently inhibiting PGM1 expression using siRNA and assaying effects on proliferation in CaSki and HepG2 cells. Experiments were conducted in different media concentrations of glucose (25, 10, 5 and 2.5 mM) as standard culturing media typically contains glucose levels that far exceed physiological serum concentrations (which is around 5.0 *mmol/L*) (Marín-Hernández et al. 2011; Dubois et al. 2010). Our results show that inhibition of PGM1 had little effect on cell proliferation in all conditions (Figure 4.8 A-H) expect a marginal increase in proliferation observed in CaSki cells grown in 2.5 mM glucose (Figure 4.8 D).

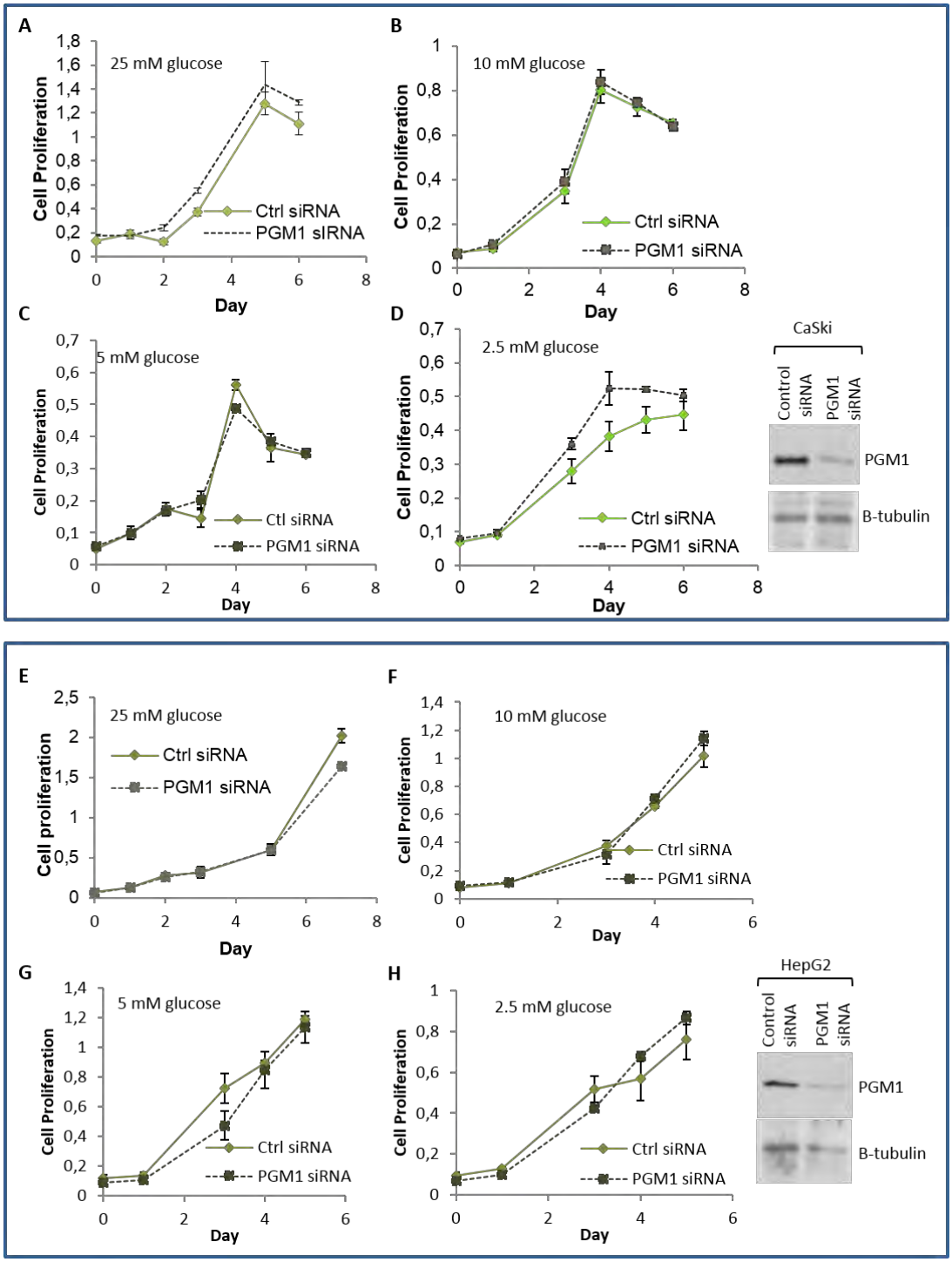

Figure 4.8. PGM1 knockdown in cancer cells does not influence cell proliferation in physiological to high glucose levels. PGM1 expression was inhibited in **A-D.** CaSki cells and **E-H.** HepG2 cells using PGM1 targeted siRNA and a scrambled sequence was used as a control (ctrl). Effects on cell proliferation were assayed using of MTT assays in cells cultured in media containing 25, 10, 5 and 2.5 mM glucose concentrations. Cells were transfected with Ctl and PGM1 siRNA, after 24 hrs re-plated into 96 well dishes containing media of different concentration. Accompanying western blots were run to verify PGM1 inhibition cells after 24 hrs post transfection with siRNA.

We next inhibited PGM1 in conditions of oxygen deprivation and hypoglycaemia. These stresses go hand-in-hand in late-stage tumour presentation, thereby creating a simplified version of an *in vitro* mimic of the tumour microenvironment as described by Onozuka et al, (2011). Our results show that when cells encounter the double stress of low glucose and hypoxia PGM1 inhibition results in a reduction in cell proliferation within 24 hrs of hypoxia and low glucose. Our data suggest that under a combination of severe stress such as hypoglycaemia and hypoxia, PGM1 is in part required for cancer cell proliferation.

A

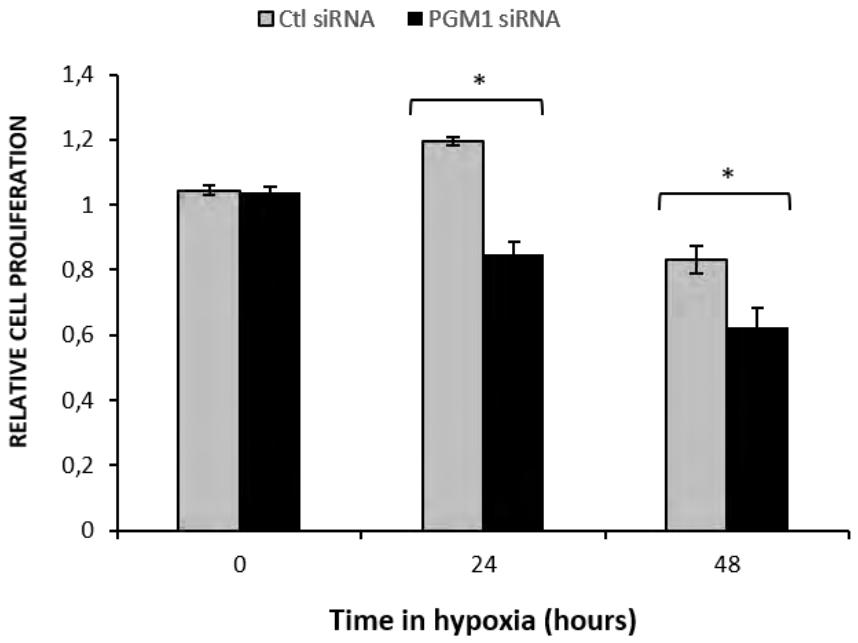

B

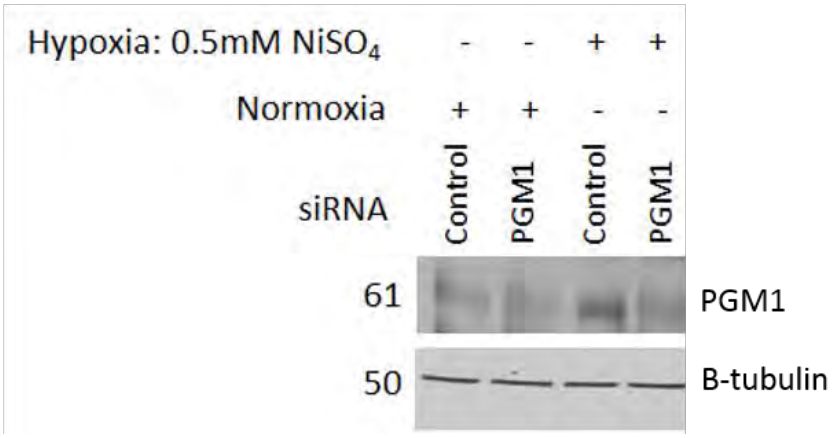

Figure 4.9. Cell viability in low glucose (2.5 mM) and normoxia vs. hypoxia. A CaSki cells grown in 2.5 mM glucose were subjected to treatment with 0.5 mM $NiSO_4$to mimic hypoxia and proliferation was assayed. **B** Protein lysates were extracted 48 hours post transfect/24hrs after exposure to hypoxia mimicking agent. The Western blot below the bar charts was run to verify PGM1 inhibition in the experiment. Results are the mean ±SD of experiments performed in quadruplicate and repeated at least two independent times *p <0.05.

4.3 DISCUSSION

Conditions in the extracellular environment of cancer cells or *in vivo*-tumour microenvironment are understood to be quite variable due to spatial challenges that often follow rapid cell proliferation and consequent expansion of the tumour mass. What is generally known and acknowledged is that the tumour microenvironment often experiences periods of hypoxia and hypoglycaemia and often acidic, a factor that has been largely attributed to the cancer cell's preference for aerobic glycolysis that results in the production and excretion of lactate into the extracellular space.

Our data, in agreement with current literature (Pelletier et al. 2012; Bae et al. 2014) shows that PGM1 inhibition results in reduced glycogen content in cancer cells. Our data using transient siRNA to inhibit PGM1 in cervical and liver cancer cell lines (CaSki, HeLa and HepG2 cells) support the findings of Bae et al. (2014). The decrease in glycogen content was seen outside of hypoxic stress conditions and interestingly, the extracellular glucose concentration was sufficient to influence the levels of stored glycogen in cancer cells. Our results support the hypothesis that PGM1 is closely involved in the modulation of glycogen content in response to extracellular glucose levels.

The question as to whether the stored glycogen proved beneficial for cancer cells in conditions of nutrient deprivation was addressed by looking at glycolytic output and effects on the pentose phosphate pathway. Our data showed that while glycogen content was directly influenced by PGM1 inhibition there was minimal effects on, glycolytic output as measured by lactate production. As the glucose concentration was decreased in the media, lactate production also declined but the presence or absence of PGM1 did not significantly influence yields regardless of the extracellular glucose concentration that the cells were

exposed to. It therefore seems that PGM1 function appears to mainly support glycogen synthesis, and not necessarily glycogen mobilization in this context, in contrast to findings done in yeast systems (Fu et al. 2000). Yeast systems have traditionally been extrapolated to have implications in cancer cells metabolism (Gururaj et al. 2004), however do not take into into account the impact of abnormal signalling that is often a feature of the cancer phenotype.

We hypothesised that PGM1 could be enabling activities of the PPP, supporting macromolecular synthesis of lipids and nucleotides while also assisting in the scavenging ROS. Our data showed that PGM1 inhibition led to a significant increase in NADPH, particularly in hypoglycaemic conditions. This observation was surprising as we anticipated that inhibiting PGM1 would result in a decrease in NADPH levels. PGM1 inhibition led to a decrease in glycogen content, while having little effect on glycolysis. It is therefore conceivable that the remaining outlet for the glucose processing would be through flux into the pentose phosphate pathway and hence the subsequent increase in NADPH under low glucose conditions. Another explanation as to why NADPH production was increased in response to PGM1 inhibition is that NADPH is not only produced through the pentose phosphate pathway. Although the PPP plays as major part, other NADPH sources include the malic enzymes Me 1 and 2 as well as IDH (Jiang et al. 2014). Given the important role played by NADPH in maintaining cellular functions and its activity as a cofactor for many enzymes, breaking the balance between NADP+ and NADPH by blocking one or two of the pathways required to maintain this homeostasis would influence the activity of the others. It is possible that in our assay conditions, a compensatory effect between these NADPH-generating enzymes may be involved, as suggested by Jiang et al, (2014), in which NAPDH production via the malic enzymes and respond to the reduced outputs of the PPP due to depletion in hypoglycaemic stress in low glucose media. Our experimental design did not exclude or isolate out only the

NADPH produced via the PPP but assayed global NAPDH production making it likely that the other pathways could contribute towards NADPH production and even overcompensate for the limited outputs of PPP.

An increase in NADPH production as literature would suggest, should yield increased macromolecular synthesis and reduced levels of ROS however, our data showed that while NADPH production increased in response to PGM1 knockdown, ROS levels were left unaffected irrespective of the extracellular environment. A possible reason to account for this observation may be that the changes in NADPH via the PPP were not sufficient to counteract or overcome the high levels of ROS. Hypoglycaemia stress would likely cause cells prioritize glucose metabolism via glycolysis over the PPP as the two process are co-ordinated together (Berg et al. 2002).

Increased PGM1 expression was observed in late-stage cervical cancer specimens. A common characteristic of late stage cancer presentation is the emergence of hypoxic regions and a hypoglycaemic environment that is often associated with the insufficiency of the tumour vasculature. To find out whether cancer cells show a dependence on PGM1 for their survival and proliferation, we investigated responses to PGM1 inhibition in ambient and sufficient nutrient availability conditions as well as in sustained hypoglycaemic and hypoxic stress conditions. The proliferation of cells grown in high glucose was not affected by PGM1 inhibition. This result was not surprizing as it is unlikely for cells to rely on glycogen content in an environment of glucose sufficiency. Bae et al, (2014) demonstrate that PGM1 inhibition did not show effects on cell number when cell were left to grow in 25 mM glucose. Reduced proliferative rates were only visible subsequent to a complete depletion of glucose in the culture media for 2 hrs followed by re-feeding of cells with 10 mM glucose (Bae et al. 2014).

The control cells were able to recover from the short-lived glucose deprivation while PGM1 knockdown cells proliferated at a diminished rate. Our data, while complementing findings by Bae et al, (2014) in high glucose, showed that both CaSki and HepG2 cells were not affected by PGM1 knockdown in low glucose environments for prolonged periods. PGM1 knockdown cells grown in 10 to 2.5 mM glucose concentrations proliferated at comparable rates to the control cells, suggesting that PGM1 function was non-essential for survival under sustained hypoglycaemic stress. While both CaSki and HepG2 cells underwent cell proliferation in low glucose (2.5 mM) conditions, neither cell could survive and conditions of zero glucose (data not shown).

When exposing cells to a combination of hypoglycaemic stress, and to a hypoxia mimicked environment, PGM1 knockdown cells showed significantly reduced proliferation. This could be explained by the fact that control cells treated with hypoxia can access their glycogen stores and even store up more glycogen in response to HIF signalling as reported by (Pelletier et al. 2012; Pescador et al. 2010; Favaro et al. 2012)). PGM1 knockdown cells on the other hand have had no access to stored glycogen in low glucose and hypoxia conditions. These findings support the theories demonstrating that cancer cells rely on their own intracellular reservoirs of energy when grown in deficient and depreciating nutrient environments.

CHAPTER 5

CONCLUSIONS

5.1 MAIN CONCLUSIONS

Altered metabolism as an additional hallmark of cancer cells has been subject to much discussion in the past decade (Hanahan & Weinberg 2011; Ward & Thompson 2012). Cancer cells deregulate metabolic pathways as a means to maximize energy utilization and metabolite outputs to support biosynthetic processes occurring in highly proliferating cells (Vander Heiden et al. 2009). Differential expression patterns in metabolic gene expression have been observed in a number of cancers with links to clinical outcomes observed in a few, these include alterations in glucose metabolism which have been described and associated with cell survival in cancers such as pancreatic and colorectal cancer (Cavalieri et al. 2007; Chaika et al. 2012; Gapstur et al. 2007).

The targeting of metabolic pathways has shown promise in cancer therapy, and currently there are numerous small molecule inhibitors targeted against metabolic pathways under investigation as cancer therapeutic strategies. Evading metabolic blocks through bypass pathways and redundancy is possibly one of the major challenges to this approach to cancer treatment (Jones 2011). The need to understand key nodal points and possible combination strategies remains essential. Our interest in PGM1 stems from its position three-way of important pathways in glucose metabolism. Understanding this specific traffic point would bring insight into some of the metabolic priorities of cancer cells (Gururaj et al. 2004).

Our study is a first to show higher expression of PGM1 in cancer patient specimen compared to normal cervical biopsies. We also showed PGM1 expression to be high in cancer cell lines of other tissue origins compared to their normal counter parts, such as oesophageal cancer. Previous studies have shown a number genes involved in glucose management to have elevated expression in cancer, these include genes directly playing a part in glycolysis such as Phosphoglucose isomerase (PGI), Enolase 1 (Eno 1), Phosphoglycerate kinase 1 (PGK1) and Lactate dehydrogenase A (LDHA) (Tsutsumi et al. 2009; Capello et al. 2011; Chen et al. 2003; Ahmad et al. 2013; Billiard et al. 2013) and those participating in glycogen metabolism Glycogen Phosphorylase, muscle isoform (PYGL) and glycogen synthase (GYS) (Favaro et al. 2012). The elevated expression of genes involved in glucose management of cancer cells confirms the significance metabolic pathways to cancer survival (Altenberg & Greulich 2004; Dang 2012).

Through an analysis of the PGM1 promoter, we identified HIF1α and E2F proteins to be regulators of PGM1 transcription by directly binding to the PGM1 promoter and inducing expression. The DP1/E2F complex which is known to play a prominent role in cervical cancer development (Karstensen et al. 2006) was shown to influence PGM1 expression and directly bind to the PGM1 promoter at various regions. A recent study showed that E2F1 silenced oxidative metabolic gene expression and increased glycolytic gene expression, the predominant energy manufacturing pathway in cancer cells (Blanchet et al. 2013). Our data suggest a role for E2F/DP1 proteins in the control of glucose metabolism via PGM1 regulation.

Under conditions of hypoxia we found PGM1 expression levels were significantly increased. Our data supports studies reporting an increase PGM1 expression in hypoxia with an

associated increase to glycogen accumulation (Pelletier et al. 2012; Favaro et al. 2012). Our study suggests that cancer cells already have higher PGM1 levels compared to normal which are further increased in hypoxia. Consequently, even without the introduction of hypoxia, glycogen levels were found to be significantly decreased following PGM1 inhibition. Our data showed increase PGM1 mRNA and protein expression and promoter activity in response to treatment with hypoxia mimicking agents. Reinforcing the idea that upregulation of PGM1 under hypoxic conditions is a result of transcriptional events. PGM1 function is central to three metabolically significant pathways; glycolysis, glycogen synthesis and pentose phosphate pathway. HIF1α is known to have over a hundred target genes (Ke & Costa 2006) and many of these functioning in glucose management by these pathways under hypoxic conditions. In this study we show that HIF1α binds to the 5'UTR of the PGM1 gene supporting studies that have suggested an interaction between HIF1α and PGM1.

We showed that PGM1 to have minimal effects on secreted lactate levels however, it was found to be integral to glycogen synthesis. PGM1 was also shown to influence the production of NADPH via the pentose phosphate pathway. Interestingly, cancer cell proliferation appeared unaffected in standard culture conditions (25 mM glucose and normoxia). However cancer cell viability was decreased following PGM1 inhibition with the introduction of a 'multiple-stress' conditions of (hypoglycaemia and hypoxia), suggesting that PGM1's role is to help cancer cells cope with conditions of severe stress while under amicable conditions its role is mainly in storing glycogen which can be released in periods of glucose deprivation and energy deficit (i.e., high ADP/ATP ratios). While we focused on the effects on cell viability seen under combined hypoglycaemic and hypoxic stress other studies have investigated the efficacy of cancer therapeutics that target metabolic targets under induced oxidative stress

conditions for example, and seen augmented drug sensitivity when cells were subjected to additional stress (Estan et al. 2014). A recent study reported that combined inhibition of glycolysis, the pentose cycle, and thioredoxin metabolism selectively increased cytotoxicity and oxidative stress in human breast and prostate cancer (Li et al. 2015). Many such investigations are underway that look at combined approaches to exploiting the unique features of the tumour microenvironment in cancer. These approaches selectively increase the environmental stress conditions within and around tumours based on the hypothesis that this will lead increased drug efficacy.

5.2 SUMMARY OF KEY FINDINGS

1. PGM1 expression is elevated in cervical, oesophageal and breast cancer cells
2. Elevated PGM1 expression in cancer cells is as a result of increased transcriptional activation.
3. PGM1 expression is elevated under conditions of hypoxia
4. E2F and HIF1α are regulators of PGM1 expression. The exact regions in the PGM1 promoter responsible for this regulation is not clear at present.
5. PGM1 expression in cancer cells is required for glycogen accumulation
6. PGM1 is necessary for the proliferation of cancer cells under conditions of severe stress conditions such as glucose depletion and hypoxia

5.3 LIMITATIONS AND FURTHER DISCUSSIONS

Our investigation were not without limitations, most of our experiments involving hypoxia were done in hypoxia-mimicked conditions, i.e., nickel sulphate or cobalt chloride treatments. While valuable information could be deducted and the experimental setting allowed for sustained inhibition of the prolyl hydroxylases that are responsible for HIF degradation, thereby HIF 1 expression and activity. We cannot discount other adverse effects that these agents may have had on cells apart from mimicking hypoxia. The ideal setting would be to perform hypoxia experiments in a hypoxic chamber designed for diverse experimental applications, particularly for tissue culture work, without a limited supply of nitrogen gas in order to maintain the oxygen potential. The hypoxic chamber used in some of these studies (chapter 4 for example) came with limitations such as those associated with the short half-life of HIF proteins, making it difficult to sustain hypoxia and its responses for long enough to allow for downstream processing.

There were difficulties also with interpreting promoter assays relative to the pTK-Renilla plasmid used as an internal control following other external treatments. This promoter showed increased activity in response to treatments with hypoxia mimicking agents as well as siRNA. To combat this limitation however, the pTK-Renilla control was used only where no further treatments were require and total protein used as an alternative where necessary.

Recommended future work may include evaluating an approach in which glucose management is disrupted by blocking PGM1 expression and/or function while simultaneously subjecting cells to a cytotoxic agents and determining whether the agents show enhanced efficacy.

There is often an inherent difficulty in replicating *in vivo* conditions in culture. This undoubtedly influences the accuracy of our assessments of cancer cell metabolism. In culture, cancer cells are 'bathed' in metabolic substrates (high glucose and the addition of glutamate) to support their proliferation and this would likely influence resultant metabolic programs (Papandreou et al. 2011). Recent studies contrasting responses to drugs such as Dichloroacetate (a drug that blocks glycolytic metabolism, and promotes mitochondrial respiration), *in vitro* versus *in vivo*, have seen modest effectiveness in killing cancer cells in culture while showing more dramatic cytotoxic effects *in vivo* (Chen et al. 2009). On this basis, possible future perspectives in this study could explore inhibiting PGM1 in xenograft mouse models and investigating effects on cancer cell biology and metabolism in this context.

CHAPTER 6

MATERIALS AND METHODS

6.1 MATERIALS

6.1.1 Cervical tissue specimen

All cervical tissue specimen was obtained previously from Groote Schuur Hospital, Observatory, South Africa (Transcriptional Regulation and Cancer Biology Group, Medical biochemistry, UCT, RSA) upon consent from all patients involved in the study and the approval of the Research Ethics Committee of the University of Cape Town (REC REF153/2004). Cancerous tissue biopsies were collected from patients treated for cervical dysplasia and carcinoma, while non-cancerous (normal) tissue specimen were obtained from patients that were undergoing hysterectomies for reasons other than cervical cancer. A pathologist certified all specimen as either normal or diseased. RNA was previously isolated from the biopsies, genotyped and identified as HPV positive (Transcriptional Regulation and Cancer Biology Group, Medical biochemistry, UCT).

6.1.2 Cell lines

The cervical cancer cell lines; HeLa (HPV18), SiHa (HPV16), CaSki (HPV16 &18), Me180 (similar to HPV39), Ms751 (HPV18) and C33A (HPV negative) and the following normal and transformed fibroblasts; WI38 (normal lung) and its SV-40 transformed matched cell line, SVWI38 (transformed lung), CCD1068-SK (normal breast skin) as well as the non-tumorigenic breast epithelial cell line MCF12A and breast cancer cell lines (T47D, MCF7 and MDA-MB-231), were all obtained from the American Type Culture Collection (ATCC) (Rockville, MD, USA). All the above with the exception of MCF12 A cells were cultured under adherent

conditions at 37℃ in Dulbecco's Modified Eagle's Medium (DMEM), supplemented with an antibiotic cocktail of penicillin (100 U/ml) and streptomycin (100µg/ml) with 10 % (v/v) heat-inactivated Fetal Bovine Serum (FBS) (Gibco, Paisley, Scotland). Cells were cultured in a 5% CO_2 conditioned humidified incubator and were routinely passaged every 2-3 days. MCF12A cells however, were maintained in media containing 50% Ham's F12 media (Gibco) and 50% DMEM media with 10% heat-inactivated FBS, 100 U/ml penicillin and 100 µg/ml streptomycin with 20 ng/ml EGF (Gibco), 100 ng/ml Cholera toxin (Sigma, Aldrich, Germany), 500 ng/ml Hydrocortisone (Sigma) 10 µg/ml Insulin (Gibco).

The primary cervical epithelial cells, HCX, were obtained from Drs. C Baker and A Baege at the National institute of Health, USA, the cells were cultured as described by Berger et al., 2002. Briefly, The HCX cells were retrieved from normal cervical tissue and kept in keratinocytes growth medium supplemented with EGF (10 ng/ml) and pituitary extract (50 µg/ml, cultured as described by van der Watt P et al., 2009 at 37°C, in an atmosphere of 95 % air and 5% CO_2.

The normal h-TERT-immortalized human oesophageal keratinocytes, EPC2 cells, were obtained as a gift from Prof A.K. Rustgi (University of Pennsylvania, Philadelphia, USA). FGo normal skin fibroblasts were acquired from the Department of Medicine, UCT, and transformed fibroblasts, CT1 as referred to in Namba et al., 1980. Oesophageal carcinoma cell line, WHCO1 cell line was established from a South African patient with oesophageal squamous cell carcinoma, and obtained as a gift from Dr R. Veale. Oesophageal carcinoma cell lines, KYSE30, 70, 150, 180 and 450, were obtained from DSMZ (Berlin, Germany). The epithelial liver cancer cells, HepG2, were acquired from the UCT Heart foundation and cultured adherently in antibiotic free, DMEM and 10% (v/v) non-heat-inactivated FBS. All cell lines were kept in a 5% CO_2 humidified incubator and routinely passaged every 2-4 days.

6.1.3 siRNA

For the inhibition of gene expression, short-interfering RNA (siRNA) was used; PGM1 siRNA (ID: s10407) (Ambion-Life technologies, California, USA) and p53 siRNA (sc-29435), DP1 siRNA (sc-37813), Santa Cruz Biotechnology, Santa Cruz, CA, USA). Control siRNA-A consisting of a scrambled sequence (sc-37007, Santa Cruz Biotechnology) was used as a non-silencing control. siRNAs were provided as lyophilised powders and were reconstituted in nuclease-free water to give a stock concentration of 10 µM. E7 siRNA was designed as described by Tang et al., 2006. RNA oligos were synthesised by Ella Biotech GmBH (Germany) and annealed in a reaction containing 30 µl each RNA oligo (50 µM) and 15 µl annealing buffer (100 mM Potassium acetate, 20 mM Hepes, pH 7.4, 2 mM Magnesium acetate) at 90°C for 1 minute, followed by 37°C for 1 hour, to give a final siRNA concentration of 20 µM.

6.1.4 2', 7'-Dichlorodihydrofluorescein Diacetate (H_2DCFDA)

H_2DCFDA is a cell-permeable non-fluorescent probe used for quantitation of reactive oxygen species (ROS) was obtained from Sigma (Aldrich, Germany). ROS was measured in response to PGM1 inhibition in different extracellular environments. Kept as 50 mM stock, dissolved in DMSO at -80^{o}C.

6.1.5 Hypoxia mimics: Nickel Sulphate (II) and Cobalt (II) Chloride

Hypoxia mimicking agents which function by attenuating activity of prolyl hydroxylases therefore rendering HIF active to bind to its target genes as would be in hypoxia. These were obtained from Sigma, kept at a stock concentration of 0.25 M and stored at -20 °C.

6.1.6 Actinomycin D

A polypeptide antibiotic, obtained from Sigma (Aldrich, Germany) used as an inhibitor of de novo transcription, was dissolved in DMSO and kept at -80 °C at a concentration of 400 µg/ml.

6.1.7 Plasmids

The pGEM-T Easy plasmid (Promega, Madison, WI, USA) was used as a tool for sub-cloning PCR products of the PGM1 promoter region. The pGL3-Basic reporter plasmid (Promega) was used for the cloning of sequence-confirmed promoter fragments upstream of a luciferase construct. pRL-TK (Promega) encoding the Renilla reporter gene was used to normalize for transfection efficiency unless otherwise specified. To assay for the effect of Rb overexpression on PGM1 promoter activity, cells were co-transfected with 400 ng pCMV or RcCMV/Rb (Addgene plasmid 1763, provided by Bob Weinberg).

6.2 Methods

6.2.1 Quantitative real time PCR (qRTPCR)

To validate microarray data in cervical tissue specimen and investigate differential gene expression in cells, qRTPCR was employed. For patient specimen, RNA was previously extracted from normal and cervical cancer patient tissue samples using the Trizol reagent

(phenol/guanidine isothiocyanate) (Invitrogen, Rockville, MD, USA), according to the manufacturer's instructions, van der Watt et al., 2009. First strand cDNA was then synthesized in following manner; 2 µg of RNA was used as template and mixed with T7 oligo dT primers per sample then reverse transcribed in 20 µl reaction consisting of 1 µl ImPromII Reverse Transcriptase II (Promega), 1 µl RNAsin (Promega), 2 mM $MgCl_2$, 1 mM dNTPs and 1 X ImPromII reaction buffer (Promega). Quantitative real time RT-PCR was done using a Step One Instrument according to the manufacture's operator's manual (Applied Biosystems, CA, USA). A master mix was prepared containing nuclease free water, Kapa SyBr green fast (Kapa Biosystems), a pair of forward and reverse primers (refer to the Table 6.1 below) in separate master mixes for each target gene and housekeeping genes. For patient cDNA β-glucuronidase (Gus B) and Cyclophilin D Ct values were averaged used as a single reference value to normalize data. 2 µl of synthesised cDNA was used as a template for the qRTPCR reaction.

Table 6.1 Primers used for real-time RT-PCR

Gene	Sequence	PCR product size (bp)	Ta (°C)
PGM1 Forward	5'-ATGATTACGAGGAGGTGGAAG-3'	150	55
PGM1 Reverse	5'-CTGGGTCGCTGTATTCAAAG-3'		
PGK1 Forward	5'-AAGAAGTATGCTGAGGCTGTC-3'	150	55
PGK1 Reverse	5'-GCAAGTGGCAGTGTCTCC-3'		
VEGF A Forward	5-TTCATGGATGTCTATCAGCG-3'	236	60
VEGF A Reverse	5'-GCTCATCTCTCCTATGTGCT-3'		
Enolase 1 Forward	5'-GCCGTGAACGAGAAGTCC-3'	150	55

Enolase 1 Reverse	5’-CAGGTCAGCGATGAAGGTATC-3’		
Cyclophilin D Forward	5’-TGAGACAGCAGATAGAGCCAAGC-3’	94	60
Cyclophilin D Reverse	5’-TCCCTGCCAATTTGACATCTTC-3’		
GusB Forward	5’-CTCATTTGGAATTTTGCCGATT-3’	81	55
GusB Reverse	5’-CCGAGTGAAGATCCCCTTTTTA-3’		
B-Actin Forward	5’-ATCGTGCGTGACATTAAGGA-3’	178	60
B-Actin Reverse	5’-AGGAAGGAAGGCTGGAAGAG-3’		

Ta being the annealing temperature used in the cycling stages of the real-time PCR reaction

6.2.2 Western blot analysis

Media was removed and cells were washed twice in ice cold 1X PBS. A fresh mixture of 10 X complete protease inhibitor cocktail (Roche, Basel, Switzerland) was added to RIPA lysis buffer as well as phosphatase inhibitor (0.1 M Sodium validate). The mixture was then added to cells and lysates were collected by scraping using a rubber police man. The protein lysate was separated from debris by centrifugation and protein concentrations were determined using the BCA protein assay kit (Thermo Fisher Scientific Pierce, Illinois, USA). The protein molecular weight marker, Spectra-BR (Thermo Fisher Scientific Fermentas, Illinois, USA) for the determination of protein size. 20-30 µg of total protein was loaded onto SDS Polyacrylamide gels prepared according to (Table 6.2) and ran at 185 V for 1 h. Protein was then transferred to a Hybond^{TM} –ECL ^{TM} nitrocellulose membrane (Amersham Biosciences, Buckinghamshire, UK) at 100 V, for 1 hour. Membranes were blocked for either 1 hour with shaking at room temperature or overnight at 4^{o}C in 5 % milk (in TBST) and incubated in primary and secondary antibodies according to the conditions indicated in (Table 6.3) below. Detection of bands was done by chemiluminescence, using Lumiglo or Lumiglo Reserve (KPL

Inc., Gaithersburg, MD, USA), depending on the strength of the signal. In detection of different antibodies on the same blot, the membranes were stripped in 1 M Glycine, pH 2.5 for 5 minutes then neutralised with 1/10 volume 1 M Tris-Cl, pH 7.5. The membranes were then washed four times with TBST after which blocking and re-probing with the primary antibody could proceed.

Table 6.2 Preparation of resolving and stacking gels for thickness and pore sizes (%)

Resolving Gel Solution	**10%** **(1.5 mm gel)**	**7.5 %** **(1.5 mm gel**	**15%** **(1.5 mm gel)**
Resolving gel buffer	3 ml	3 ml	3 ml
30 % Acrylamide	3ml	2.25 ml	4.5 ml
dH_2O	3ml	3.75 ml	1.5 ml
10 % Ammonium Persulphate (APS)	180 µl	180 µl	180 µl
TEMED	18 µl	18 µl	18 µl
Stacking Gel Solution	**1.5 mm gel**	**1 mm gel**	
Stacking gel buffer	1.5 ml	750 µl	
30 % Acrylamide	1 ml	500 µl	
dH_2O	3.5 ml	1.75 ml	
10% APS	60 µl	30 µl	
TEMED	6 µl	3 µl	

Table 6.3 Antibody concentrations and incubation conditions

Primary Antibody	Primary Antibody conditions	Secondary Antibody	Secondary Antibody conditions	Detection Substrate
PGM1 [Ab55616, Abcam]	1:1000 in 5% milk (in TBST)	Goat anti-mouse [[Bio-rad]	1:5000 in TBST	Lumiglo
DP1 (k-20) [Sc-601, Santa Cruz Biotechnology]	1:1000 in TBST	Goat anti-rabbit [Bio-rad]	1:5000 in TBST	Lumiglo
Phospho-RB (Ser 807/811) [9308S, Cell Signalling]	1:500 in 5% BSA (in TBST)	Goat anti-rabbit [Bio-rad]	1:5000 in 5% milk	Lumiglo
HIF 1-α [sc-13515, Santa Cruz Biotechnology]	1: 500 in 2.5 % milk (in TBST)	Goat anti-mouse [Bio-rad]	1:25000 in 5 % milk	Lumiglo
β-Tubulin (H-235) [sc-9104, Santa Cruz Biotechnology]	1:1000 in TBST	Goat anti-rabbit [Bio-Rad]	1:5000 in TBST	Lumiglo
p53 [M7001, DakoCytomation, Glostrup, Denmark]	1:500 in TBST	Goat anti-mouse [Pierce]	1:2000 in TBST	Lumiglo Reserve
p21 (H-164) [sc-756, Santa Cruz Biotechnology]	1:250 in 2.5 % milk in TBST	Goat anti-rabbit [Bio-Rad]	1:5000 in TBST	Lumiglo Reserve

6.2.3 Immunofluorescence

Cells were cultured on cover-slips then washed 3 x 5 minutes each in 1 x PBS and then fixed in 4% paraformaldehyde in PBS. They were then permeabilized using 0.5 % Triton X 100 in PBS for 5 minutes. The cells were washed again in PBS and quenched in 50mM NH_4Cl in PBS for 5minutes. NH_4Cl was removed and the cells were blocked for 30 min in 0.2% gelatine. After blocking, the cover slips were removed from culture dishes and inverted on to primary antibody: mouse anti-PGM1 [1:100 in 0.2 % gelatine], the cover-slips were incubated at room temperature in a humidified chamber for 45 minutes, then washed in PBS for 3 x 5 minutes

and then incubated in secondary antibody: Alexa 488-conjugated donkey anti-mouse [1:200 in 0.2 % gelatine] for 45 minutes in a humidified chamber and washed again. The nuclei of cells were stained with DAPI (at 100 ng/ml) and cover slips were washed again in PBS and mounted on slides in mowiol. Slides were allowed to dry in the dark and fluorescence was visualised by standard fluorescence microscopy using a Zeiss Axiovert 200M fluorescence microscope with optical filters that were used for the separate imaging of Alexa 488 and DAPI signals. Images were analysed by selecting regions of equal size using an interactive graphics screen as a feature of the AxioVision Release 4.5 software.

6.2.4 Transfections with siRNA

Cells were plated in 35 mm dishes or 60 mm dishes at a concentration of 150 000-200 000 cells or 400 000-500 000 cells per dish respectively. The next day a transfection mixture was prepared using DMEM (Gibco) media free of antibiotics and fetal calf serum (FCS), transfectin lipid reagent (biorad) 0.625 µl or 1.25 µl for 35 mm or 60 mmm dishes respectively and added to the above media and left for five minutes after which siRNA was added. For control dishes a scrambled sequence siRNA, control siRNA-A (Santa Cruz) was used to treat cells, the mixture was left for 15 to 20 minutes after which it was added drop-wise to cells suspended in 1 ml DMEM with 10% FCS for 35 mm dishes and 2 ml media when 60 mm dishes were used making up a final siRNA concentration of 20 nM in each dish. Cells were left to incubate for either 6 hours or overnight in siRNA containing media. The Media was removed and replaced with normal complete media (DMEM, 10% FCS and Penicillin and streptomycin antibiotics). Effect of treatment with targeting siRNA was then investigated and knockdown was validated by western blotting or qRT-PCR.

6.2.5 Cell Proliferation assays

Cells were transfected according to the above transfection protocol and counted for plating 2000 cells/well in a 96 well plate. After plating a tetrazolium salt, MTT (3–(4,5-dimethylthiazol-2-yl)-2,5-diphenyltetrazolium bromide)(Sigma), was added to cells which was metabolised by the active mitochondria of live cells to a purple formazan dye. Solubilisation reagent consisting largely of sodium duodecyl sulphate (SDS) (Merck, Darmstadt, Germany), was added to cells 4 hours later to lyse the cells releasing the dye. Samples were then left overnight to create a homogenous solution and an absorbance reading was taken at 595 nm on a calorimetric plate reader (BioTek, Winooski, VT, USA) and related to the amount of cells. Cells treated with control siRNA and PGM1 targeting siRNA were compared in terms of their rate of proliferation over 5 or 6 days.

6.2.6 Periodic Acid Schiff (PAS) assay

Cells were plated at 150 000 cells/dish in 35 mm dishes on cover slips for the PAS experiment and without cover slips for protein extractions. The next day they were transfected with control (scrambled) siRNA and PGM1 siRNA. 72 hrs post transfection the PAS experiment was conducted as follows:

Cells were washed thrice with ice-cold PBS, the cells fixed in methanol at 20°C for 5 min. Methanol was removed and cells were immersed in freshly made-up Periodic acid (Merck) 1% (w/v) in 70 % ethanol for 30 min a room temperature. The cells were then rinsed twice with water and consequently stained with Schiff's reagent (Merck) for 5 min at room temperature then rinsed continually for at least 30 minutes.

To mount coverslips on slides, cells were dehydrated by immersing coverslips in different concentrations of ethanol, 70% and 96% respectively once and absolute alcohol twice, then in Xylene twice. The cells were then mounted in non-aqueous mounting fluid Entellan (Merck) and viewed under a bright-field microscope for glycogen staining.

6.2.7 Glycogen titration assay

To quantitatively determine the levels of glycogen after inhibition PGM1 expression, the glycogen assay was employed using the Glycogen Assay Kit (Abcam) according to the manufactures instructions. Cells were grown in 25 mM glucose containing DMEM media and transfected for 72 hrs with PGM1 targeted siRNA, cells transfected with scrambled siRNA were used as a control. The same cells were then transfected again for 96 hours. Cells were washed twice in ice cold PBS to remove all glucose and harvested in 200 µl dH_2O. Samples were then boiled for 5 minutes to inactivate enzymes and centrifuged at 14000 xg. The supernatant was then kept for further processing. Glycogen samples were then subjected to hydrolysis using gluco-amylase in hydrolysis buffer to obtain the total amount of released glucose. A sample containing no enzyme was used to control for free background glucose. The released glucose from the glycogen hydrolysis reaction was then oxidized in a development reaction to produce a detectable product with an OxiRed probe. The coloured product from this reaction was then measured calorimetrically at 570 nm. The glycogen content of the sample was calculated by subtracting free background glucose present in samples prior to hydrolysis and normalized to protein concentration.

6.2.8 NADPH assay

The assay to determine levels of NADPH was employed using the NADP/NADPH assay kit-ab6534, according to the manufacturer's instructions (Abcam, Cambridge, UK). Briefly

samples are prepared as follows: Cells are plated in 60 mm dishes and transfected with siRNA over 72 hours, the cells (approx. 10^5 cells) are then washed in PBS to remove media and trypsinized and re-suspended in extraction buffer 200µl. The lysate was then homogenised by sonicating for 30 seconds on ice. Samples were then heat treated (by heating samples on a heating block at 60^{o}C for 30 min) to eliminate the any NADP present in the sample on order to quantitate only NADPH. NADPH standard stock solution of 1 nmol/µl is diluted in NADP/NADPH extraction buffer to create a concentration series in duplicate of 0, 20, 40, 60, 80 and 100pmol/µl. The extracted cell lysate was diluted in 1:3 in NADP/NADPH extraction buffer in duplicate in a 96 well plate. NADP cycling enzyme was added to standards and samples and left to incubate for 5min, then NADPH developer was added to the sample mixtures. The reaction was allowed to develop for 3 hours at least with OD reading taken at 450 nm after every hour. The concentration NADPH in each sample was determined using the standard curve.

6.2.9 ROS assays

To investigate the effect of PGM1 inhibition on intracellular ROS generation in low (2.5 mM glucose containing media), high (25 mM glucose containing media) normoxia and hypoxic conditions, the cell-permeant 2',7'-dichlorodihydrofluorescein diacetate (H_2DCFDA) (also known as dichlorofluores*cin* diacetate) was used. H_2DCFDA is a chemically reduced form of fluorescein used as an indicator for reactive oxygen species (ROS) in cells. Briefly, 10 000 cells/well were plated in white, sterile flat bottom 96 well plates in media containing 2.5 or 25 mM glucose. The next day cells were transfect with control or PGM1 siRNA, then the next day an additional 100 µl of media (2.5 or 25 mm glucose containing media) was added to neutralize the transfection reagent and prevent dehydration. Cells were left for 48 hours and

then assayed for ROS generation, 72hrs post transfection in normoxia. In hypoxia however, before staining cells with H_2DCFDA, plates were incubated for 2h30 in a hypoxic chamber (1% oxygen and 98.8% Nitrogen). Alternatively for hypoxia treatments with hypoxia mimicking compounds (i.e. Nickel 0.5 mM Nickel (II) Sulphate), cell were left instead for 24 hours post transfection and the next day subjected to NiSO4 treatment for 24 hrs. 72 hrs post transfection with siRNA, media was removed and cells were washed once with 100 µl pre-warmed (37^{o}C) Krebs ringer buffer then treated with 25 µM H_2DCFDA in Krebs ringer buffer for 30 min in the dark after which fluorescence was read at Ex:485 nm and Em: 530 nm. Treatment with 5 µM Doxorubicin at different time points (15 min, 30 min, 1, 2, 3 and 4 hours) was done concurrently as a positive control and unstained cells were set aside as a negative control for background fluorescence.

6.2.10 PCR amplification of the PGM1 (-1988 to +101) promoter

In order to retrieve the DNA fragment consisting of the 5'-regulatory region of PGM1 to investigate PGM1 promoter activity in cells, PCR primers to amplify the region approximately 2 kb upstream and 100 bp downstream of the PGM1 transcription start site (TSS) were designed using Primer-BLAST (http://www.ncbi.nlm.nih.gov/tools/primer-blast/) based on the sequence information in GenBank (accession number NC_000001.10). The primers were designed to incorporate restriction enzyme sites flanking either end with the forward primer containing the NheI site (G^CTAGC) and the reverse primer with a HindIII site (A^AGCTT) respectively for cloning into a pGL3-Basic vector. Importantly the restriction enzyme sites selected for the primer design had to be absent in the promoter insert but and the pGEMT-easy shuttle vector but only present in multiple cloning site of the pGL3-Basic vector. On each

primer, an extra two based was added on the 5'-end of each restriction enzyme site in order to aid with binding. Sequences and positions of the primers are shown in (Table 6.4).

The PCR reaction as performed using 100 ng genomic DNA from normal blood as the template in 5 µl of 10 X PFU Buffer, 1.25 µl each of 20 µM primers (Forward and Reverse), 1 µl 10 mM dNTPs, 2.5 µl of 5% DMSO and 3µl of 25 mM $MgCl_2$ added to reduce non-specific binding with 0.5 µl of the high fidelity enzyme PFU DNA polymerase (Fermentas, Thermo Fischer Scientific, Waltham, MA, USA) to minimize PCR errors and filled up with nuclease-free water to make up a 50 µl reaction. The conditions used for the PCR reaction were initially denaturation at 95°C for 5 min, followed by 30 cycles of denaturation at 95°C for 30 s, annealing at 55°C for 30s, and extension at 72°C for 3 min, with the final extension at 72°C for 15 mi to allow for the amplification of lengthy DNA fragments. However due to difficulty in seeing a clear and precise PCR product, the PCR reaction was optimized by setting up gradient PCR experiment in which the annealing temperature is ramped from 55 to 65.1°C. 63.4°C was found to be the optimal annealing temperature for amplification of the correct product.

Table 6.4 Sequences of primers used for cloning the 2 Kb, 5'-regulatory region of PGM1

Primer name	Sequence	Position	PCR product size (bp)	Ta (°C)
PGM1 F	5' AG**GCTAGC**GGCCACAGTAACCCTGTCCAGA 3'	-1988 to -1966	2089	63.4
PGM1 R	5' AGAAGCTTACTCTAGGCCGGCGTTTGGC 3'	+81 to +101		

The NheI site is in bold and the HindIII site is underlined. The position of the primers represents the matching sequence in the 5'-regulatory region of the PGM1 gene, not including the added restriction sites and extra bases, and therefore not represent the exact size of the primer. The relative positioning is based on numbering the first base of the transcription start site as +1, with upstream sequences indicated as negative numbers. Ta being the annealing temperature of PCR cycling reactions.

6.2.11 PCR products purification and A-tailing for cloning the promoter into pGEM-T Easy

The products from the PCR reaction were run on a 1 % agarose gel and visualized using ethidium bromide and UV. The PCR product bands were then excised from the gel using a sharp blade and the DNA was cleaned up using the Wizard SV gel and PCR Clean-up System (Promega) according to the manufacturer's instructions. The cleaned up PCR products were then A-tailed using 5 U Taq polymerase (Stratagene) in a reaction containing 1X Taq buffer, 2.5 mM $MgCl_2$ and 0.2 mM dATP in a total volume of 10 µl incubated at 70°C for 30 min. This was done because the Taq polymerase enzyme yielded blunt ends, therefore A-tailing was necessary to facilitate the PCR product ligation into the pGEM-T Easy plasmid.

6.2.12 Sub-cloning of PGM1 promoter PCR products into pGEM-T Easy

A ligation reaction was then set up and incubated overnight at 4°C consisting of 3µl of the A-tailed promoter PCR product and 50 ng pGEM-T Easy in 5µl of 2 X Rapid ligation buffer and 3 U/µl of T4 DNA-Ligase (Promega) in a total volume of 10 µl. Half of the ligated plasmid preparation was then used to transform 30 µl competent JM109 cells (Promega) for 20 min on ice. The bacterial cells were then heat-shocked at 42°C for 2 min to facilitate uptake of the plasmid DNA and placed back on ice for another 2 min. 450 µl of LB broth was then added to the mix and incubated at 37°C for 1 hr, after which 100 µl and 400µl were spread on separate agar plates containing 100 µg/ml Ampicillin, and onto which 100 µl 0.1 M IPTG and 20 µl 50 mg/ml Xgal. The plates were incubated overnight at 37°C to allow for the bacterial to form.

6.2.13 Preparation of recombinant pGEM-T Easy clones for screening of correct inserts

White colonies were then selected for screening. Representative colonies were pick inoculated from the agar plate into 5 ml Luria broth (LB) and incubated at 37°C, overnight with shaking at 200 rpm. The next day glycerol stocks were made by mixing 500 µl of bacterial culture with 500 µl of sterile 80% glycerol. Glycerol stocks were then kept at -80°C for long-term storage. The remaining 4 ml of the bacterial culture was then used to extracted plasmid DNA using a Pure-Yield Mini-prep System (Promega). The 4 ml culture was split into two 2 ml epperndorf tubes then span down to collect the cells. The supernatant was discard and the pellets re-suspended in 600 µl of water. The suspension was then lysed in a blue Cell Lysis Buffer and neutralized using a Neutralizing solution after which the mixture was centrifuged at maximum speed using a small bench-top centrifuge (or microcentrifuge) at room temperature for 3 minutes. The supernatant (~900µl) was transferred to a PureYield Minicolumn without disturbing the cell debris pellet. After spinning for 15 sec the flowthrough was discarded and endotoxins were removed by washing the cells with 200µl and again with 400µl of Column Wash Solution. DNA was eluted in 30µl of nuclease-free water, and plasmid stored at –20°C. The correct clones were identified from false positives, by doing a restriction enzyme double digested using 5 U Nhe I and 5 U HindIII (both from Promega) in 1x Buffer B and 0.5 µg DNA, overnight at 37°C. Digests were then run alongside uncut plasmid on a 1 % agarose gel. Positive clones were then selected for downstream experiments.

6.2.14 Preparation and large scale retrieval of high quality pGEM-T Easy recombinant clones with the 2kb PGM1 promoter fragment for sequencing.

A large-scale retrieval of high quality recombinant pGEM-T Easy clones containing the PGM1 5'-regulatory region was performed using the Qiagen Maxi-prep. Bacterial cultures were first

grown up from glycerol stocks by inoculating into 5 ml LB containing 60 µg/ml Ampicillin and incubated for approximately 4 hrs at 37°C with shaking at 200 rpm to make up a starter culture which was then transferred into 100 ml LB containing 100 µg/ml Ampicillin and incubated for overnight (approximately 16 hrs) at 37°C with shaking at 200 rpm.

Bacterial cultures were then span down at 6000 rpm, supernatant discarded and pellet re-suspended in Buffer P1 containing 100 µg/ml RNAse. The re-suspension was lysed in Buffer P2 for 5 minutes at room temperature, and the solution was then neutralised using Buffer P3 for 20 minutes on ice. The supernatant was isolated by centrifugation at 13000 rpm for 30 minutes, followed by an additional centrifugation step for 15 minutes to ensure complete exclusion of the suspended material (containing genomic DNA, proteins and cell debris), the supernatant was applied to a Qiagen-tip according to the manufacturer's instructions. After several washes, the eluate was precipitated using 0.7 volumes isopropanol and centrifuged. The DNA pellet was then washed with 70 % Ethanol and then air-dried and re-suspended in 50 µl TE buffer, pH 8.0. The plasmids were cut with NheI and HindIII restriction enzymes, and electrophoresed to verify the isolation of the correct plasmids.

6.2.15 Sequence confirmation to verify correct PGM1 promoter insert

To confirm the correct sequence of the PGM1 promoter within the pGEM-T Easy plasmid vector, sequencing reactions were performed using the BigDye Terminator v3.1 Cycle Sequencing Kit (Applied Biosystems), according to the manufacturer's instructions. Reactions were set up using the primers in (Table 6.5). (2 mM primer solution was made up from a 20 mM stock of primers) with 6.4 pmol sequencing primer and 0.5 µg template plasmid DNA was used in each sequencing reaction. The following cycling conditions were used: 96°C for 1

minute, followed by 25 cycles of 96°C for 10 seconds, 45 °C for 5 seconds, and 60°C for 4 minutes.

Table 6.5. Sequencing primers

Primer	Sequence	Position in promoter	Ta (°C)
T7 primer	5' TAATACGACTCACTATAGGG 3'	In pGEM-T Easy	45
SP6 primer	5' CGATTTAGGTGACACTATAG 3'	In pGEM-T Easy	45
PGM1 seq primer 1 (F)	5' GGTAATGATATGCTCTGG 3'	-758 to -740	45

Ta refers to the annealing temperature used in the cycling stages of the PCR.

6.2.16 Cloning of PGM1 promoter upstream of the luciferase construct in pGl3-Basic

10µg of recombinant pGEM-T Easy constructs containing the sequence verified PGM1 promoter fragments were digested with the restriction enzymes NheI and HindIII to release the cloned inserts and 5 µg of the pGL3-Basic vector was digested with the same enzymes to linearize the vectors. Digest were then run on a 1% agarose gel at 80 V for 2 hours, the released inserts and linearized pGL3-Basic vector were then excised from the gel and cleaned up using the Wizard SV gel and PCR Clean-up System (Promega) according to the manufacturer's instructions.

The amount of insert DNA to be used for ligation was determined using the equation:

ng vector/Kb vector x Kb insert x molar ratio (insert:vector) = ng insert

(where 100 ng vector DNA was used, and an insert:vector ratio of 2.5:1).

The cleaned up linearized vector and promoter inserts were then quantified and ligated using T4-DNALigase (Fermentas) in a reaction containing 10 X ligation buffer (Fermentas) 10 % polyethylene glycol (PEG) to facilitate the ligation reaction, 100 ng of plasmid and 250 ng of

insert, filled up with water to 10 µl. The ligation was done at 4°C overnight (± 16 hrs). The entire ligation reaction mix was used to transform 40 µl of competent JM109 cells as described previously in Section 6.2.14. The next day colonies were picked and screened for the correct insert. Positive clones were identified by restriction digestion analysis and grown up for large-scale plasmid preparations as described in Section 6.2.16.

6.2.17 Luciferase assays

400 ng of each promoter construct was transfected into 300 000 CaSki cervical cancer cells/well of a 6-well plate, using 1.2 µl Transfectin (Bio-Rad) (i.e. the DNA (µg) to Transfectin (µl) ratio was 1:3). The pRL-TK plasmid (that encodes Renilla luciferase) along with the promoter constructs was used normalise for transfection efficiency, cells were co-transfected with 50 ng Renilla plasmid. In the case of cells that were treated with hypoxia mimicking agents following transfection, based on the effect of hypoxia on the pRL-TK Renilla plasmid luciferase readings were normalized to protein concentration instead. Transfection mixes were made up in 100 µl serum-free, p/s-free DMEM and after a 20 minute incubation, added drop-wise to the cells in 1 ml media (containing 10 % FCS and p/s). 24 hours post transfection, media was removed from cells. Cells were washed with 1x PBS and total cell lysates were extracted from cells in 200 µl of 0.25 mM Tris, pH 8.0, and firefly luciferase activity was assayed using the Dual Luciferase Kit (Promega). Luminescence was monitored using the Glomax 96 microplate luminometer (Promega). Promoter activity was normalised to the Renilla luciferase activity from pRL-TK in the same extract.

6.2.18 Rb overexpression

To assay for the effect of Rb overexpression on PGM1 promoter activities, cells were co-transfected with 400 ng pCMV or RcCMV/Rb (Addgene plasmid 1763, provided by Bob Weinberg), 400ng pGL3-pPGM1 (-1988/+101) construct and 50 ng Renilla, using 2.4 µl Transfectin per well in a 6 well plate. Cells were incubated for 48 hours after transfection, and luciferase assays performed.

6.2.19 Generating deletion constructs

PGM1 promoter deletion constructs were generated using gene-specific forward primers with a Nhe I restriction site incorporated into each respective primer shown in (Table 6.6) to create the promoter fragments shown in (Figure 6.1)**,** and PGM1 R (containing the HindIII site) was used as the reverse primer. A PCR was done using the cloned pGL3-Basic constructs described previously as the template DNA. The PCR products were purified and cloned into the pGL3-Basic vector to generate shorter constructs of the PGM1 promoter. High-quality plasmid DNA was required for luciferase assays therefore large-scale plasmid preparations were performed for each construct.

Table 6.6. Primers used to generate PGM1 promoter deletion constructs

Primer name	Sequence (5'-3')	Position	Size of Fragment
PGM1F587	5' AG**GCTAGC**AAATCATGGGAAGAGAGCC 3'	-587 to -571	688 bp
PGM1F135	5'AG**GCTAGC**GTTCTTACCCCAACCTCTGC 3'	-135 to -116	336 bp

Both constructs were designed to include a Nhe I site indicated in bold

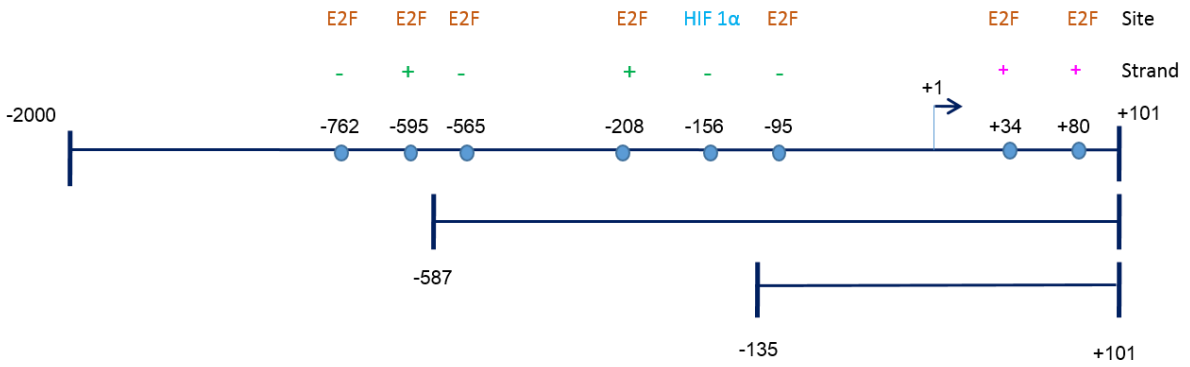

Figure 6.1 Co-ordinates of promoter deletion constructs and the putative transcription factor binding sites in the -2 Kb to +101 bp region of the PGM1 promoter. Seven putative E2F sites are shown and one hypoxia responsive element is shown in blue.

6.2.20 Site-directed mutagenesis

Putative transcription factor binding sites in the -1988/+101 and -135/+101 region of PGM1 promoter were disrupted by site-directed mutagenesis. Specific primers were designed to mutate and incorporate a restriction enzyme site within the binding region of the transcription factors, HIF (in the hypoxia responsive element) and E2F to allow for identification of positive clones. Primer X (http://www.bioinformatics.org/primerx/) was used to design optimal primers and these are depicted in (Table 6.7) below. Primers were designed in such as not to introduce any additional sites verified using the MatInspector software programme (https://www.genomatix.de/). The melting temperature (Tm) for each primer was calculated to be >75°C using the following equation (obtained from the Stratagene QuikChange site-directed mutagenesis kit instruction manual):

$$Tm = 81.5 + 0.41\ (\%\ GC) - 675/N - \%\ mismatch$$

where N is the primer length in bases.

Table 6.7 Mutagenic primers used to disrupt transcription factor binding site

Name	Primer sequence	Plasmid template	Enzyme incorporated
-156HREmut_F	5' CTTTTTTCCACCCTGCCTCggaTCCTTGCCCTATGACCG 3'	pGL3pPGM1 -1988/+101	BamHI
-156HREmut_R	5' CCGGTCATAGGGCAAGGATccGAGGCAGGGTGGAAAAAA 3'		
+19HREmut_F	5' CTTTCCCCTCCCGCCGGAtCcGCCAGGAGGTGGGCTGG 3'	pGL3pPGM1 -135/+101	BamHI
+19HREmut_R	5' CCAGCCCACCTCCTGGCgGaTCCGGCGGGAGGGGAAAG 3'		
-95E2Famut_F	5' CACTTAGGGGAGGAGTctCGaGCCTCTTTTTACAGTG 3'	pGL3pPGM1 -135/+101	Xho1
-95E2Famut_F	5' CACTGTAAAAAGAGGCtCGagACTCCTCCCCTAAGTG 3'		
+34E2Fbmut_F	5' CTGCCAGGAGGTGGGCgctaGCGGAGGGAGGGCCCTG 3'	pGL3pPGM1 -135/+101	NheI
+34E2Fbmut_R	5' CAGGGCCCTCCCTCCGCtagcGCCCACCTCCTGGCAG 3'		
+80E2Fcmut_F	5' CCCTGTCCCTTTAAGGAGGAGGGCtAgcCGCCGGCCTAGAG 3'	pGL3pPGM1 -135/+101	NheI
+80E2Fcmut_R	5'CTCTAGGCCGGCGgcTaGCCCTCCTCCTTAAAGGGACAGGG 3'		

mutated bases are indicated in lower case and the restriction enzyme sites are underlined. The position of the first base on the 5'end of the putative TF binding site in included in the primer name.

The different PCR reactions were set up as follows: 50 ng of plasmid DNA was used as template, 125 ng each of forward and reverse primers, 10x PFU buffer and 5 U PFU DNA polymerase, 3µl of 25mM MgCl2 and 5% DMSO, and 0.2mM dNTPs in 50 µl total volume. However, due to difficulties in cloning the +19HRE and -95E2Fa mutants, a different reaction recipe was used in order to optimize product output with each respective primer. The PCR reaction set up in the following manner: 30 ng of the plasmid DNA template was used together with 1.5 µl each of the forward and reverse primers indicated in (Table 6.7), at a stock concentration of 2µM, 1 µl of 10 mM dNTPs, 5µl of 10x PFU buffer (Fermentas) 5U of

PFU DNA polymerase and 1.5mM of $MgSO_4$ made up to 50µl in nuclease-free dH_2O.PCR was performed using the following cycling conditions: 95^oC for 30 seconds, followed by 18 cycles of 95^oC for 30 seconds, 55^oC for 1 minute, and 72^oC for 6 minutes, followed by a final extension step of 72^oC for 20 minutes with an exception of the +19HREmut and -99E2Famut where the annealing temperature was increased to 61^oC instead of 55^oC. Following PCR amplification, 10 U DpnI (Promega) was added to the reaction mix and digestion carried out at 37^oC for 90 minutes, before transformation into highly competent JM109 cells (Promega). Restriction digestion analysis was used to identify clones carrying the mutation.

6.2.21 Chromatin immunoprecitation (ChIP)

In order to determine whether specific transcription factors bind directly to the PGM1 5'regulatory region ChIP assays were performed. Cells were grown till were about 90 % confluent in 2 x 150 mm culture dishes or 5 x 10 cm dishes, a fraction of cells were treated with hypoxia mimicking agent (nickel sulphate (II)) for experiments involving hypoxia responsive elements. When cells were at the correct confluency, 1 % formaldehyde was added and cells were incubated for 10 min at room temperature with shaking to cross-link the protein-DNA complexes. Then 0.125 M Glycine, pH 2.5 was added for 5 min to neutralise the reaction. Cells were then quickly rinsed twice in ice-cold 1X PBS and scraped into 1 ml of PBS, samples of the same experimental conditions were pooled together. The cell suspension was then spun down at 3000 rpm for 2 minutes at 4°C and the cell pellets re-suspended in 300 µl lysis buffer and placed on ice for 10 min. The released chromatin from lysed cells was sheared using a sonicator to lengths of between 400 and 1000 bp on ice and the cell debris removed by centrifugation at 13000 rpm for 10 minutes. 20 µl of chromatin was kept and

diluted in 100 µl dilution buffer and stored at -20°C. The remainder of the chromatin was also diluted 1:10 in dilution buffer. Beads were prepared by blocking in 100 mg/ml salmon sperm DNA and 5% BSA overnight at 4°C with rotation. The chromatin was then pre-cleared using protein-A agarose beads (Merck, NJ, USA) for 2 hr, then incubated with 2 mg antibody a-DP1 (K-20, sc-610, Santa Cruz Biotechnology); HIF 1-α (sc-13515, Santa Cruz Biotechnology), or no antibody negative control) at 4°C overnight with rotation. Protein-A agarose beads were added for another 2hr at 4°C, and immuno-complexes bound by the beads recovered by centrifugation and washed twice sequentially in TSE I buffer, TSE II, Buffer III and TE, pH 7.4. Bound chromatin was eluted using elution buffer (1% SDS, 0.1 M NaHCO3) at room temperature for 10 minutes, and the input and eluted samples heated at 65°C overnight to reverse the cross-links from formaldehyde treatment. DNA was purified using the Wizard SV gel and PCR Clean-up System (Promega) and used for real-time PCR, using primers designed to span the E2F and HIF binding sites Primers 1, 2 and 3 and 2 respectively (Figure 6.8). Then PCR products were electrophoresed on 2% agarose gel and visualized.

Table 6.8. Primers used for ChIP assays

Primer	Sequence	Position	Ta (°C)	PCR product
PGM1F-Primer-1	5' GTTGACCTTGCTATCCCCCG 3'	-784 to -765	60	205 BP
PGM1R-Primer-1	5' CATGATTTGCCCCGCTGTGAC 3'	-600 to -579	60	
PGM1F-Primer 2	5'TCTGACCCTCCCAACAGGT 3'	-257 to -238	60	180 bp
PGM1R-Primer 2	5'TGAAAAAGAGGCCCGCAACT 3'	-97 t0 -77	60	
PGM1F-Primer 3	5' CACTTAGAGGAGGAGTTGCGG 3'	-110 to -90	60	187 BP
PGM1R-Primer 3	5' TCCTTAAAGGGACAGGGGACA 3'	+56 to +77	60	

6.3 Solutions

6.3.1 Tissue culture solutions

Cell-freezing media

70 % DMEM, 20 % Fetal Calf Serum and 10 % DMSO

10 X PBS

40 g NaCl, 1 g KCl, 5.75 g $Na_2HPO_4.7H_2O$, 1 g KH_2PO_4, make up to 500 ml with dH_2O

MTT (5 mg/ml)

100 mg MTT, 20 ml 1 X PBS, Vortex and incubate at 37°C for 15 min, Filter through a 0.2 µm filter, Wrap in foil and store at 4°C for up to one month

Solubilisation Reagent

25 g SLS, make up to 250 ml with dH_2O then adding 76.6 µl conc. HCl

6.3.2 RNA solutions

10 X MOPS Buffer

0.2 M MOPS, 0.05 M Sodium Acetate and 0.01 M EDTA

RNA Loading Buffer

0.72 ml Formamide, 0.16 ml 10 X MOPS Buffer, 0.26 ml 37 % Formaldehyde, 0.18 ml dH_2O, 0.1 ml 80 % Glycerol and 0.08 ml 0.25 % Bromophenol Blue

1.5 % agarose gel with formaldehyde

0.75 g Agarose, 50 ml 1 X MOPS, 2.7 ml 37 % Formaldehyde and 2.5 µl Ethidium Bromide

6.3.2 Protein solutions

RIPA Buffer

150 mM Sodium Chloride, 1 % Triton X-100, 1 % Sodium Deoxycholate, 0.1 % SDS and 10 mM Tris-Cl, pH 7.4

Resolving gel buffer

36.2 g Tris, 0.8 g SDS, Dissolve in 150 ml dH2O, pH to 8.9 with 1 N HCL or 1 N NaOH and make up to 200 ml with dH_2O. Stored at 4°C.

Stacking Gel Buffer

5.9 g Tris, 0.4 g SDS, Dissolve in 70 ml dH2O, pH to 6.8 with 1 N HCL or 1 N NaOH and make up to 100 ml with dH_2O. Stored at 4°C.

10x Running buffer

30.2 g Tris, 144 g Glycine, 10 g SDS, make up to 1 L with dH2O

1x Running buffer

100 ml of 10x running buffer 900 ml of dH2O

10x Transfer Buffer

144 g Glycine 38 g Tris, make up to 1 L with dH2O

1x Transfer Buffer

100 ml 10x transfer buffer (in this order) 700 ml dH2O, 200 ml methanol/isopropanol

10x Tris Buffered Saline (TBS)

60.5 g Tris, 87.6 g NaCl, dissolve in 700 ml dH2O, pH to 7.5 with 1 N HCL or 1 N NaOH and make up to 1 L with dH_2O.

1x TBST

100 ml 10x TBS, 900 ml dH2O and 1 ml Tween 20

4 X Laemmli Loading Dye

250 mM Tris-Cl, pH 6.8 6 % SDS, 0.005 % Bromophenol Blue, 40 % Glycerol and 10 % β-mercaptoethanol

Rapid Coomassie Staining Solution

0.024 % Coomassie Brilliant Blue, 10 % Acetic Acid and 90 % dH_2O

Destain

10 % Acetic Acid

6.3.3 DNA solutions

TE Buffer

10 mM Tris-Cl, pH 8.0 and 1 mM EDTA, pH 8.0

10 X TBE

108 g Tris, 55 g Boric Acid, 7.4 g EDTA up to 1 L with dH_2O

6.3.5 Bacterial solutions

Luria Broth (LB) medium

10 g Tryptone, 5 g Yeast Extract, 10 g NaCl, 1 mM NaOH, make up to 1 L with dH_2O

LB agar

Same as LB medium, but with 15 g Agar per litre

Ampicillin (10 mg/ml)

1 mg Ampicillin in 10 ml dH_2O, filter-sterilise and store at -20°C

X-gal (50 mg/ml)

50 mg X-gal in 1 ml DMSO and store at -20°C in the dark

IPTG (0.1 M)

72 mg IPTG in 3 ml dH_2O, filter-sterilise and store at 4°C

6.3.6 ChIP Solutions

Lysis buffer

1% SDS, 5 mM EDTA, 50 mM Tris-Cl, pH 8.1 and

1 X Complete Protease Inhibitor (Roche)

Dilution buffer

1% Triton X-100, 2mM EDTA, 150 mM NaCl, 20 mM Tris-Cl, pH 8.1 and

1 X Complete Protease Inhibitor

TSEI

0.1 % SDS, 1% Triton X-100, 2mM EDTA, 20 mM Tris-Cl, pH 8.1 and 150 mM NaCl

TSEII

0.1% SDS, 1% Triton X-100, 2mM EDTA, 20 mM Tris-Cl, pH 8.1, 500 mM NaCl

Buffer III

0.25 M LiCl, 1% NP-40, 1% Sodium Deoxycholate, 1mM EDTA, 10 mM Tris-Cl, pH 8.1

Elution Buffer

1% SDS and 0.1M $NaHCO_3$

References

Ahmad, S.S. et al., 2013. Phosphoglycerate kinase 1 as a promoter of metastasis in colon cancer. *International journal of oncology*, 43(2), pp.586–90.

Allison, D.B. et al., 2006. Microarray data analysis: from disarray to consolidation and consensus. *Nature reviews. Genetics*, 7(1), pp.55–65.

Altenberg, B. & Greulich, K.O., 2004. Genes of glycolysis are ubiquitously overexpressed in 24 cancer classes. *Genomics*, 84(6), pp.1014–20.

Avril, N., 2004. GLUT1 Expression in Tissue and 18F-FDG Uptake. *Journal of Nuclear Medicine*, 45, pp.930–932.

Bae, E. et al., 2014. Phosphoglucomutase1 is necessary for sustained cell growth under repetitive glucose depletion. *FEBS letters*, pp.1–7.

Bae, S. et al., 2006. Protein Expression Profile using Two-Dimensional Gel Analysis in Squamous Cervical Cancer Patients. *Cancer Research and Treatment*, 38(2), pp.99–107.

Balasenthil, S. et al., 2004. p21-activated Kinase-1 Signaling Mediates Cyclin D1 Expression in Mammary Epithelial and Cancer Cells. *Journal of Biological Chemistry*, 279(2), pp.1422–1428.

Bao, Y. et al., 2013. Energy management by enhanced glycolysis in G1-phase in human colon cancer cells in vitro and in vivo. *Molecular cancer research*, 11(9), pp.973–85.

Berg, J.M., Tymoczko, J.L. & Stryer, L., 2002. *Biochemistry* 5th ed., New York: W H Freeman. Available at: http://www.ncbi.nlm.nih.gov/books/NBK21190/.

Billiard, J. et al., 2013. Quinoline 3-sulfonamides inhibit lactate dehydrogenase A and reverse aerobic glycolysis in cancer cells. *Cancer & metabolism*, 1(1), p.19.

Blanchet, E. et al., 2013. E2F transcription factor-1 regulates oxidative metabolism. *Nature cell biology*, 13(9), pp.1–16.

Bracher, J.C., 2009. *Expression and regulation of N-Myc Downstream-Regulated Gene 1 in squamous cell carcinoma of the oesophagus*. University of Cape Town. Available at: http://uctscholar.uct.ac.za/PDF/4375_Bracher_JC.pdf.

Brahimi-Horn, M.C., Bellot, G. & Pouysségur, J., 2011. Hypoxia and energetic tumour metabolism. *Current opinion in genetics & development*, 21(1), pp.67–72.

Brown, A.M. & Ransom, B.R., 2007. Astrocyte Glycogen and Brain Energy Metabolism. *GLIA*, 55(July), pp.1263–1271.

Cairns, R.A., Harris, I.S. & Mak, T.W., 2011. Regulation of cancer cell metabolism. *Nature reviews. Cancer*, 11(2), pp.85–95.

Capello, M. et al., 2011. α-Enolase: a promising therapeutic and diagnostic tumor target. *The FEBS journal*, 278(7), pp.1064–74.

Carew, J.S. & Huang, P., 2002. Mitochondrial defects in cancer. *Molecular cancer*, 1, p.9.

Cavalieri, D. et al., 2007. Analysis of gene expression profiles reveals novel correlations with the clinical course of colorectal cancer. *Oncology research*, 16(11), pp.535–48.

Chaika, N. V et al., 2012. Differential expression of metabolic genes in tumor and stromal components of primary and metastatic loci in pancreatic adenocarcinoma. *PloS one*, 7(3), p.e32996.

Chakrabarti, O. & Krishna, S., 2003. Molecular interactions of "high risk" human papillomaviruses E6 and E7 oncoproteins: implications for tumour progression. *Journal of biosciences*, 28(3), pp.337–348.

Chen, G. et al., 2003. Protein profiles associated with survival in lung adenocarcinoma. *Proceedings of the National Academy of Sciences of the United States of America*, 100(23), pp.13537–42.

Chen, Y. et al., 2009. Oxygen consumption can regulate the growth of tumors, a new perspective on the Warburg effect. *PloS one*, 4(9), p.e7033.

Choi, J. et al., 2014. The Nuclear Matrix Protein, NRP/B, Acts as a Transcriptional Repressor of E2F-mediated Transcriptional Activity. *Journal of Cancer prevention*, 19(3), pp.187–98.

Clem, B.F. & Chesney, J., 2012. Molecular pathways: regulation of metabolism by RB. *Clinical cancer research : an official journal of the American Association for Cancer Research*, 18(22), pp.6096–6100.

Curry, J.M. et al., 2013. MCT1 and MCT4 are functional biomarkers of metabolic symbiosis in head and neck cancer Cancer metabolism , stemness and tumor recurrence. *Cell Cycle*, 12(9), pp.1371–1384.

Dang, C. V, 2012. Links between metabolism and cancer. *Genes & development*, 26(9), pp.877–90.

Dang, C. V et al., 2008. The interplay between MYC and HIF in cancer. *Nature reviews. Cancer*, 8(January), pp.51–56.

Darnell, J.E., 2002. Transcription factors as targets for cancer therapy. *Nature reviews. Cancer*, 2(10), pp.740–9.

DeBerardinis, R.J. et al., 2008. The biology of cancer: metabolic reprogramming fuels cell growth and proliferation. *Cell metabolism*, 7(1), pp.11–20.

DeGregori, J. & Johnson, D.G., 2006. Distinct and Overlapping Roles for E2F Family Members in Transcription, Proliferation and Apoptosis. *Current molecular medicine*, 6(7), pp.739–48.

Druker, B.J. et al., 2006. Five-year follow-up of patients receiving imatinib for chronic myeloid leukemia. *The New England journal of medicine*, 355(23), pp.2408–17.

Dubois, S. et al., 2010. Glucose inhibits angiogenesis of isolated human pancreatic islets. *Journal of molecular endocrinology*, 45(2), pp.99–105.

Dyson, N., 1998. The regulation of E2F by pRB-family proteins. *Genes & development*, (617), pp.2245–2262.

Edwards, B.K. et al., 2002. Annual Report to the Nation on the status of cancer, 1973-1999, featuring implications of age and aging on U.S. cancer burden. *Cancer*, 94(10), pp.2766–2792.

Elstrom, R.L. et al., 2004. Akt Stimulates Aerobic Glycolysis in Cancer Cells. , pp.3892–3899.

Emmert-Streib, F. & Glazko, G. V, 2011. Pathway analysis of expression data: deciphering functional building blocks of complex diseases. *PLoS computational biology*, 7(5), p.e1002053.

Estan, M.C. et al., 2014. Apoptotic Efficacy of Etomoxir in Human Acute Myeloid Leukemia Cells . Cooperation with Arsenic Trioxide and Glycolytic Inhibitors , and Regulation by Oxidative Stress and Protein Kinase Activities. *PloS one*, pp.1–26.

Estrella, V. et al., 2013. Acidity generated by the tumor microenvironment drives local invasion. *Cancer research*, 73(5), pp.1524–35.

Favaro, E. et al., 2012. Glucose utilization via glycogen phosphorylase sustains proliferation and prevents premature senescence in cancer cells. *Cell metabolism*, 16(6), pp.751–64.

Feron, O., 2009. Pyruvate into lactate and back: from the Warburg effect to symbiotic energy fuel exchange in cancer cells. *Radiotherapy and oncology : journal of the European Society for Therapeutic Radiology and Oncology*, 92(3), pp.329–33.

Fiaschi, T. & Chiarugi, P., 2012. Oxidative stress, tumor microenvironment, and metabolic reprogramming: a diabolic liaison. *International journal of cell biology*, 2012, p.762825.

Flamant, L. et al., 2012. TMEM45A is essential for hypoxia-induced chemoresistance in breast and liver cancer cells. *BMC cancer*, 12, p.391.

Földi, M. et al., 2007. Transketolase protein TKTL1 overexpression : A potential biomarker and therapeutic target in breast cancer. *Oncology reports*, 17, pp.841–845.

Frezza, C. et al., 2011. Metabolic profiling of hypoxic cells revealed a catabolic signature required for cell survival. *PloS one*, 6(9), p.e24411.

Fu, L. et al., 2000. Loss of the Major Isoform of Phosphoglucomutase Results in Altered Calcium Homeostasis in Saccharomyces cerevisiae. *Journal of Biological Chemistry*, 275(8), pp.5431–5440.

Gapstur, S.M., Gann, P.H. & Lowe, W., 2007. Abnormal Glucose Metabolism and Pancreatic Cancer Mortality. *Journal of American Medical Association*, 283(19), pp.2552–2558.

Giacinti, C. & Giordano, a, 2006. RB and cell cycle progression. *Oncogene*, 25(38), pp.5220–7.

Grupp, K. et al., 2013. High mitochondria content is associated with prostate cancer disease progression. *Molecular cancer*, 12(1), p.145.

Günther, V., Lindert, U. & Schaffner, W., 2012. Biochimica et Biophysica Acta The taste of heavy metals : Gene regulation by MTF-1 ☆. *BBA - Molecular Cell Research*, 1823(9), pp.1416–1425.

Gururaj, A. et al., 2004. Regulation of phosphoglucomutase 1 phosphorylation and activity by a signaling kinase. *Oncogene*, 23, pp.8118–8127.

Hanahan, D., 2014. Rethinking the war on cancer. *Lancet*, 383(9916), pp.558–63.

Hanahan, D. & Coussens, L.M., 2012. Accessories to the crime: functions of cells recruited to the tumor microenvironment. *Cancer cell*, 21(3), pp.309–22.

Hanahan, D. & Weinberg, R.A., 2011. Hallmarks of cancer: the next generation. *Cell*, 144(5), pp.646–674. Hanahan, D., Weinberg, R.A. & Francisco, S., 2000. The Hallmarks of Cancer. , 100, pp.57–70.

Harbour, J.W. & Dean, D.C., 2000. The Rb/E2F pathway: Expanding roles and emerging paradigms. *Genes and Development*, 14(314), pp.2393–2409.

Vander Heiden, M.G., 2011. Targeting cancer metabolism: a therapeutic window opens. *Nature reviews. Drug discovery*, 10(9), pp.671–84.

Vander Heiden, M.G., Cantley, L.C. & Thompson, C.B., 2009. Understanding the Warburg Effect: The Metabolic Requirements of Cell Proliferation. *Science*, 324(5930), pp.1029–1033.

Holroyde, P. et al., 1979. Lactate Metabolism in Patients with Metastatic Colorectal Cancer. *Cancer research*, 39(December), pp.4900–4905.

Horsman, M.R. et al., 2012. Imaging hypoxia to improve radiotherapy outcome. *Nature reviews. Clinical oncology*, 9, pp.674–87.

Hu, C. et al., 2003. Differential Roles of Hypoxia-Inducible Factor 1 α (HIF-1 α) and HIF-2 α in Hypoxic Gene Regulation. *Molecular and Cellular Biology*.

Huang, W. et al., 2013. A proposed role for glutamine in cancer cell growth through acid resistance. *Cell research*, 23(5), pp.724–7.

Icard, P. & Lincet, H., 2012. A global view of the biochemical pathways involved in the regulation of the metabolism of cancer cells. *Biochimica et biophysica acta*, 1826(2), pp.423–33.

Ishida, S. et al., 2001. Role for E2F in control of both DNA replication and mitotic functions as revealed from DNA microarray analysis. *Molecular and cellular biology*, 21(14), pp.4684–99.

Jemal, A., Bray, F. & Ferlay, J., 2011. Global Cancer Statistics. *CA Cancer J Clin*, 61(2), pp.69–90.

Jiang, B.-H. et al., 1996. Hypoxia-inducible factor 1 levels vary exponentially over a physiologically relevant range of O2 tension. *The American Physiological Society*, 2(45), pp.1172 –1180.

Jiang, P., 2011. p53 regulates biosynthesis through direct inactivation of glucose-6-phosphate dehydrogenase. *Nature cell biology*, 13(3), pp.310–316.

Jiang, P., Du, W. & Wu, M., 2014. Regulation of the pentose phosphate pathway in cancer. *Protein & cell*. Available at: http://www.ncbi.nlm.nih.gov/pubmed/25015087

Jones, N.P., 2011. Targeting target cancer metabolism what is fuelling the resurgence? *Drug Discovery World Fall*, pp.64–75.

Jones, R.G. & Thompson, C.B., 2009. Tumor suppressors and cell metabolism: a recipe for cancer growth. *Genes & development*, 23(5), pp.537–48.

Junttila, M.R. & de Sauvage, F.J., 2013. Influence of tumour micro-environment heterogeneity on therapeutic response. *Nature*, 501(7467), pp.346–54.

Karstensen, B. et al., 2006. Gene expression profiles reveal an upregulation of E2F and downregulation of interferon targets by HPV18 but no changes between keratinocytes with integrated or episomal viral genomes. *Virology*, 353(1), pp.200–9.

Ke, Q. & Costa, M., 2006. Hypoxia-Inducible Factor-1 (HIF-1). *MOlecular Pharmacology*, 70(5), pp.1469–1480.

Keith, B., Adelman, D.M. & Simon, M.C., 2001. Targeted mutation of the murine arylhydrocarbon receptor nuclear translocator 2 (Arnt2) gene reveals partial redundancy with Arnt. *Proceedings of the National Academy of Sciences of the United States of America*, 98(12), pp.6692–7.

Kennedy, K.M. & Dewhirst, M.W., 2010. Tumor metabolism of lactate: the influence and therapeutic potential for MCT and CD147 regulation. *Future Oncology*, 6(1), pp.1–32.

Kim, W. et al., 2012. Dual functions of DP1 promote biphasic Wnt-on and Wnt-off states during anteroposterior neural patterning. *The EMBO Journal*, 31(16), pp.3384–3397. Kondoh, H. et al., 2005. Glycolytic Enzymes Can Modulate Cellular Life Span. *Cancer research*, 2005(65), pp.177–185.

Kondoh, M. et al., 2013. Hypoxia-induced reactive oxygen species cause chromosomal abnormalities in endothelial cells in the tumor microenvironment. *PloS one*, 8(11), p.e80349.

De La Luna, S. et al., 1999. Integration of a growth-suppressing BTB/POZ domain protein with the DP component of the E2F transcription factor. *EMBO Journal*, 18(1), pp.212–228.

Langbein, S. et al., 2006. Expression of transketolase TKTL1 predicts colon and urothelial cancer patient survival: Warburg effect reinterpreted. *British journal of cancer*, 94(4), pp.578–85.

Lee, C.-H. et al., 2010. Down-regulation of phosphoglucomutase 3 mediates sulforaphane-induced cell death in LNCaP prostate cancer cells. *Proteome science*, 8(1), p.67.

Lee, W.-N.P. et al., 2004. Metabolic sensitivity of pancreatic tumour cell apoptosis to glycogen phosphorylase inhibitor treatment. *British journal of cancer*, 91(12), pp.2094–100.

Lee, Y. et al., 2014. Compromised Catalysis and Potential Folding Defects in in Vitro Studies of Missense Mutants Associated with Hereditary Phosphoglucomutase 1 Deficiency. *Journal of Biological Chemistry*, 289(46), pp.32010–32019.

Li, L. et al., 2015. Combied inhibition of glycolysis , the pentose cycle , and thioredoxin metabolism selectively increases cytotoxicity and oxidative stress in human breast and prostate cancer. *Redox Biology*, 4, pp.127–135.

Liao, S.-H. et al., 2009. Proteomics-based identification of two novel direct targets of hypoxia-inducible factor-1 and their potential roles in migration/invasion of cancer cells. *Proteomics*, 9(15), pp.3901–12.

Lingwood, R.J. et al., 2008. The challenge of cancer control in Africa. *Nature cell biology*, 8, pp.398–403.

Liu, H. et al., 2010. Fructose induces transketolase flux to promote pancreatic cancer growth. *Cancer research*, 70(15), pp.6368–76.

Liu, H. et al., 2004. New roles for the RB tumor suppressor protein. *Current opinion in genetics & development*, 14(1), pp.55–64.

Liu, W. et al., 2012. Targeted genes and interacting proteins of hypoxia inducible factor-1. *International journal of biochemistry and molecular biology*, 3(2), pp.165–78.

Locasale, J.W., 2012. Metabolic rewiring drives resistance to targeted cancer therapy. *Molecular systems biology*, 8(597), p.597.

Logue, J.S. & Morrison, D.K., 2012. Complexity in the signaling network: insights from the use of targeted inhibitors in cancer therapy. *Genes & development*, 26(7), pp.641–50.

Lu, W., Logsdon, C.D. & L Abbruzzese, J., 2013. Cancer Metabolism and Its Therapeutic Implications. *Journal of Cell Science & Therapy*, 4(2), p.1000143.

Lum, J.J. et al., 2007. The transcription factor HIF-1alpha plays a critical role in the growth factor-dependent regulation of both aerobic and anaerobic glycolysis. *Genes & development*, 21(9), pp.1037–49.

Ma, Y. et al., 2009. Searching for serum tumor markers for colorectal cancer using a 2-D DIGE approach. *Electrophoresis*, 30(15), pp.2591–9.

Macaluso, M. et al., 2005. Modulation of Cell Cycle Components by Epigenetic and Genetic Events. *Seminars in Oncology*, 32(5), pp.452–457.

Marín-Hernández, A. et al., 2011. Modeling cancer glycolysis. *Biochimica et biophysica acta*, 1807(6), pp.755–67.

Masson, N. & Ratcliffe, P.J., 2014. Hypoxia signaling pathways in cancer metabolism: the importance of co-selecting interconnected physiological pathways. *Cancer & metabolism*, 2(1), pp.2–17..

Mclaughlin-drubin, M.E. & Münger, K., 2010. The Human Papillomavirus E7 Oncoprotein. *Virology*, 384(2), pp.335–344.

Miao, P. et al., 2013. Lactate dehydrogenase A in cancer: a promising target for diagnosis and therapy. *IUBMB life*, 65(11), pp.904–10.

Moreno-Sánchez, R. et al., 2007. Energy metabolism in tumor cells. *The FEBS journal*, 274(6), pp.1393–418.

Morey, J.S., Ryan, J.C. & Van Dolah, F.M., 2006. Microarray validation: factors influencing correlation between oligonucleotide microarrays and real-time PCR. *Biological procedures online*, 8(1), pp.175–93.

Moscato, S. et al., 2000. Surface expression of a glycolytic enzyme, alpha-enolase, recognized by autoantibodies in connective tissue disorders. *European journal of immunology*, 30(12), pp.3575–84.

Muller, P. a J., Vousden, K.H. & Norman, J.C., 2011. P53 and Its Mutants in Tumor Cell Migration and Invasion. *The Journal of cell biology*, 192(2), pp.209–18.

Nakajima, E.C. & Van Houten, B., 2013. Metabolic symbiosis in cancer: refocusing the Warburg lens. *Molecular carcinogenesis*, 52(5), pp.329–37.

Nardinocchi, L. et al., 2009. Inhibition of HIF-1alpha activity by homeodomain-interacting protein kinase-2 correlates with sensitization of chemoresistant cells to undergo apoptosis. *Molecular cancer*, 8(1).

Nevins, J.R., 2001. The Rb/E2F pathway and cancer. *Human molecular genetics*, 10(7), pp.699–703. Available at:

Nevins, R., 1998. Toward an Understanding of the Functional Complexity of the E2F and Retinoblastoma Families. *Cell Growth & Differentiation*, 9(August), pp.585–593.

Obel, L.F. et al., 2012. Brain glycogen-new perspectives on its metabolic function and regulation at the subcellular level. *Frontiers in neuroenergetics*, 4(March), p.3.

Ondruskova, N. et al., 2014. Glycogen storage disease-like phenotype with central nervous system involvement in a PGM1-CDG patient. , 35(2), pp.137–141.

Onozuka, H., Tsuchihara, K. & Esumi, H., 2011. Hypoglycemic/hypoxic condition in vitro mimicking the tumor microenvironment markedly reduced the efficacy of anticancer drugs. *Cancer science*, 102(5), pp.975–82.

Papandreou, I., Goliasova, T. & Denko, N.C., 2011. Anticancer drugs that target metabolism: Is dichloroacetate the new paradigm? *International journal of cancer. Journal international du cancer*, 128(5), pp.1001–8.

Pelicano, H., Carney, D. & Huang, P., 2004. ROS stress in cancer cells and therapeutic implications. *Drug resistance updates : reviews and commentaries in antimicrobial and anticancer chemotherapy*, 7(2), pp.97–110.

Pelletier, J. et al., 2012. Glycogen Synthesis is Induced in Hypoxia by the Hypoxia-Inducible Factor and Promotes Cancer Cell Survival. *Frontiers in oncology*, 2(February), p.18.

Perl, A. et al., 2012. Oxidative stress, inflammation and carcinogenesis are controlled through the pentose phosphate pathwat by transaldose. *Trends in Molecular Medicine*, 17(7), pp.395–403.

Pescador, N. et al., 2010. Hypoxia promotes glycogen accumulation through hypoxia inducible factor (HIF)-mediated induction of glycogen synthase 1. *PloS one*, 5(3), p.e9644.

Pfeiffer, T., Schuster, S. & Bonhoeffer, S., 2001. Cooperation and competition in the evolution of ATP-producing pathways. *Science*, 292, pp.504–7.

Polanska, U.M. & Orimo, A., 2013. Carcinoma-associated fibroblasts: non-neoplastic tumour-promoting mesenchymal cells. *Journal of cellular physiology*, 228(8), pp.1651–7.

Porporato, P.E. et al., 2011. Anticancer targets in the glycolytic metabolism of tumors: a comprehensive review. *Frontiers in pharmacology*, 2(August), p.49.

Pouysségur, J., Shiu, R.P. & Pastan, I., 1977. Induction of two transformation-sensitive membrane polypeptides in normal fibroblasts by a block in glycoprotein synthesis or glucose deprivation. *Cell*, 11(4), pp.941–947.

Pray, L.A., 2008. Gleevec: the breakthrough in cancer treatment. *Nature Education*, 1(1), p.37.

Puzio-Kuter, A.M., 2011. The Role of p53 in Metabolic Regulation. *Genes & cancer*, 2(4), pp.385–91.

Rajeevan, M.S. et al., 2001. Use of real-time quantitative PCR to validate the results of cDNA array and differential display PCR technologies. *Methods*, 25, pp.443–51.

Ravazzolo, R., Sessarego, M. & Barresi, R., 1985. Demonstration of Phosphoglucomutase 1 in a Subclone of the K-562 Cell Line. *Cancer research*, pp.1296–1299.

Rohren, E.M., Turkington, T.G. & Coleman, R.E., 2004. Radiology Clinical Applications of PET in Oncology. *Radiology*, 231, pp.305–320.

Rohwer, N. & Cramer, T., 2011. Hypoxia-mediated drug resistance: novel insights on the functional interaction of HIFs and cell death pathways. *Drug resistance updates : reviews and commentaries in antimicrobial and anticancer chemotherapy*, 14(3), pp.191–201.

Rousset, M., Zweibaum, A. & Fogh, J., 1981. Presence of Glycogen and Growth-related Variations in 58 Cultured Human Tumor Cell Lines of Various Tissue Origins. *Cancer research*, 41, pp.1165–1170.

Salceda, S. & Caro, J., 1997. Hypoxia-inducible Factor 1 alpha (HIF-1 alpha) Protein Is Rapidly Degraded by the Ubiquitin-Proteasome System under Normoxic Conditions. *The Journal of Biological Chemistry*, 272(36), pp.22642–22647.

Santos, C.R. & Schulze, A., 2012. Lipid metabolism in cancer. *The FEBS journal*, 279(15), pp.2610–23.

Saydam, N. et al., 2002. Regulation of Metallothionein Transcription by the Metal-responsive Transcription Factor MTF-1. , 277(23), pp.20438–20445.

Schumacker, P.T., 2006. Reactive oxygen species in cancer cells: live by the sword, die by the sword. *Cancer cell*, 10(3), pp.175–6.

Semenza, G.L., 2013. HIF-1 mediates metabolic responses to intratumoral hypoxia and oncogenic mutations. *The Journal of Clinical Investigation*, 123(9), pp.3664–3671.

Semenza, G.L., 2010. HIF-1: upstream and downstream of cancer metabolism. *Current opinion in genetics & development*, 20(1), pp.51–6.

Semenza, G.L., 2009. Regulation of oxygen homeostasis by hypoxia-inducible factor 1. *Physiology*, 24, pp.97–106.

Semenza, G.L., 2008. Tumor metabolism : cancer cells give and take lactate. *Journal of Clinical Investigation*, 118(12), pp.3835–3837.

Seyfried, T.N. & Shelton, L.M., 2010. Cancer as a metabolic disease. *Nutrition & metabolism*, 7(7), pp.1–22.

Shim, H. et al., 1997. c-Myc transactivation of LDH-A : Implications for tumor metabolism and Growth. *Proceedings of the National Academy of Sciences*, 94(June), pp.6658–6663.

Smith, N.R. et al., 2013. Tumor stromal architecture can define the intrinsic tumor response to VEGF-targeted therapy. *Clinical cancer research : an official journal of the American Association for Cancer Research*, 19(24), pp.6943–56.

Som, P. et al., 1980. A Fluorinated Glucose Analog , 2-fluoro-2-deoxy-D-glucose (F-18): Nontoxic Tracer for Rapid Tumor Detection A FluorinatedGlucose Analog , 2-fluoro-2-deoxy-D-glucose (F-18): Nontoxic Tracer for RapidTumor Detection ofacute orchronic. *J Nucl Med*, 21, pp.670–675.

Song, Y. et al., 2014. Alpha-enolase as a potential cancer prognostic marker promotes cell growth, migration, and invasion in glioma. *Molecular cancer*, 13(1), p.65.

Sonveaux, P. et al., 2008. Targeting lactate-fueled respiration selectively kills hypoxic tumor cells in mice. *Journal of Clinical Investigation*, 118, pp.3930–3942.

Sonveaux, P. et al., 2012. Targeting the lactate transporter MCT1 in endothelial cells inhibits lactate-induced HIF-1 activation and tumor angiogenesis. *PloS one*, 7(3), p.e33418.

Sørensen, T.S. et al., 1996. Functional interaction between DP-1 and p53. *Molecular and cellular biology*, 16(10), pp.5888–5895.

Stenger, C. et al., 2011. The cell death response to the ROS inducer, cobalt chloride, in neuroblastoma cell lines according to p53 status. *International journal of oncology*, 39(3), pp.601–9.

Stojkovic, T. et al., 2009. Muscle glycogenosis due to phosphoglucomutase 1 deficiency. *The New England journal of medicine*, 361(4), pp.425–427.

Szatrowski, T. & Nathan, C., 1991. Production of large amounts of hydrogen peroxide by human tumor cells. *Cancer research*, pp.794–798.

Tang, J. et al., 2013. Target inhibition networks: predicting selective combinations of druggable targets to block cancer survival pathways. *PLoS computational biology*, 9(9), p.e1003226.

Tegtmeyer, L. et al., 2015. Multiple Phenotypes in Phosphoglucomutase 1 Deficiency. , 72(4), pp.377–385.

Tong, Y. et al., 2013. HIF1 regulates WSB-1 expression to promote hypoxia-induced chemoresistance in hepatocellular carcinoma cells. *FEBS letters*, 587(16), pp.2530–5.

Trachootham, D. et al., 2006. Selective killing of oncogenically transformed cells through a ROS-mediated mechanism by beta-phenylethyl isothiocyanate. *Cancer cell*, 10(3), pp.241–52.

Tsin-Wah, L., 2013. *The Role of Human Papillomavirus (HPV) -related Molecular Markers in Cervical Neoplasia , with emphasis on p-21 Activated Kinase Type 1 (PAK 1)"*. University of Hong Kong.

Tsouko, E. et al., 2014. Regulation of the pentose phosphate pathway by an androgen receptor-mTOR-mediated mechanism and its role in prostate cancer cell growth. *Oncogenesis*, 3(5), p.e103..

Tsutsumi, S. et al., 2009. Phosphoglucose isomerase enhances colorectal cancer metastasis. *International journal of oncology*, 35, pp.1117–1121.

Upadhyay, M. et al., 2013. The Warburg effect: insights from the past decade. *Pharmacology & therapeutics*, 137(3), pp.318–30.

Varmus, H. & Kumar, H.S., 2013. Addressing the Growing International Challenge of Cancer: A Multinational Perspective. *Science translational medicine*, 5(175), pp.1–5.

Vaupel, P., Kallinowski, F. & Okunieff, P., 1989. Blood flow, oxygen and nutrient supply, and metabolic microenvironment of human tumors: a review. *Cancer research*, 49(23), pp.6449–65.

Vogel, C.L. et al., 2003. Efficacy and Safety of Trastuzumab as a Single Agent in First-Line treatment of HER2-Overexpressing Metastatic Breast Cancer. *Journal of Clinical Oncology*, 20(3), pp.719–726.

Wang, C. et al., 2011. Identification of transaldolase as a novel serum biomarker for hepatocellular carcinoma metastasis using xenografted mouse model and clinic samples. *Cancer letters*, 313(2), pp.154–66.

Wang, G.L. et al., 1995. Hypoxia-inducible factor 1 is a basic-helix-loop-helix-PAS heterodimer regulated by cellular 02 tension. *Proceedings of the National Academy of Sciences*, 92(June), pp.5510–5514.

Warburg, O., 1956. On the origin of cancer cells. *Science*, 123(3191), pp.309–314.

Ward, M.C. et al., 2011. Deregulated LAP2α expression in cervical cancer associates with aberrant E2F and p53 activities. *IUBMB life*, 63(11), pp.1018–26.

Ward, P.S. & Thompson, C.B., 2012. Metabolic reprogramming: a cancer hallmark even warburg did not anticipate. *Cancer cell*, 21(3), pp.297–308.

Van der Watt, P., 2009. *Expression and regulation of the nuclear transport proteins, Crm1 and Kpnβ1, in cervical cancer and transformed cells*. University of Cape Town. Available at: http://uctscholar.uct.ac.za/PDF/90882_Van_der_Watt_P.pdf.

Van der Watt, P.J., Ngarande, E. & Leaner, V.D., 2011. Overexpression of Kpnβ1 and Kpnα2 importin proteins in cancer derives from deregulated E2F activity. *PloS one*, 6(11), p.e27723.

Whitaker-Menezes, D. et al., 2011. Evidence for a stromal-epithelial “lactate shuttle” in human tumors: MCT4 is a marker of oxidative stress in cancer-associated fibroblasts. *Cell Cycle*, 10(11), pp.1772–1783.

Wilson, W.R. & Hay, M.P., 2011. Targeting hypoxia in cancer therapy. *Nature reviews. Cancer*, 11, pp.393–410.

Wise, D.R. & Thompson, C.B., 2010. Glutamine Addiction: A New Therapeutic Target in Cancer. *Trends in Biochemical Sciences*, 35(8), pp.427–433.

Wong, N., De Melo, J. & Tang, D., 2013. PKM2, a Central Point of Regulation in Cancer Metabolism. *International journal of cell biology*, 2013, pp.1–11.

World Health Organization, 2008. *The Global Burden of Disease: 2004 Update*, Geneva.

Xu, R., Pelicano, H. & Zhou, Y., 2005. Inhibition of Glycolysis in Cancer Cells : A Novel Strategy to Overcome Drug Resistance Associated with Mitochondrial Respiratory Defect and Hypoxia. *Cancer research*, 65(2), pp.613–621.

Xue, F. et al., 2006. F-18 fluorodeoxyglucose uptake in primary cervical cancer as an indicator of prognosis after radiation therapy. *Gynecologic oncology*, 101(1), pp.147–51.

Yeo, H.C. et al., 2011. Integrated transcriptome and binding sites analysis implicates E2F in the regulation of self-renewal in human pluripotent stem cells. *PloS one*, 6(11), p.e27231.

Zaragoza, K. et al., 2010. Repression of transcriptional activity of C/EBPalpha by E2F-dimerization partner complexes. *Molecular and cellular biology*, 30(9), pp.2293–304.

Zeng, W. et al., 2014. Hypoxia and hypoxia inducible factors in tumor metabolism. *Cancer letters*, pp.1–5.

Zhao, Y., Butler, E.B. & Tan, M., 2013. Targeting cellular metabolism to improve cancer therapeutics. *Cell death & disease*, 4(3), p.e532.

Zhuang, Y. et al., 2014. Mechanisms by which low glucose enhances the cytotoxicity of metformin to cancer cells both in vitro and in vivo. *PloS one*, 9(9), p.e108444.

Zwerschke, W. et al., 2000. Allosteric Activation of Acid alpha -Glucosidase by the Human Papillomavirus E7 Protein. *Journal of Biological Chemistry*, 275(13), pp.9534–9541.

Zwerschke, W. & Mazurek, S., 1999. Modulation of type M2 pyruvate kinase activity by the human papillomavirus type 16 E7 oncoprotein. *Proceedings of the National Academy of Sciences of the United States of America*, 96(February), pp.1291–1296.